

# **Effects of Lamin A Progeric Mutation (LMNA- $\Delta$ 50) in Tau Reporter Cell Culture Models**

by

Zhuang Zhuang Han

A thesis submitted in partial fulfillment of the requirements for the degree of

Master of Science

Department of Biochemistry

University of Alberta

© Zhuang Zhuang Han, 2021

## **Abstract**

Chronological aging is one of the greatest risk factors of tauopathies, yet our understanding about the underlying molecular mechanism is limited. Studying physiological aging often requires an extended timeline and thus presents a significant hurdle for modeling late-onset disorders. In this study, we present an attempt to mimic chronological aging with pathological premature aging. Our approach involves expression of progerin, a truncated form of lamin A found primarily in Hutchinson Gilford progeria syndrome, in established cell culture models for tau protein aggregation. We find that induced aging sensitizes tau inclusion-free cells to tau misfolding events when cells are exposed to pathogenic tau. Significant aggravation of nuclear deformation is observed in cells that are already burdened with tau aggregates. To further investigate progerin-induced cellular changes, mass spectrometry is employed to determine the cellular proteome with and without progerin expression. Our proteomics dataset shows that progerin results in notable but complex alterations in nuclear and endosome-associated proteins, shedding light on their potential involvements in chronological aging.

## **Preface**

This thesis is an original work by Zhuang (George) Han. The transgenic mice used in this research project were generated in previous animal studies (AUP00000358 and AUP00000356) which were approved and reviewed by the Animal Care and Use Committee of the University of Alberta.

Some of the research conducted for this thesis forms part of a research collaboration, led by Dr. David Westaway and Dr. Olivier Julien in the Department of Biochemistry. The mass spectrometric analysis described in Chapter 3 was designed by myself and performed by Mr. Erik Gomez. The data analysis was conducted by myself, with general guidance from Mr. Erik Gomez, Dr. Olivier Julien and Dr. Michael Schultz.

This dissertation is dedicated to Dr. Ignaz Semmelweis,  
a true hero who (almost) single-handedly cured puerperal fever with hand washing.

He was unfortunately ridiculed and mistreated by fellow physicians,  
and he died long before hand washing finally became a routine procedure for obstetricians.

Let's all remember Dr. Ignaz Semmelweis, the savior of mothers.

I pray that I will have the same enthusiasm in the most difficult moments in my career.

“When I look back upon the past, I can only dispel the sadness which falls upon me by gazing into that happy future when the infection will be banished. But if it is not vouchsafed for me to look upon that happy time with my own eyes ... the conviction that such a time must inevitably sooner or later arrive will cheer my dying hour.”

Ignaz Semmelweis (1818-1865)

## **Acknowledgements**

Above all, I want to thank God Almighty for giving me enough energy and perseverance when I encountered obstacles in this journey. It was God's mercy that brought all these wonderful people into my life and it was God's grace that brought me this far despite "many dangers, toils and snares" in this career path.

I would like to express my sincere gratitude to the University of Alberta for the opportunity of becoming a Master's student. I would also like to thank the Department of Biochemistry and the Centre for Prion and Protein Folding Diseases (CPPFD) for allowing me to participate in a variety of meaningful dementia-related research projects. Most importantly, I want to thank my supervisor, Dr. David Westaway, who provided guidance for me through these years. Beyond an exceptional scientist and mentor, David is also such an extremely generous and caring individual with great enthusiasm that working with him certainly became one of the most rewarding experiences in my life. I have no doubt that David will become my lifelong mentor and role model. I would also like to thank the members of my thesis committee, Dr. Michael Schultz and Dr. Sue-Ann Mok, as they have given me immeasurable guidance and support since the beginning of my project. I am grateful to all my colleagues who are, and were Dr. Serene Wohlgemuth, Dr. Sang-Gyun Kang, Dr. Andrew Castle, Dr. Nathalie Daude, Dr. Jing Yang, Dr. Ivana Machado, Dr. Ghazaleh Eskandari-Sedighi, Dr. Zelin Fu, Dr. Olivier Julien, Luis Arce, Klinton Shmeit, Erik Gomez and Natasha Wismark. They all have provided me with training, technical expertise, encouragement, general advice and logistics support.

I would like to acknowledge with gratitude, the support and love of my parents, without whom it would have been impossible for me to focus on the coursework and research projects. Thank you, Mom and Dad, for your unconditional love through all these years!

## Table of Contents

<b>Chapter 1: Introduction</b> .....	1
1.1: Tauopathies and dementias .....	1
1.1.1: Microtubule-associated protein tau .....	1
1.1.2: Disease-causing tau and tauopathies .....	3
1.1.3: Pathogenicity of tau in dementias .....	6
1.1.4: Tau pathogenic conformers .....	9
1.1.5: Tau and non-neurological disorders .....	11
1.2: Aging and dementia .....	15
1.2.1: Natural aging and pathological aging .....	15
1.2.2: Aging of the brain .....	23
1.2.3: Aging models for dementia research .....	24
1.2.4: Involvement of <i>LMNA</i> in brain aging – to be or not to be? .....	28
1.3: Hypothesis .....	32
<b>Chapter 2: Materials and Methods</b> .....	33
2.1: Construction of <i>LMNA</i> ( $\Delta$ 50 or WT) expression vectors .....	33
2.1.1: Construction of mCherry-pBudCE vector .....	33
2.1.2: Construction of mCherry- <i>LMNA</i> WT-pBudCE and mCherry- <i>LMNA</i> $\Delta$ 50-pBudCE vectors .....	35
2.2: Expression of <i>LMNA</i> $\Delta$ 50, <i>LMNA</i> WT and mCherry in HEK293 tauRD-YFP cells .....	36

2.2.1: Cell culture.....	36
2.2.2: Transient transfection of LMNA ( $\Delta$ 50, WT and empty vector) in HEK293 tauRD-YFP cells .....	36
2.2.3: Generation of stable progeric cell lines (HEK293 tauRD-YFP LMNA $\Delta$ 50 and ES1 LMNA $\Delta$ 50).....	37
2.2.4: Confocal microscopy .....	37
2.2.5: Analyses of protein expression with capillary western immunoassay .....	38
2.3: Tau protein transduction in HEK293 tauRD-YFP cells .....	38
2.4: Limited proteolysis .....	40
2.5: Mass spectrometric analysis of cell lysate.....	41
2.6: Statistical analysis.....	42
<b>Chapter 3: Results.....</b>	<b>43</b>
3.1: Construction of mCherry-pBudCE, mCherry-LMNA WT-pBudCE and mCherry-LMNA $\Delta$ 50-pBudCE vectors .....	43
3.2: Transient transfection of LMNA-WT or - $\Delta$ 50 in HEK293 tauRD-YFP reporter cell line....	46
3.3: Generation of stable progeric HEK293 tauRD-YFP reporter cell lines .....	48
3.4: Seeding of progeric HEK293 tauRD-YFP reporter cell lines.....	52
3.5: Generation and characterization of polyclonal progeric ES1 cell lines.....	58
3.6: Mass spectrometric analysis of progeric and non-progeric tau reporter cell lines .....	61
3.6.1: Progeric and non-progeric HEK cell lines .....	61

3.6.2: HEK and ES1 cell lines .....	66
3.6.3: Non-progeric HEK and progeric ES1 cell lines.....	70
<b>Chapter 4: Discussion</b> .....	<b>74</b>
4.1: Progeric HEK cell lines – progerin-induced aging in a tau inclusion-free cell culture model .....	74
4.2: The ES1 cell line harboring tau aggregates exhibits changes in splicing and endosomal proteins.....	76
4.3: Progeric ES1 cell lines – progerin-induced aging in a tau inclusion-positive cell culture model.....	78
4.4: Technical considerations.....	79
4.5: Modeling aging to study tau biology – what is next? .....	80
4.6: Summary .....	81
<b>Chapter 5: References</b> .....	<b>83</b>

## List of Tables

Table 1: Polar and charged amino acid composition of six tau splicing isoforms .....	2
Table 2: Tauopathies and predominant tau isoforms in the inclusions.....	4
Table 3: Global socioeconomical burden of dementia from 2000 to 2016.....	6
Table 4: Braak staging system of Alzheimer’s disease .....	8
Table 5: Tauopathy-associated mutations in the <i>MAPT</i> gene.....	13
Table 6: Summary of genetic progeroid syndromes .....	16
Table 7: Properties associated with HGPS .....	22
Table 8: Tauopathy mouse models .....	28
Table 9: Summary of primers used.....	34
Table 10: Primary antibodies used in confocal microscopy. ....	38
Table 11: Primary antibodies used in capillary western immunoassay .....	38

## List of Figures

Figure 1: Six isoforms of tau produced by alternative splicing from the <i>MAPT</i> gene. ....	3
Figure 2: Cryo-EM structures of tau filaments. ....	7
Figure 3: Lamin A and the nuclear lamina. ....	18
Figure 4: Normal and HGPS prelamin A processing.....	19
Figure 5: Research timeline of the functions of nuclear lamins in brain physiology. ....	32
Figure 6: Schematic illustrating methods used to transduce brain-derived or cell lysate-derived tau extracts into HEK293 tauRD-YFP cells (progeric or non-progeric). ....	40
Figure 7: Schematic illustration of mass spectrometric analysis of different cell lines with/without progerin expression. ....	42
Figure 8: Construction of mCherry-pBudCE vector with molecular cloning.....	44
Figure 9: Construction of mCherry-LMNA WT-pBudCE and mCherry-LMNA $\Delta$ 50-pBudCE vectors. ....	46
Figure 10: Transient transfection of progerin in HEK293 tauRD-YFP cells. ....	48
Figure 11: Characterization of progeric HEK293 tauRD-YFP clones. ....	51
Figure 12: Wes capillary immunoassay of tau in progeric and non-progeric HEK cell lines. ....	51
Figure 13: Tau seeding efficiency was quantified with the high content screening fluorescence microscopy.....	53
Figure 14: Tau-liposome titration assay used to determine the working ratio between tau extracts (from Tg mouse brain extracts or ES1 cell lysate) and lipofectamine 3000.....	55
Figure 15: Quantitation of tau seeding efficiency.....	57
Figure 16: Correlation analysis for progerin-induced increase of seeding efficiency and the proportion of seeded cells that display nuclear envelope-bound tau. ....	57

Figure 17: Characterization of polyclonal progeric ES1 cell lines. ....	60
Figure 18: Limited proteolysis of ES1 cell-derived sedimented tau.....	60
Figure 19: Adjustment of total protein abundance for cell lysate samples analyzed by mass spectrometry.....	61
Figure 20: Mass spectrometric analysis of up/downregulated proteins in progeric HEK cells (PH2 and PH3) compared to non-progeric HEK cells (NPH). ....	65
Figure 21: Preliminary analysis for pathways significantly modulated in progeric HEK cell lines (PH2/PH3) when compared to non-progeric HEK control. String pathway analysis reveals proteins involved in mRNA splicing (A), protein linear deubiquitination (B) and endosomal/lysosomal trafficking (C).....	66
Figure 22: Mass spectrometric analysis of up/downregulated proteins in non-progeric ES1 cells (NPH) compared to non-progeric HEK cells (NPH). ....	69
Figure 23: Mass spectrometric analysis of up/downregulated proteins in progeric ES1 cells (PE7 and PE9) compared to non-progeric HEK cells (NPH). ....	72
Figure 24: Analysis for pathways significantly modulated in progeric ES1 cell lines (PE7/PE9) compared to non-progeric HEK control. ....	73
Figure 25: Schematic summary of main findings in progeric HEK cells, non-progeric ES1 cells and progeric ES1 cells. ....	82

## Glossary of Terms, Abbreviations and Acronyms

A $\beta$	Beta-amyloid
AD	Alzheimer's disease
AGD	Argyrophilic grain disease
APP	Amyloid precursor protein
BCA	Bicinchoninic acid
CBD	Corticobasal degeneration
CDI	Conformation-dependent immunoassay
CMV	Cytomegalovirus
Cryo-EM	Cryo-electron microscopy
CSA	Conformational stability assay
CTE	Chronic traumatic encephalopathy
DMEM	Dulbecco's Modified Eagle Medium
EF1 $\alpha$	Elongation factor 1 alpha
ES1	Edmonton strain 1
FTD	Frontotemporal dementia
FTLD	Frontotemporal lobar degeneration
GGT	Globular glial tauopathies
HD	Huntington's disease
HGPS	Hutchison-Gilford progeria syndrome
hIAPP	Human pancreatic islets amyloid polypeptide
IBNC	Idiopathic brainstem neuronal chromatolysis
iPSC	Induced pluripotent stem cell
MAPT	Microtubule associated protein tau
miR-9	MicroRNA-9
MRI	Magnetic resonance imaging
NFT	Neurofibrillary tangle
NL	Nuclear lamina
NPE	Non-progeric ES1
NPH	Non-progeric HEK
PART	Primary age-related tauopathy
PD	Parkinson's disease
PE	Progeric ES1
PET	Positron emission tomography
PH	Progeric HEK
PHF	Paired helical filament
PiD	Pick's disease
PK	Proteinase K
PrP	Prion protein

PS	Progeroid syndrome
PSP	Progressive supranuclear palsy
PTM	Post-translational modification
sAD	Sporadic Alzheimer's disease
SAMP	Senescence-accelerated mouse prone
SF	Straight filament
T1D	Type-1 diabetes
T2D	Type-2 diabetes
TI	Tau inclusion
TOR	Target of rapamycin
Tpr	Translocated promoter region
UTR	Untranslated region
WS	Werner syndrome
WT	Wildtype
YFP	Yellow fluorescent protein

## **Chapter 1: Introduction**

### **1.1: Tauopathies and dementias**

#### **1.1.1: Microtubule-associated protein tau**

Tau proteins represent a group of six low molecular weight microtubule-associated protein isoforms produced by alternative splicing from the *MAPT* gene located on chromosome 17q21 [1][2]. Tau is expressed in animal species, including but not limited to human, mouse, rat, bovine, guinea pig and zebrafish[3][4][5]. Although tau was once thought to be a nervous system-specific protein, tau mRNA has been detected in various other tissues, such as kidney, liver and testis in rat, and muscle in both rat and human[6][7].

In the nervous system, tau mRNA is expressed predominantly in neuronal cells, although a lower expression level of tau has been detected in various types of glial cells, such as oligodendrocytes and astrocytes[8]. Similar to other microtubule-associated proteins (MAPs), one of the physiological functions of tau is to bind microtubules, stabilize and mediate their assembly and modulate vesicle/organelle transport on microtubules[9][10]. Intracellular tau is primarily located in the axons and to a lesser extent in somatodendritic compartments such as the cell membrane[11], mitochondria[12] and nucleus[13]. Depending on its cellular localization, tau also plays important roles in axonal transport[14][15], nucleic acid protection[16][17], synaptic plasticity[18][19] and neuronal maturation[20].

Amongst 16 exons in the tau primary transcript, exons 2, 3, 4a, 6, 8 and 10 are subject to alternative splicing and exons 1, 4, 5, 7, 9, 11, 12 and 13 are constitutive[21][22]. The promoter lies in exon 1 (Fig. 1)[23]. Exons 0 and 14 are transcribed but not translated as they are a part of the 5'-untranslated sequence (5'-UTR) and the 3'-untranslated sequence (3'-UTR),

respectively[23][24]. In the adult human brain, alternative splicing of exons 2, 3 and 10 gives rise to all six isoforms of tau; exons 4A, 6 and 8 are exclusive to the peripheral nervous system and absent in human brain[21]. Tau splicing isoforms differ by the number of N-terminal regions (0N, 1N or 2N) as well as the number of conserved repeat motifs (3R or 4R)[2]. Due to its high content of polar and charged amino acids (Table 1), tau is a highly hydrophilic and water-soluble protein. The proline-rich domain (PRD) links the C-terminal assembly domain and the N-terminal projection domain. It serves as binding site for signaling proteins with SRC homology 3[25] and, has recently been suggested to influence tau liquid-liquid phase separation in cells[26]. Structural biology techniques (nuclear magnetic resonance and small-angle X-ray scattering) show that natively folded tau is an intrinsically disordered protein (IDP)[27][28]. Functionally, the N-terminal regions may influence spacing between microtubules[29], subcellular distribution of neuronal tau[30][31] and aggregation kinetics of tau[32]. The repeat motifs constitute the microtubule-binding domain of tau. Due to the additional repeat motif R2, 4R tau displays higher affinity to microtubule than 3R tau, and is thus more efficient at mediating microtubule assembly[33]. 3R and 4R tau are found in adult human brain with an approximate 1:1 ratio[34] and 3R:4R tau isoform imbalance may have significant implications in tau-related pathogenesis[35].

Table 1: Polar and charged amino acid composition of six tau splicing isoforms

Tau isoform	Length (amino acids)	Ser	Thr	Asp	Glu	Lys	Arg	Polar and charged amino acid %
2N4R	441	45	35	29	27	44	14	44%
1N4R	421	45	31	27	24	20	14	38%
0N4R	383	40	26	25	18	42	14	43%
2N3R	410	41	35	27	27	39	14	45%
1N3R	381	41	31	25	24	38	14	45%
0N3R	352	36	26	23	18	37	14	44%

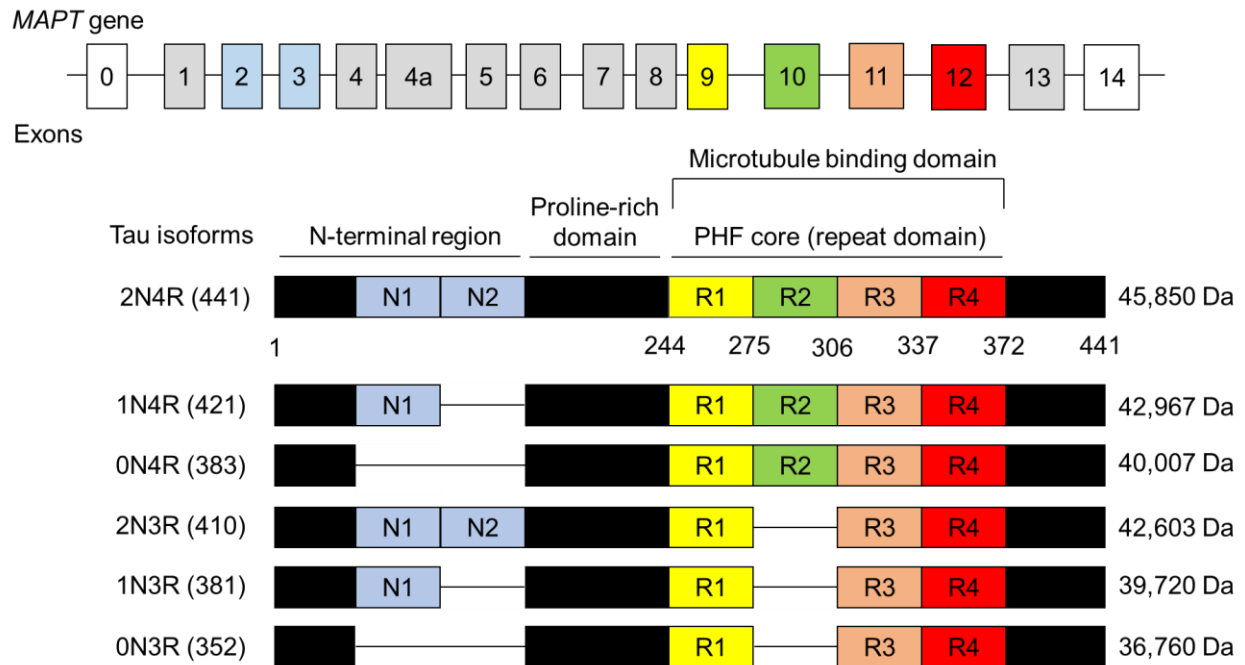


Figure 1: Six isoforms of tau produced by alternative splicing from the *MAPT* gene.

### 1.1.2: Disease-causing tau and tauopathies

The physiological function of tau is further highlighted when tau converts into a pathogenic state. The term “tauopathy” represents a family of neurodegenerative disorders pathologically characterized by the presence of insoluble intracellular tau inclusions in the central nervous system and clinically characterized by dementia and/or parkinsonism[36][37]. Classical tauopathies include, but are not limited to, Alzheimer’s disease (AD), frontotemporal dementia with parkinsonism-17 (FTDP-17T, also known as FTL D-MAPT), Pick’s disease (PiD), progressive supranuclear palsy (PSP), corticobasal degeneration (CBD), argyrophilic grain disease (AGD)[38][25] and sporadic multiple system tauopathy with dementia[39]. In recent years, multiple neurological disorders are now recognized to fall within the spectrum of tauopathies, such as primary age-related tauopathy (PART)[40], Huntington’s disease (HD)[40], Parkinson’s disease (PD)[41], globular glial tauopathies (GGT)[42], chronic traumatic

encephalopathy (CTE)[43], nodding syndrome[41], progressive ataxia and palatal tremor[42][43] and autism spectrum disorder[44]. Accumulation of tau aggregates can also occur in non-human mammals, such as domestic cat[45], cow (idiopathic brainstem neuronal chromatolysis, IBNC)[46], rabbit, spectacled bear and rhesus monkey[47]. It is noteworthy that 3R or 4R tau may become the predominant pathological tau isoform in different diseases (Table 2).

Table 2: Tauopathies and predominant tau isoforms in the inclusions

Disease	Predominant tau isoforms
AD	3R and 4R
PART	3R and 4R
CTE	3R and 4R
Nodding syndrome	3R and 4R
FTLD-MAPT	3R and 4R, 4R, 3R
Tauopathy in aged cat	3R and 4R, 4R
PD	3R, 4R
PiD	3R
IBNC	3R
PSP	4R
CBD	4R
AGD	4R
GGT	4R
HD	4R
Progressive ataxia and palatal tremor	4R
Sporadic multiple system tauopathy with dementia	4R

In terms of clinical signs, various tauopathies share similar symptoms, including motor symptoms (e.g., stiffness of muscles, speech/limb apraxia and early gait freezing), cognitive and behavioral symptoms (e.g., memory loss, personality change and difficulties with calculations) and miscellaneous symptoms (e.g., depression, constipation and urinary incontinence)[48]. Large overlap in symptoms makes accurate diagnosis of tauopathy subtypes challenging in the absence of specific biomarkers. Despite recent advancement in neuroimaging technology (positron

emission tomography and magnetic resonance imaging[49]), autopsy remains to be the only method to make definite diagnoses.

There are two forms of tauopathies, familial and sporadic. Familial tauopathies are caused by mutations in the *MAPT* gene and are often autosomal dominant. Over 100 tau mutations have been discovered[50] yet not all associate with pathogenesis. Most pathogenic mutations lie in the coding regions of exons 9, 10, 11 and 12 (see extended table; Table 5 on page 13), corresponding to the repeated microtubule-binding domain of tau. Other intronic mutations affect the ratio of 3R:4R spliced mRNAs. Familial tauopathies generally associate with early onset of symptoms. Sporadic tauopathies, on the other hand, have delayed onset of symptoms. Not linked to tau genetic mutations or any specific environmental factors, sporadic tauopathies occur in a seemingly unpredictable manner, suggesting a complex and multifactorial nature of its etiology. The molecular events in the “headwater” of sporadic tauopathy pathogenesis remain to be mysterious.

Currently, there are 40-50 million people living with dementia. Alzheimer’s disease, being the most common neurodegenerative disorder, accounts for 24 million of these dementia victims globally[51][52]. Regarding cost of care (Table 3), dementias alone represent a significant socioeconomical challenge worldwide as the cost for dementia care shares a significant portion of global GDP[53]. As human life expectancy continues to increase[54], the number of Alzheimer victims is anticipated to double by 2040[51], assuming no changes in incidence, mortality and current treatments.

Table 3: Global socioeconomical burden of dementia from 2000 to 2016

Year	Global societal cost of dementia (US. billion)	GDP real (US. billion)[55]	Cost of dementia/ GDP
2000	\$278[56]	\$50,131	5.55‰
2005	\$315[57]	\$60,720	5.19‰
2010	\$604[53]	\$66,036	9.17‰
2015	\$818[53]	\$75,834	10.8‰
2016	\$948[56]	\$77,797	12.2‰

Despite the urgent need of finding an efficacious treatment for AD and other types of tauopathies, there are currently no effective, disease-modifying interventions available other than temporary symptomatic relief, such as using selective serotonin reuptake inhibitors to relieve behavioral symptoms and employing physical therapy to improve functional abilities[58]. Slow progress in therapeutics development is at least partly owing to 1) heterogeneity of the disease (different types of tauopathies and different neurological manifestations in each type); 2) complexity of disease-specific biomarkers, difficult diagnosis, and late intervention – neurons have often been irreversibly damaged already at the beginning of treatment; 3) heterogeneity of clinical trial participants[59]; 4) lack of accurate *in vitro* and *in vivo* models. The conflicts between the increasing prevalence of tauopathies and the limited number of effective medical interventions cry out for a more in-depth understanding of tau biology in general.

### 1.1.3: Pathogenicity of tau in dementias

Despite its disordered and soluble character in native conformation, tau exhibits structural plasticity and tendency to change its global conformations to form protein aggregates that are energetically favorable, detergent-resistant, protease-resistant[60] and can be stained with amyloid dyes (e.g., Thioflavin S and Congo red). In tauopathies, the hallmark lesion is neurofibrillary tangles (NFTs) - insoluble, fibrillar intraneuronal deposition of misfolded forms

of the tau protein. Structurally, neurofibrillary tangles consist of paired helical filaments (PHF), straight filaments (SF) and twisted ribbons[61]. Cryo-electron microscopy (cryo-EM) reveals a double helical stack of C-shaped paperclip-like subunits in the cores of PHFs and SFs (Figure 2), where they display cross- $\beta$  structure[62][63]. The “fuzzy-coat” structures surrounding the core, on the other hand, are highly flexible and therefore difficult to visualize with current structural biology techniques.

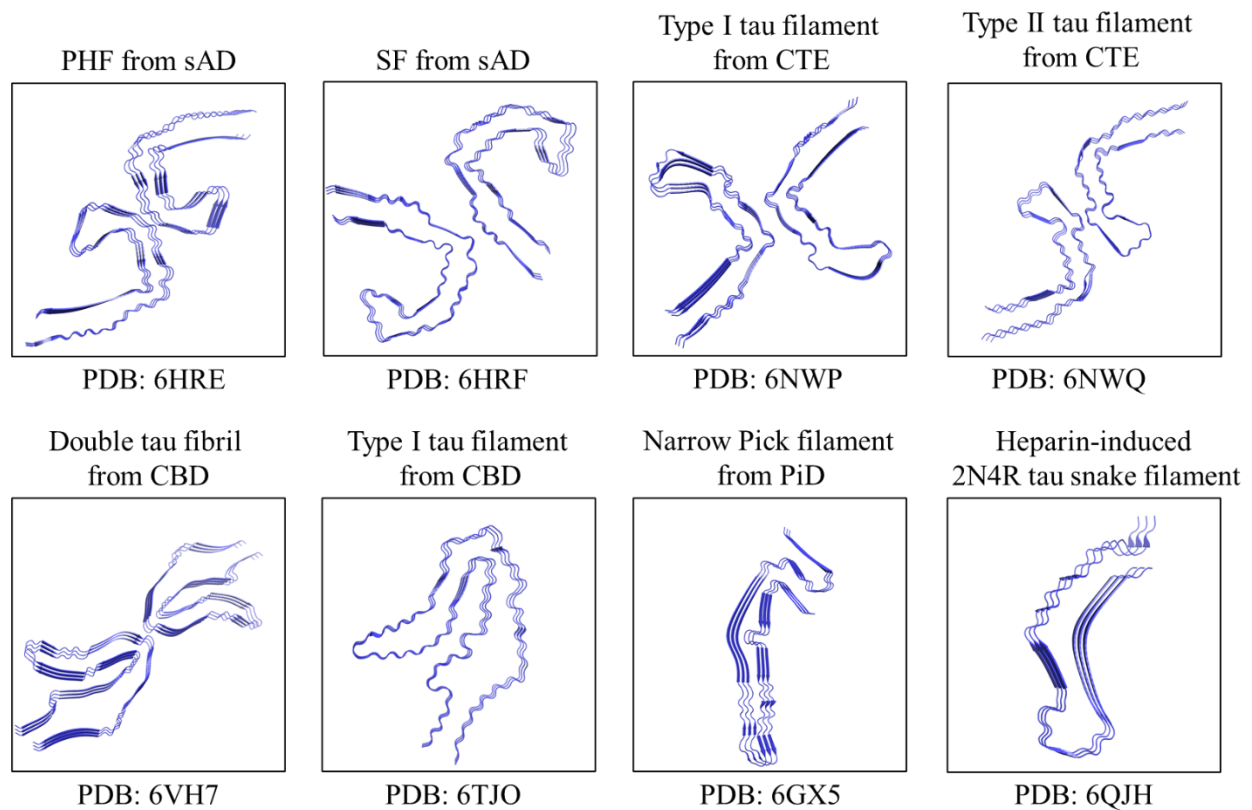


Figure 2: Cryo-EM structures of tau filaments. Samples extracted from sporadic Alzheimer’s disease (sAD), chronic traumatic encephalopathy (CTE), corticobasal degeneration (CBD), Pick’s disease (PiD), or induced by heparin *in vitro*.

Pathologically, neurofibrillary lesions in brain directly correlates with the progression of AD as pathogenic tau propagates through connected neural network. The Braak staging system (Table 4) of AD indicates that certain anatomical regions in brain are “infected” with pathogenic tau in

each clinical stage of the disease and there is at least a loose correlation between tau spreading and disease progression[64].

Table 4: Braak staging system of Alzheimer’s disease

Braak’s Stages	Brain areas affected by NTFs	Clinical stage
I-II	Entorhinal cortex	Preclinical (clinically silent)
III-IV	Limbic system	Prodromal (incipient AD)
V-VI	Neocortex	Advanced AD

Although pathogenic tau is not infectious in a classical sense, experiments performed in tissue culture[65] and in animal models[66] both demonstrated that misfolded tau can be released to into extracellular space and be taken up by neighboring cells. Several mechanisms may support intercellular tau transfer: 1) ectosomes and exosomes carry pathogenic tau in vesicles, which, upon simple fusion and endocytosis, may release tau seeds to recipient cells[67][68]; 2) tunneling nanotubes act as intercellular bridges to facilitate tau fibril transfer[69]; 3) heparan sulfate proteoglycan mediates micropinocytosis of tau seeds[70]. When taken in by naïve cells, pathogenic tau conformers stimulate natively folded tau to adopt an alternative conformation (misfold), leading to the spread of tau pathology. Interestingly, natively folded monomeric tau is also subject to efficient intercellular trafficking between neurons, suggesting that transport of tau may be a constitutive biological process as well as occurring in disease[71]. In an experimental realm, the “infectious” nature of pathogenic tau can be exploited to establish models of tauopathies – inoculation of tau seeds (*in vivo* or *in vitro* generated) into transgenic animal models[72], organoids[73] and tissue culture[74] has become a common experimental approach. Functions of tau are largely dependent on its post-translational modifications (PTMs), including phosphorylation, glycation, nitration, acetylation, oxidation, sumoylation, ubiquitylation, polyamination, isomerization and addition of  $\beta$ -linked *N*-acetylglucosamine[75]. Abnormally

hyperphosphorylated tau, which is a cardinal component of neurofibrillary tangles, is seen in various types of tauopathies, including but not limited to AD, FTDP-MAPT and PSP[76]. The phosphorylation state of tau has significant implications on neuronal health in various ways: 1) it alters the binding property of tau to microtubules, hence detach tau from MTs and destabilize them[77][78]; 2) it alters the binding property of tau to other interacting partners and disturb tau-mediated signaling pathways[79]; 3) it results in local high concentration of tau[80], possibly promoting its aggregation; 4) it disrupts the intracellular route of tau degradation[81]. The mechanisms by which tau contributes to neurological disorders is a multifaceted matter. It is noteworthy that loss of normal tau function does not explain the whole picture of tau-related neurodegeneration as tau knock-out mice only display mild phenotypes (e.g., muscle weakness and hyperactivity), instead of neurodegeneration[82]. Thus, gain-of-function abnormalities caused by tau misregulation appear to be the major contributor to tau pathologies.

#### **1.1.4: Tau pathogenic conformers**

Similar to the prion protein (PrP<sup>c</sup>), tau misfolding does not only produce one type of pathogenic tau but instead gives rise to an array of conformationally distinct conformers of tau. These pathogenic species self-assemble and propagate indefinitely in living systems. Due to their similarities to classical infectious agents (bacterium and virus), these covalently heterogeneous tau species are often called strains and they have been postulated to be an underlying factor of tau transmission and diversity in neuropathology. To contrast different types of misfolded tau, multiple biochemical assays are often employed together for holistic assessments. Different banding patterns produced by limited proteolysis provide a qualitative comparison of different tau strains[74][83][84]. Guanidine denaturation curves generated in conformational stability assay offer a quantitative measurement[84] and may suggest the number of tau conformers

within a sample. Biophysical assays, such as electron-electron resonance spectroscopy[85][86], yield accurate and quantitative structural information of tau misfolding.

In the process of misfolding, tau monomers, oligomers and fibrils represent three unique stages of templated conversion. Since distinct tau strains associate with diverse downstream effects (aggregation kinetics, cellular internalization and propagation rates)[87][88], a question arises as to which tau species (monomers vs oligomers vs fibrils) encodes these specific strain properties. To date, most tau strain research has been performed with detergent-insoluble fibrillar tau species[72][84][74][83]. However, using chronically infected tau reporter cell lines, the Diamond Lab showed for the first time that seed competent tau monomers encode strains[89]. Investigation of multimeric tau species remains to be a challenge, partially due to their ambiguous definition, their unstable biochemical nature and limitations of current separation technology.

Despite intensive research on the determinant of tau strain properties, it is still unclear what pre-defines tau misfolded conformation. Post-translational modification may play a role in this process as an acetylation-mimic substitution modulates tau pathology and phosphorylation status[90]. Using mouse models of tauopathy, He *et al.* suggested that the transmission of distinct tau conformers is independent of the composition of alternatively spliced isoforms (3R:4R ratio)[91]. While it remains unanswered how different tau conformers evolve and propagate in brain, recent development of high-resolution separation methods (e.g., Asymmetric Flow Field-Flow Fractionation[92]) and sensitive conformation-dependent biophysical assays[86] will enable us to more accurately characterize different tau conformers with a holistic approach.

### 1.1.5: Tau and non-neurological disorders

Neurodegenerative diseases and cancer may appear unrelated and opposite phenomena; one that may feature premature cell death and the other one that may feature resistance to programmed cell death. However, recent studies pointed out a great overlap between these diseases. Emerging epidemiological evidence shows an inverse correlation between the incidences of neurodegenerative diseases and cancer. A longitudinal study in 2005 suggested that participants with pre-existing Alzheimer's disease tend to develop cancer at a slower rate and participants with a history of cancer tend to develop Alzheimer's disease at a slower rate[93]. Furthermore, a cognition study in 2010 demonstrated that the Alzheimer victims associate with a 60% reduced risk of cancer; and individuals suffering from prevalent cancer associate with a 30% reduced risk of AD[94][95]. A similar type of "protection" was observed for Parkinson's disease: PD patients associate with a lower risk of all types of cancer except thyroid cancer and melanoma[96].

Though the molecular details underlying this general "protection mechanism" are largely missing, it has been proposed that tau may be one of the determinants at the interface of neurodegeneration and cancer. In gliomas (brain tumor of glial origin), there is an inverse correlation between the expression of the *MAPT* gene and the clinical development of tumors[97]. Tau is involved in cancer biology by several proposed pathomechanisms. First, tau is a modifier of wild-type p53 function and a regulator of DNA damage-induced cell death[98].

Second, because spindle formation is crucial for rapid cell division and this process is regulated by phosphorylation of tau protein, tau overexpression may impair mitosis, induce cell death and slow down tumor progression[99]. More recently, Gargini *et al.* showed that overexpression of tau protein inhibits angiogenesis and reduces glioma aggressiveness through stabilization of microtubules and epidermal growth factor receptor inhibition[100].

Diabetes is another instance in which tau protein is involved in non-neurological diseases. Although the correlation between Type-1 Diabetes (T1D) and AD remains unestablished with epidemiological data[101], AD-like cognitive and intellectual decline (e.g., reduced mental speed and flexibility[102], memory impairment[103]) is common in T1D-afflicted individuals. Type-2 Diabetes (T2D) is also closely related to AD as T2D-afflicted individuals have a 1.54-fold higher risk to develop AD[104]. Beyond correlation in incidence and overlaps in neurological manifestation, diabetes and AD share common features related to pathogenesis. Due to their structural compatibility in the  $\beta$ -sheet regions[105], human pancreatic islet amyloid polypeptide (hIAPP, a major secretory product of  $\beta$ -cells of the pancreatic islets of Langerhans) and beta amyloid ( $A\beta$ , a hallmark of Alzheimer's disease) have cross-seeding interactions and co-oligomerize into  $A\beta$ -hIAPP heterocomplexes[106]. In addition, hIAPP is identified in the cerebrospinal fluid of both AD and T2D patients[107]; elevated levels of tau and phosphorylated tau are detected in the cerebrospinal fluid for both T1D[108] and T2D[109], as in patients with AD. Animal models offered a valuable tool to investigate the molecular linkage between diabetes and AD. Ke *et al.* showed that streptozotocin injection, which mimics the pancreatic damage in T1D, accelerates onset of cerebral tau pathology in a transgenic TauP301L mouse model (Line pR5) that has predisposition to accumulate hyperphosphorylated tau and neurofibrillary tangles[110]. Regarding T2D, Platt *et al.* transduced a Type-2 diabetic mouse line (*Lepr<sup>db/db</sup>*) with TauP301L via adeno-associated virus and discovered that the level of tau phosphorylation and neurofibrillary tangles undergo a drastic increase in the hippocampus compared to the non-diabetic control group[111].

Broad involvement of tau protein in various subtypes of neurodegenerative diseases and non-neurological disorders (such as cancer and diabetes) suggests a cardinal role of tau in cellular

physiology, including cell proliferation/death, cell migration and signaling transduction. It further highlights the need of understanding the functions of tau in different cell types.

Table 5: Tauopathy-associated mutations in the *MAPT* gene

Exons	Disease-associated mutation	Codon change	Neurological phenotype[50]
Exon 1	R5C	CGC > TGC	PD
	R5H	CGC > CAC	FTLD-MAPT
	R5L	CGC > CTC	PSP
	A41T	GCT > ACT	PD
Exon 2	G55R	GGC > AGA	FTLD-MAPT
Exon 3	V75A	GTG > GCG	FTLD-MAPT
	A90V	GCC > GTC	AD
Exon 4a	G213R	GGG > AGG	AD
	V224G	GTC > GGC	AD
	Q230R	CAA > CGA	AD
	D285N	GAC > AAC	PSP
	A297V	GCC > GTC	AD
	S318L	TCG > TTG	AD
Exon 6	L410F	CTT > TTT	AD
Exon 7	A152T	GCC > ACC	AD, FTLD-MAPT, PSP, PD, CBD
Exon 8	S427F	TCC > TTC	AD, PD
	R448*	CGA > TGA	PD
	P512H	CCC > CAC	AD
Exon 9	A239T	GCC > ACC	FTLD-MAPT
	D252V	GAC > GTC	FTLD-MAPT
	K252T	AAG > ACG	PiD-like
	I260V	ATC > GTC	FTLD-MAPT
	L266V	CTG > GTG	FTLD-MAPT
	G272V	GGC > GTC	FTLD-MAPT, PiD-like
	G273R	GGG > AGG	FTLD-MAPT
Exon 10	N279K	AAT > AAG	FTLD-MAPT
	K289del	AAG > del	AD, FTLD-MAPT, PiD-like
	L284L	CTT > CTC	FTLD-MAPT
	L284R	CTT > CGT	PSP
	S285R	AGC > AGA	PSP
	V287I	GTC > ATC	AD
	C291R	TGT > CGT	Speech apraxia, CBD
	N296del	AAT > del	PSP, PD
	N296D	AAT > GAT	FTLD-MAPT
N296H	AAT > CAT	FTLD-MAPT	

	N296N	AAT > AAC	FTLD-MAPT, PSP
	P301L	CCG > CTG	FTLD-MAPT
	P301P	CCG > CCA	FTLD-MAPT
	P301S	CCG > TCG	FTLD-MAPT
	P301T	CCG > ACG	FTLD-MAPT, CBD, GGT
	G303V	GGC > GTC	PSP
	S305I	AGT > ATT	AGD
	S305N	AGT > AAT	FTLD-MAPT
	S305S	AGT > AGC	FTLD-MAPT, PSP
Exon 11	L315L	CTG > CTA	FTLD-MAPT
	L315R	CTG > CGG	FTLD-MAPT
	K317M	AAG > ATG	Tauopathy with Parkinsonism
	K317N	AAG > AAC	GGT
	S320F	TCC > TTC	FTLD-MAPT, PiD-like
	S320Y	Unclear	PiD-like
	P332S	CCA > TCA	FTLD-MAPT
Exon 12	G335A	GGC > GCC	FTLD-MAPT
	G335S	GGC > AGC	FTLD-MAPT
	G335V	GGC > GTC	FTLD-MAPT
	Q336H	CAG > CAC	Pick's disease
	Q336R	CAG > CGG	FTLD-MAPT
	V337M	GTG > ATG	FTLD-MAPT
	E342V	GAG > GTG	FTLD-MAPT
	S352L	TCG > TTG	Other tauopathy (reduced tau-microtubule binding and accelerated tau filament formation)
	S356T	TCC > ACC	FTLD-MAPT
	I360V	ATC > GTC	PD
	V363I	GTC > ATC	FTLD-MAPT
	P364S	CCT > TCT	FTLD-MAPT
	G366R	GGA > AGA	FTLD-MAPT
	K369I	AAA > ATA	FTLD-MAPT, PiD-like
Exon 13	E372G	GAA > GGA	FTLD-MAPT
	G389_I392del	GGG GCG GAG ATC GTG > GTG	FTLD-MAPT
	G389R (G>A)	GGG > AGG	FTLD-MAPT, Pick's disease
	G389R (G>C)	GGG > CGG	FTLD-MAPT
	P397S	CCA > TCA	FTLD-MAPT
	R406W	CGG > TGG	AD, FTLD-MAPT
	N410H	AAT > CAT	CBD
	T427M	ACG > ATG	FTLD-MAPT, PD

## **1.2: Aging and dementia**

### **1.2.1: Natural aging and pathological aging**

Aging is a time-dependent progressive biological process which leads to declined physiological functions and compromised ability to adapt to metabolic stress. Chronological age is a main risk factor for the prevalent non-infectious ailments, including life-threatening diseases (e.g., cardiovascular disease, cancer and neurodegeneration[112]) and less lethal conditions that reduce life quality (e.g., hypertension, osteoarthritis and osteoporosis[113]). Although late-onset tauopathies are associated with unclear multifactorial molecular origins, aging has a strong positive correlation with the prevalence of tauopathies. The general age at symptom onset is >65 years for sporadic Alzheimer's disease, 45-65 years for FTLD-MAPT, 40-60 years for PiD and 40-80 for PSP[114]. For sporadic Alzheimer's disease, chronological age is often considered the greatest known risk factor[115]. Despite the clear epidemiological relationship between aging and tauopathies, the age-dependent risk for tauopathies remains obscure at a molecular level.

Two types of aging process have been considered: inborn normal (chronological) aging and premature pathological aging. Normal physiological aging associates with various defects in cells, such as genome instability[116], telomere shortening[117], mitochondrial dysfunction[118], alterations in epigenetics[119] and nuclear membrane impairment[120]. Premature aging syndromes, also known as progeroid syndromes (PS), are rare congenital disorders that recapitulate some pathological features of normal aging in an accelerated manner and thus provide potential insights into the aging process at the molecular, cellular and organismal levels (Table 6). Premature aging often associates with perturbations to the nucleus, leading to deteriorated nuclear lamina or compromised DNA replication/transcription/repair

mechanisms. Table 6 offers a non-exhaustive summary of common progeroid syndromes caused by gene mutations.

Table 6: Summary of genetic progeroid syndromes

Progeroid syndromes	Dominant/recessive	Mutated gene(s)	Affected protein(s)	Affected cellular mechanism
Hutchinson-Gilford progeria syndrome	Dominant	<i>LMNA</i>	Lamin A	Nuclear lamina
Restrictive dermopathy	Recessive	<i>ZMPSTE24</i>	Lamin A	Nuclear lamina
Cockayne syndrome	Recessive	<i>ERCC8; ERCC6</i>	CSA, CSB	Nucleotide excision repair
Xeroderma pigmentosum	Recessive	<i>DDB2; ERCC2; ERCC3; ERCC4; CC5; XPA; XPC</i>	XP DNA repair proteins	Nucleotide excision repair
Trichothiodystrophy	Recessive	<i>TTDN1; XPB; XPD; TTDA</i>	Transcription factor II	Nucleotide excision repair
Bloom syndrome	Recessive	<i>BLM</i>	BLM helicase	RecQ protein-like helicase
Werner syndrome	Recessive	<i>WRN</i>	WRN helicase	RecQ protein-like helicase
Rothmund-Thomson syndrome	Recessive	<i>RECQ4</i>	RECQL4	RecQ protein-like helicase
Wiedemann-Rautenstrauch syndrome[121]	Recessive	<i>POLR3GL</i>	RNA Polymerase III Subunit GL	RNA polymerase III
Keppen-Lubinsky syndrome[122]	Dominant	<i>KCNJ6</i>	GIRK2	K <sup>+</sup> channel
Gottron acrogeria[123][124]	Recessive	<i>COL3A1</i>	Collagen Type III Alpha 1 Chain	Collagen production
Ehlers-Danlos syndrome progeroid type[125][126]	Recessive	<i>B4GALT7</i>	Beta-1,4-galactosyl-transferase 7	Proteoglycan synthesis

Hutchinson-Gilford Progeria Syndrome (HGPS) and Werner Syndrome (WS) are by far the best-characterized segmental progeroid disorders in humans. HGPS is an ultra-rare, genetically encoded, autosomal dominant, lethal childhood aging disorder; the estimated overall prevalence of HGPS is 1 in 18 million and the average life expectancy of affected individuals is 14.6 years[127]. In terms of clinical features, the faces of HGPS affected individuals become wrinkle and aged looking due to loss of subcutaneous fat; prominent eyes, scalp veins, alopecia, bone density reduction and high-pitched voice are other common features[128]. Though physically underdeveloped (short stature, low weight and absent sexual maturation)[129], children with HGPS appear to age a decade for every year of life, shown by their advanced cardiovascular, respiratory and arthritic conditions. Cardiovascular compromise is the leading cause of death in HGPS victims - myocardial infarction is by far the most common though cerebral vascular lesions, infections and others have also been reported[130]. Despite its 100% mortality and many proposed treatment options (Table 6), no intervention has been approved for this orphan disease.

Hutchinson-Gilford Progeria Syndrome is a member of the family of genetic diseases caused by defects in lamin proteins, collectively known as the laminopathies. Lamins are members of the intermediate-filament family that constitutes major components of the nuclear lamina – the three dimensional meshwork underlying the inner nuclear membrane[131]. There are two types of lamin proteins encoded by three genes. A-type lamins (lamin A and C) are product of the *LMNA* gene on chromosome 1 by alternative splicing. B-type lamins include lamin B1, B2 and B3: lamin B1 is encoded by the *LMNB1* gene on chromosome 5, and lamin B2 and B3 are product of the *LMNB2* gene on chromosome 19 by alternative splicing[132]. In eukaryotic cells, A-type and B-type lamins form heterodimers[133] and homodimers[134] to assemble the nuclear lamina. Structurally, lamins mainly consist of  $\alpha$ -helical rods and form coiled-coil dimers[135] (Figure 3).

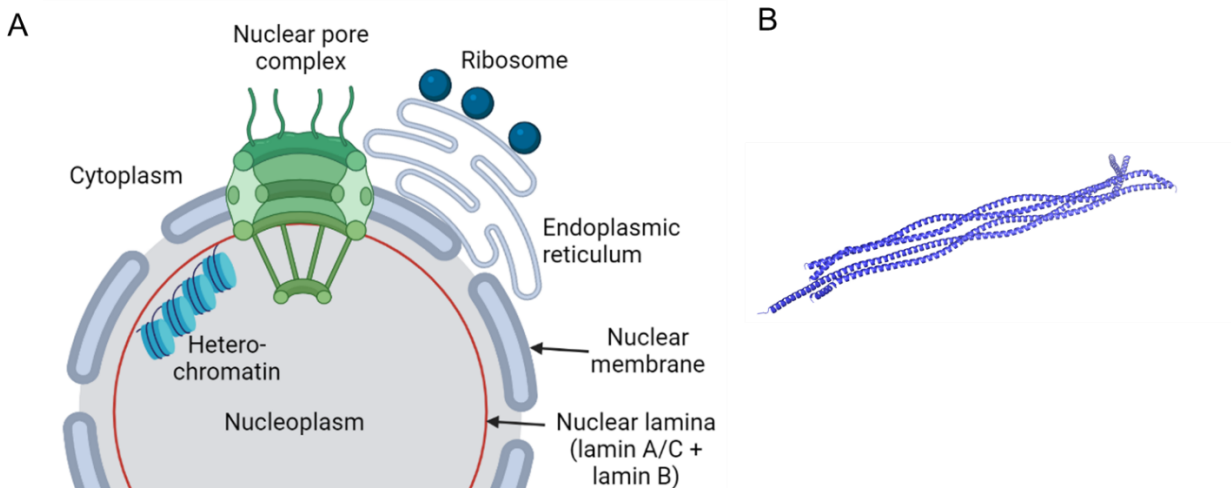


Figure 3: Lamin A and the nuclear lamina. (A). Nuclear lamina (NL) is a meshwork consist of lamin A/C and lamin B. NL has close spatial and functional association with chromatin organization and nuclear pore complex. Figures are not drawn to scale. (B). Crystal structure of human lamin A/C fragment and assembly mechanisms of intermediate filaments (PDB: 6JLB).

Although the expression level of lamins systematically increases with tissue stiffness[136], A-type and B-type lamins have different expression patterns in different tissues. In general, B-type lamins are constitutively expressed in most cell types and A-type lamins are mainly expressed in most differentiated cell types[137], such as fibroblasts. Tissue micro-stiffness also determines the expression level of A- and B-type lamins. A-type lamins often associate with high-stress, bone-like tissues (e.g., cartilage, heart and muscle) whereas B-type lamins associate with low-stress, fat-like tissues (e.g., marrow and brain)[136].

Most HGPS cases (classical HGPS) are caused by a single *de novo* nucleotide substitution at position 1824 (C>T) in exon 11 of the *LMNA* gene[129]. This silent mutation activates a cryptic splicing site that at the 3'-end of the *LMNA* mRNA and leads to a 150-nucleotide deletion from the prelamins A transcript. The mutant protein (50 amino acids truncated near its C-terminus) produced is termed lamin A- $\Delta$ 50 or “progerin”. As depicted in Figure 4, normal wildtype lamin A, once synthesized, undergoes farnesylation at its C-terminal CaaX box by farnesyltransferase.

The CaaX box is subsequently cleaved by Ras Converting CAAX Endopeptidase 1 (RCE1) and Zinc Metallopeptidase STE24 (ZMPSTE24) after the cysteine residue, and then methylated by protein-S-isoprenylcysteine carboxyl methyltransferase (ICMT). Upstream cleavage by ZMPSTE24 then removes 18 amino acids at the C-terminus, producing mature lamin A (72 kDa) that is unattached to the C-terminal farnesyl group. HGPS mutant lamin A, on the other hand, lacks the recognition site of ZMPSTE24 (-RSYLLG-) and thus cannot be cleaved at its C-terminus. As a result, mutant prelamina A (progerin) retains a farnesyl group and becomes immobilized in the nuclear lamina.

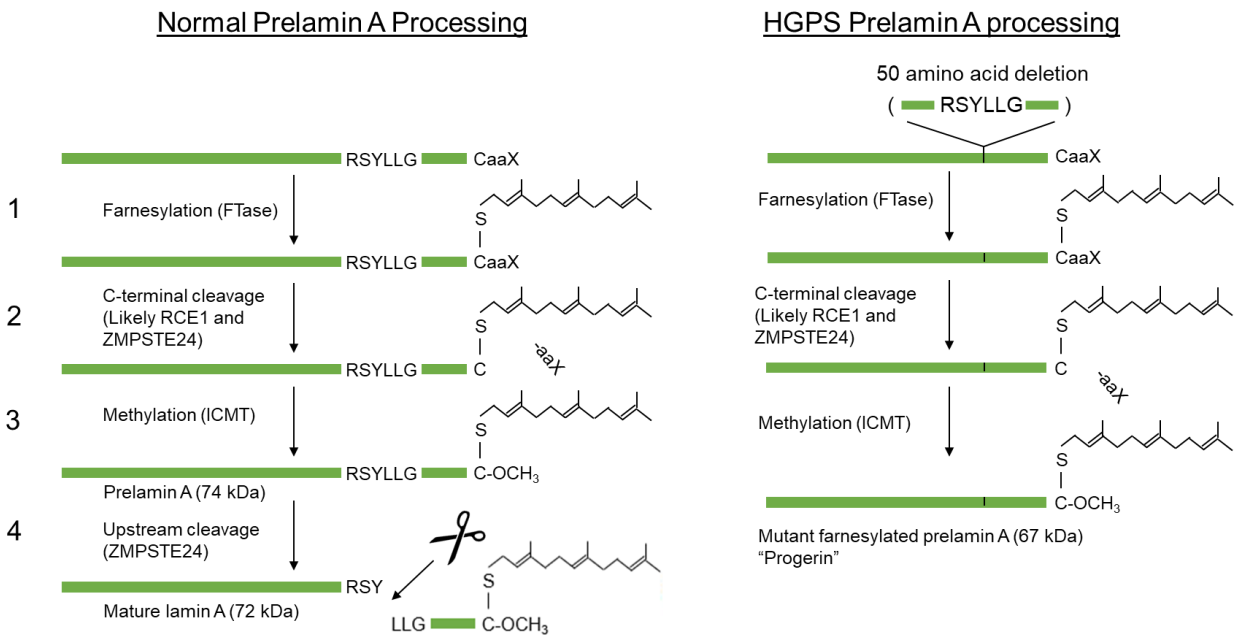


Figure 4: Normal and HGPS prelamina A processing. Adapted from Coutinho *et al* [138].

Stable association of progerin with the nuclear lamina has multiple implications. First, it thickens the lamina, alters the mechanical properties of the nuclei and increases the stiffness of cell[139]. Second, progerin alters chromatin architecture and genome stability. Since the spatial organization of chromosome depends on its attachment to the nuclear lamina, progerin-induced

loss of nuclear-lamina-chromatin interaction causes significant changes in chromosome organization[131]. In this process, alterations in the levels of key architectural chromatin proteins (e.g., HP1 $\alpha$ ) and heterochromatin-associated histones (e.g., H3K9me3) are common observations[140][141]. Additionally, progerin results in increased unrepaired DNA double-stranded breaks[141]. Third, nucleocytoplasmic transport may be affected. Progerin disrupts the nucleocytoplasmic transport of Ran protein[142] and subsequently affects transport of large protein cargoes, such as translocated promoter region (Tpr)[143].

In a lab setting the HGPS aging mutation offers a valuable tool to circumvent the fixed timeline of chronological aging. Despite lack of HGPS mutation in normal aged individuals, progerin is produced at very low frequency in certain tissues, such as skin and skeletal muscle, due to activation of progerin cryptic splice site[144][145]. The quantity of progerin displays a tendency to increase with age both *in vivo* (in skin slices) and in tissue culture (in fibroblast cultures)[146], suggesting a possible function of progerin in normal aging. Chronological aging in normal individuals and accelerated pathological aging in HGPS patients overlap in various molecular/cellular mechanisms: 1) Telomere shortening is widely regarded as a hallmark of normal aging[117] and progerin expression accelerates telomere attrition *in vivo*[147] and in tissue culture[148]. 2) Another hallmark of normal aging is genome instability, which includes chemical damage to DNA (e.g., single- or double-stranded breaks, crosslinks between bases), mutations (addition, deletion and substitution) and epigenetic erosions[116]. Expression of progerin also results in genome instability, exemplified by defects in double-stranded DNA break repair mechanism[149]. 3) Mitochondrial dysfunction and metabolic impairment are common observations in aged tissues, such as heart[150], ovary[151] and skeletal muscle[152]. In human fibroblasts and mouse models, progerin expression also leads to mitochondrial

dysfunction and alters the metabolic rate (e.g., ATP synthesis rate and oxygen consumption rate)[153]. 4) Senescence, a cellular response characterized by limited cell proliferation, is a shared phenomenon between normal aging[154] and HGPS[155]. 5) During normal aging, the diversity and activity of stem cells decline. This is a possible result of accumulated somatic mutations, epigenetic alterations and extrinsic environmental factors (e.g., inflammatory cytokines and complement proteins in plasma)[156]. Similarly, progerin expression not only interferes with the function of human mesenchymal stem cells[157] but also changes aging kinetics in human embryonic stem cells[158]. 6) The function of proteostasis network undergoes a decline with aging, resulting in dysregulated protein synthesis, conformational maintenance, post-translational modifications, compartmentation and degradation. This is possibly a consequence of accumulated stochastic mutations, energy deficit associated with aging and compromised chaperone network[159]. Similar to normal aging, protein homeostasis is also disrupted in HGPS - proteomic analysis revealed that more than 150 proteins significantly changed in concentration upon progerin expression[160].

Although HGPS pathological aging recapitulates cellular and molecular aspects of normal physiological aging, two major differences remain. First, progerin expression in normal aged tissues is a result of activation of cryptic splicing events of the *LMNA* gene, instead of the C>T silent mutation in HGPS. Second, HGPS aging is segmental in nature, meaning that only certain types of tissues are predominantly affected. As mentioned above, lamin A is mainly expressed in elastic tissues and B-type lamins (lamin B1 and B2) are primarily expressed in inelastic tissues. Progerin, as a mutant form of lamin A, has predominant disease manifestations on tissues with high micro-stiffness, such as skin, bones and joints (Table 7). Normal physiological aging, on the

other hand, results in functional decline to all tissues. Tissue specificity thus needs to be carefully considered when we use the HGPS progeric mutation to model aging.

Table 7: Properties associated with HGPS

Prevalence	1 in 18 million Little difference between male and female
Mutations	<i>LMNA</i> exon 11 (c.1824C>T; p.G608G)
Clinical features[161][162]	<p>Developmental:</p> <ul style="list-style-type: none"> <li>• Postnatal growth retardation</li> <li>• Low body weight</li> <li>• Lack of pubertal development</li> </ul> <p>Craniofacial:</p> <ul style="list-style-type: none"> <li>• Midface hypoplasia</li> <li>• Mandibular hypoplasia</li> </ul> <p>Dermatological:</p> <ul style="list-style-type: none"> <li>• Skin abnormalities (outpouchings and scleroderma)</li> <li>• Hair loss</li> <li>• Nail dystrophy</li> <li>• Loss of subcutaneous fat</li> <li>• Lipodystrophy</li> </ul> <p>Cardiovascular and cerebrovascular:</p> <ul style="list-style-type: none"> <li>• Atherosclerosis</li> <li>• Cardiac fibrosis</li> <li>• Stroke</li> </ul> <p>Skeletal:</p> <ul style="list-style-type: none"> <li>• Decreased joint mobility</li> <li>• Progressive joint contractures</li> <li>• Osteolysis</li> <li>• Low-frequency conductive hearing loss</li> </ul>
Cellular defects[162]	<p>Nuclear dysmorphology (blebbing)</p> <p>Alteration of chromatin structure and genome instability</p> <ul style="list-style-type: none"> <li>• Relaxation of heterochromatin</li> <li>• Epigenetic changes</li> <li>• Increased DNA damage</li> </ul> <p>Alteration of regulatory and stress-response pathways</p> <p>Mitochondrial and metabolic dysfunction</p> <p>Attrition of adult stem cells</p> <p>Cellular senescence</p> <p>Loss of proteostasis</p>
Diagnosis[162]	<p>Genetic testing</p> <p>Phenotype recognition and imaging (X-ray and MRI)</p>

Potential therapeutic interventions[162]	Protein farnesyltransferase inhibitors Statins and aminobisphosphonates Protein methylation inhibitors Aging treatment (rapamycin and resveratrol) Stem cell therapy Gene therapy
--	--

### 1.2.2: Aging of the brain

Aging of the brain affects neurobiological functions at various levels and often has a direct association with cognitive decline[163][164]. Using model organisms (yeast, nematodes, flies and mammals) and microarray technology, many changes in pathways associated with brain aging have been found to be evolutionarily conserved across species. Insulin/IGF-1 (insulin-like growth factor 1) signaling, TOR (target of rapamycin) signaling, mitochondrial function, sirtuins and caloric restriction are common signaling pathways that affect brain aging[165]. Recent advancement in functional brain imaging technology enabled us to explore age-related brain changes at the anatomical and functional levels. With functional magnetic nuclear resonance (fMRI), Walhovd *et al.* showed consistent age-related brain volume changes in cerebral cortex, pallidum, putamen and accumbens[166] and Nyberg *et al.* presented diminished frontal cortex function in aging with longitudinal analyses[167].

Although aging affects the entire organism, brain aging should be considered different from that of other tissues for multiple reasons. First, unlike most cell types, neurons are highly differentiated postmitotic cells and usually have limited ability to proliferate. Though recent evidence suggests a possibility for retinal ganglion cells to re-enter the cell cycle[168][169], this exception associates with tetraploidization (duplication of the DNA content) and therefore reflects a different biological process from regular dividing cells. Second, brain aging is not uniform insofar as different brain regions can experience different changes over time. In terms of brain volume, prefrontal cortex, putamen, caudate and midbrain experience most significant age-

related atrophy. Hippocampus, amygdala and temporal cortex experience milder volume changes; and brainstem is the most unaffected brain region[170].

It is worth noting that normal (non-demented) and pathological (demented) brain aging share similarities at different levels. Although NFT's are a hallmark for AD, a secondary tauopathy, and have a strong correlation with cognitive dysfunction, neurofibrillary changes were also observed in the brains of intellectually preserved individuals[171], blurring the histological fine line between cognitively intact elderly people and demented patients. Modern neuroimaging technology tau-PET scan confirms that neurofibrillary tangle abundance is an aging phenomenon in brain and suggests that tau signal is elevated in cognitively unimpaired individuals in brain regions that are considered high Braak Stage[172]. Age-dependent dysregulation of ubiquitin-proteasome system[173], alterations of the mTOR pathway[174] and inactivation of Sirtuin 1 protein deacetylase[175] may explain the accumulation of tau deposition in non-demented brains.

### **1.2.3: Aging models for dementia research**

Recapitulating age-related features of tauopathies (or any types of dementia) largely relies on the development of cell culture or animal models. In the field of neurodegeneration, there are three main approaches to study the effect of aging: 1) to use naturally occurring animal line that displays phenotypes of aging; 2) to introduce aging-associated mutations by transfection (in cell culture) or establishing transgenic animal lines; 3) to lower the expression level of disease-related proteins (e.g., tau with pathogenic mutations) and conduct experiments at the end of the animals' natural life span. Each approach offers a unique angle to investigate the biology of aging if their limitations are carefully examined when designing experiments.

A widely studied animal model for aging research is Klotho-deficient ( $KL^{-/-}$ ) mice. Klotho, named after one of the three Fates in Greek mythology, was serendipitously discovered as a monogenic trait by Kuro-o et al. in 1997, representing a recessive allele produced by a transgene insertional inactivation event[176]. As a group of transmembrane protein, Klotho has three subfamilies ( $\alpha$ -,  $\beta$ - and  $\gamma$ -Klotho) that have different physiological functions[177]. However, the term “Klotho” generally refers to the  $\alpha$ -Klotho subfamily, which has been associated with aging.  $\alpha$ -Klotho is encoded by the  $KL$  gene and it has multiple molecular functions, such as  $\beta$ -glucosidase activity and fibroblast growth factor receptor binding activity[178]. Klotho-deficient ( $KL^{-/-}$ ) mice display overt phenotypes compared to their wildtype littermates, such as hypogonadism, premature thymic involution, ectopic calcification, impaired bone mineralization, skin atrophy, hearing loss and neurodegeneration[179]. Using a  $KL^{-/-}$  mouse model, Nagai *et al.* showed that deficiency of Klotho in mouse brain results in an impairment of visual recognition memory and associative fear memory, which may be explained by an elevated level of apoptosis and oxidative stress in hippocampus[180]. More recently, Leon *et al.* showed that peripherally administered Klotho fragment ( $\alpha$ KL-F) can enhance cognitive parameters and neural resilience in transgenic  $\alpha$ -synuclein mice[181]. Dubal *et al.*, using hAPP transgenic mice that had been crossed with Klotho transgenic mice, demonstrated that elevated level of Klotho protects hAPP mice against premature mortality and cognitive impairments[182]. As expected, a longitudinal study in 2020 suggested that increased serum level of Klotho (in Klotho-VS heterozygous individuals) is associated with reduced AD risk in  $APOE4$  carriers from 60-80 years of age[183]. These observations altogether suggest a neural-protective role of Klotho and this mechanism deserves further investigation.

A different approach – pursuit of polygenic traits – results in an important contribution by workers at Kyoto University; here, senescence-accelerated mouse prone (SAMP) substrains were established through phenotypic selection from AKR/J breeding colonies. SAMP8 is one of the nine major SAMP substrains and shows features of rapid aging. Functionally, SAMP8 mice show impairment of memory and deteriorations in learning ability. Brain stem spongy degeneration, blood-brain barrier dysfunction and loss of cholinergic neurons are major anatomical changes in the central nervous system. Despite the absence of amyloid plaques and NFTs, SAMP8 mice show many cellular and molecular characteristics that mimic physiological brain aging, such as increase in phosphorylated tau, increase in oxidative stress, severe cellular senescence and downregulation of glucose metabolism[184].

Beyond these two examples, in their review, Folgueras *et al.* summarized more than 80 genetically engineered mouse models with accelerated aging phenotypes that can be employed to disentangle human aging process[185]. These mouse models are designed to mimic certain hallmarks of aging, such as genomic instability, telomere attrition, epigenetic alterations, loss of proteostasis and mitochondrial dysfunction. Currently, there are four aging mouse models with HGPS-related genetic targets. Among these, *Lmna*<sup>D257A/D257A</sup>, *Lmna*<sup>L530P/L530P</sup>, *Lmna*<sup>G609G/G609G</sup> are LMNA knockin models and *Zmpste24*<sup>-/-</sup> is a Zmpste24 knockout model. Both homozygous and heterozygous *Lmna*<sup>G609G</sup> transgenic mice well recapitulate human HGPS phenotypes, such as growth deficiency, alopecia, decreased mobility and cardiovascular alterations[186]. Lastly, beyond genetic models, another experimental approach to producing experimental aging involves a specialized type of blood transfusion procedure called parabiosis[187]. Building on the observation that infusion of blood from young mice ameliorates aging in older animals[188], a reciprocal manipulation is to "age" young mice by infusion of blood from older animals[189].

Protein expression level and the relatively short lifespan of mice have also been exploited to study relationships between aging and neurodegeneration. Many currently adapted tauopathy mouse models significantly overexpress tau to drive pathogenesis (Table 8). This involves substantial artificial acceleration of pathogenesis and thus fails to accurately depict the diseased conditions of human sporadic tauopathies (aged central nervous system expressing low levels of tau). Currently, the mouse model generated in the Westaway lab, TgTau(P301L)23027, associates with a later disease onset (12-13 months) due to its low expression level of human mutant tau estimated at 1.7x endogenous levels[190]. This slow model of primary tauopathy exhibits pathological and biochemical features of FTLN-MAPT, such as age-dependent accumulation of hyperphosphorylated tau, neuro- and grano-fibrillary tangles in the brain, and neuronal damage in the temporal and hippocampal formations[190]. With derivatives of the same mouse model (on three different genetic backgrounds), Eskandari-Sedighi *et al.* demonstrated delayed onset of symptoms in the last 40% of the animals' natural lifespan, neuronal loss and filamentous tau formation, confirming and extending observations made with the original transgenic line[72]. Since these Tg mice exhibit phenotypic diversity even within independent inbred genetic backgrounds but likely due to environmental factors[72], they may well mimic heterogeneity in human tauopathies. When the origin of heterogeneity was more thoroughly examined by Daude *et al.* using cell biological, biochemical and biophysical methods (tau seeding assay, limited proteolysis, conformation-dependent immunoassay and electron microscopy), it became clear that these lower expresser TgTau<sup>P301L</sup> mice generates diverse distinct tau aggregate species[84], which may explain heterogenous neurological phenotypes and may model heterogeneity of tau species seen in human AD patients[191]. It is unknown whether

research groups studying rapid-onset models have looked for, or would be able to detect these types of heterogeneities in young animals.

Table 8: Tauopathy mouse models

Mouse line	Transgene	Overexpression level	Onset age (months)
rTg4510[192]	HuTau <sub>4R0N</sub> <sup>P301L</sup>	13x endogenous tau	4 months
PS19[193]	HuTau <sub>4R1N</sub> <sup>P301S</sup>	5x endogenous tau	6 months
Tau43 Tg[194]	HuTau <sub>4R0N</sub> <sup>P301S</sup>	2x endogenous tau	5 months
Tau44 Tg[195]	HuTau <sub>3R0N</sub> <sup>wt</sup>	5-15x endogenous tau	1 month
JNPL3(P301L)[196]	HuTau <sub>4R0N</sub> <sup>P301L</sup>	2x endogenous tau	4.5-6.5 months
TgTau(P301L)23027[190]	HuTau <sub>4R2N</sub> <sup>P301L</sup>	1.7x endogenous tau	12-13 months

#### 1.2.4: Involvement of *LMNA* in brain aging – to be or not to be?

Although *LMNA* has been greatly implicated in pathological and chronological aging, it is important to understand that the function of *LMNA* in brain biology is still controversial, especially in comparison to B-type lamins. In the family of nuclear lamins, lamin B and lamin C play crucial roles in brain physiology. Using *Lmnb1*- and *Lmnb2*-deficient mice, Coffinier *et al.* discovered that lamin B1 and B2 are essential for neuronal migration and brain development. Specifically, *Lmnb1* deficiency results in reduced numbers of neurons in the cerebral cortex, unlaminated hippocampus, lack of foliation of cerebellum and neuronal nuclear blebbing. *Lmnb2* deficiency leads to abnormal layering of neurons in cerebral cortex, lack of foliation of cerebellum and elongated nuclei in neurons[197]. Unsurprisingly, *Lmnb1/Lmnb2* double knock-out mice and their single knock-out counterparts all died immediately after birth[198], suggesting fetal functions of B-type lamins in brain development.

In contrast to B-type lamins, the function of lamin C in brain physiology is largely unexplored despite it being the predominant A-type lamin in the brain[199]. Since lamin C-knockout mice are healthy and free of pathology[200], the unique function of lamin C remains undiscovered and

only generic functions (e.g., structural support, chromatin regulation) have been proposed. In the context of aging, Toledo *et al.*, using lamin C-only expressing mice, revealed that lamin C encourages glucose tolerance through a  $\beta$  cell-adaptive transcriptional program during metabolic stresses[201], hence established a functional linkage between lamin C and aging.

Unlike lamin B and lamin C, the involvement of lamin A in brain has been a topic of debate, partially due to its low expression level in brain. Figure 5 offers a timeline to summarize recent major findings that support or do not support the importance of lamin A in brain physiology.

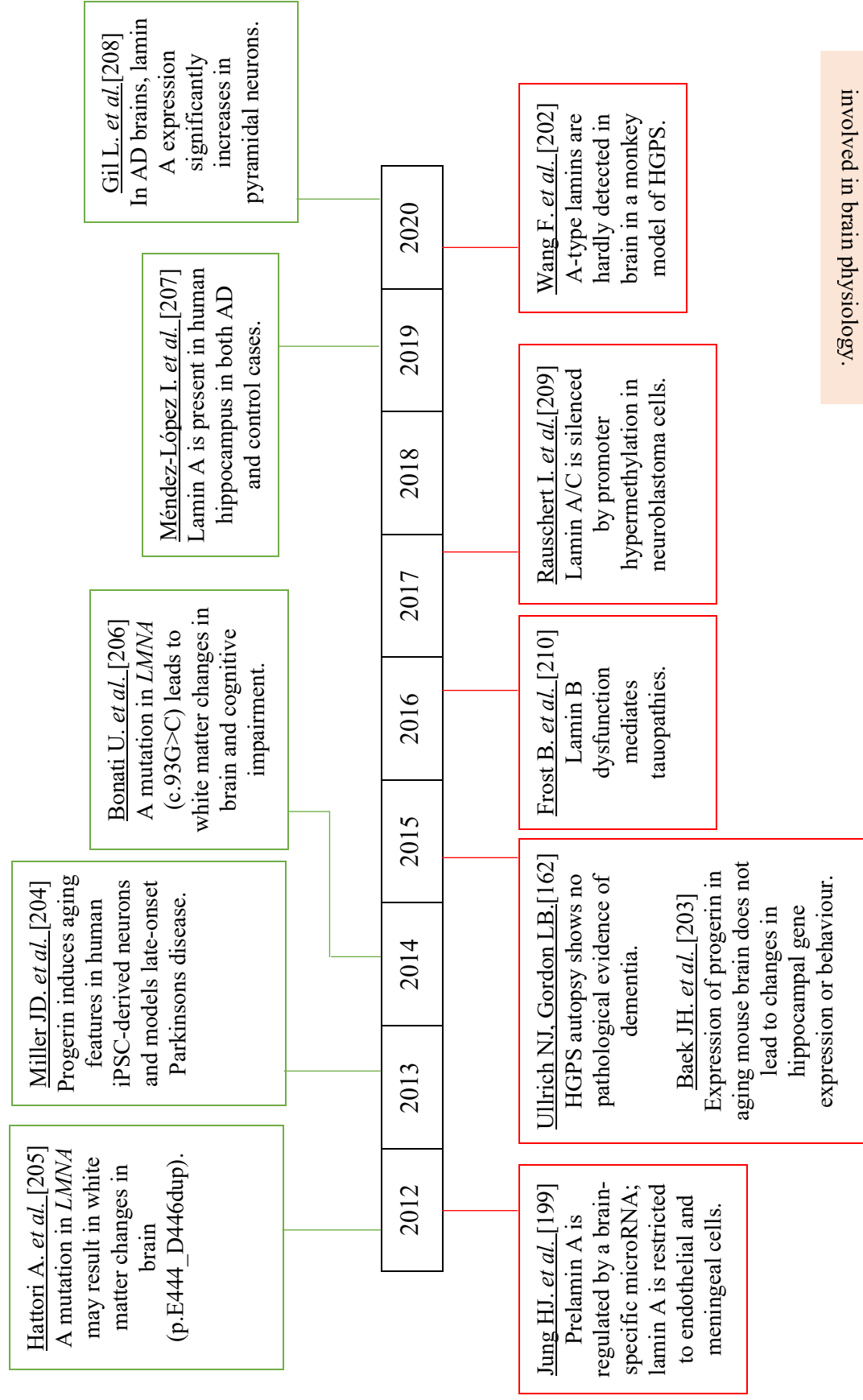
Using mouse models, Jung *et al.* demonstrated that lamin A is only marginally expressed in brain tissues (cerebellum and cortex) in comparison to other organs (liver, heart and kidney)[199]. As expected, low amount of lamin A was later confirmed in a monkey model of HGPS[202]. Jung *et al.* also unveiled a potential mechanism by which the brain reduces lamin A expression – a brain specific microRNA, namely miR-9, targets the 3' UTR of prelamin A transcript and leads to decreased lamin A expression level[199]. This discovery provides a mechanistic explanation for the absence of hippocampal and behavioral changes in transgenic mice expressing progerin[203].

Despite its low abundance in human brain, Miller *et al.* showed that progerin is a useful genetic tool for modeling late-onset Parkinson's disease in induced Pluripotent Stem Cells (iPSC)-derived neurons[204]. In the context of human neurological disorders, multiple novel LMNA mutations had been linked to white matter changes in brain, disturbed behavior and cognitive impairment[205][206], suggesting involvement of lamin A in nervous tissues. More recently, Mendez-Lopez *et al.* reported an elevated expression level of lamin A in hippocampus of AD patients[207] and Gil *et al.* showed that some pyramidal neurons have increased lamin A abundance across AD stages[208].

To understand the involvement and function of lamin A in neurobiology, we need to address the following questions in future research:

1. Why is miR-9 mediated lamin A downregulation important for normal brain function?  
What are possible consequences of when this regulation mechanism become disrupted?  
What are the consequences of lamin A upregulation in the context of Alzheimer' disease?
2. As the “culprit molecule” in HGPS, what effects will progerin have on neurophysiology if it were expressed in the brain?
3. Do A-type lamins and B-type lamins have any functions in common? What are their unique functions in brain physiology?

Laminin A (or progerin) may be involved in brain physiology.



Laminin A (or progerin) may not be involved in brain physiology.

Figure 5: Research timeline of the functions of nuclear lamins in brain physiology. There are evidence supporting the hypothesis that lamin A is involved in neuropathies (green); and there are evidence suggesting otherwise (red).

### **1.3: Hypothesis**

By introducing a HGPS progeric allele into an established cell culture model of tauopathies, we believe that we will be able to mimic an aged cellular environment and determine the effects of HGPS-accelerated aging in the context of tau misfolding. We hypothesize that LMNA-mediated pathological aging may accelerate the formation of intracellular tau aggregates.

## Chapter 2: Materials and Methods

### 2.1: Construction of LMNA ( $\Delta 50$ or WT) expression vectors

#### 2.1.1: Construction of mCherry-pBudCE vector

The DH10B strain of *E. coli* transformed with pBAD-mCherry bacterial vector was obtained as a generous gift from Dr. Robert Campbell's group. pBAD-mCherry plasmid was purified using the QIAprep Spin Miniprep Kit (Qiagen). The primers GH01 and GH02 were used to perform PCR reactions on pBAD-mCherry plasmid, introducing a *HindIII* restriction site and a *XbaI* restriction site at the 5' and 3' ends of the mCherry sequence, respectively. Products of the PCR reaction were electrophoresed on a 1% agarose gel and visualized with SYBR<sup>TM</sup> Safe DNA Gel Stain. Bands around 750 bp were extracted from the gel with the MinElute Gel Extraction Kit (Qiagen). Extracted PCR product was ligated into the pCR 2.1 TOPO vector and was transformed into DH5 $\alpha$  competent *E. coli* cells. Transformed *E. coli* were plated on LB plates containing ampicillin (50  $\mu\text{g/mL}$ ) and X-gal (20  $\text{mg/mL}$ ), cultured and the plasmid DNA was then prepared by the QIAprep Spin Miniprep Kit (Qiagen). Extracted mCherry-TOPO plasmid was test-digested with *EcoRI* restriction enzyme. DNA samples displaying a band near 750 bp after *EcoRI* digestion were sequenced. mCherry-TOPO plasmids with confirmed sequences and pBudCE4 were digested with *HindIII* and *XbaI* restriction enzymes. The bands around 750 bp in digested mCherry-TOPO samples and the bands around 5000 bp in digested pBudCE4 samples were extracted from the gel with the MinElute Gel Extraction Kit (Qiagen). Extracted *HindIII*-mCherry-*XbaI* was ligated into *HindIII*-pBudCE4-*XbaI* vector and was transformed into DH5 $\alpha$  competent *E. coli* cells. Transformed *E. coli* were plated on LB plates containing zeocin (25  $\mu\text{g/mL}$ ), cultured and the plasmid DNA was then prepared by the QIAprep Spin Miniprep Kit (Qiagen). Extracted mCherry-pBudCE4 plasmid was test-digested with *HindIII* and *XbaI*

restriction enzymes, and sequenced with primers pBud FOR, AL4 pBud Rev and T7. Confirmed mCherry-pBudCE4 plasmid was prepared at large scale with the EndoFree Plasmid Maxi Kit (Qiagen).

Table 9: Summary of primers used

Primer	Description	Sequence
GH01	<i>Hind</i> III-mCherry Forward	5'- <b>AAGCTT</b> GCCGCCACCATGGTGAGCAAGGGCGAGGAG-3'
GH02	<i>Xba</i> I-mCherry Reverse	5'- <b>TCTAGA</b> TTACTTGTACAGCTCGTCCATG-3'
GH03	<i>Not</i> I-Myc-LMNA Δ50 Forward	5'- <b>GCGGCCGC</b> CCTGCCCCGCGGGCAGCGCTGCCAACCTGC CGGCCATGGAACAAAACCTCATCTCAGAAGAGGATCTG GAGACCCCGTCCCAGCGGCG-3'
GH04	<i>Bgl</i> II-LMNA Δ50 Reverse	5'- <b>AGATCT</b> TTACATGATGCTGCAGTTCTGG-3'
GH05	LMNA Δ50 Sequencing Forward 1	5'-ACTGCTCTCAGTGAGAGGC-3'
GH06	LMNA Δ50 Sequencing Forward 2	5'-AGACCTGGAGGACTCACTGG-3'
GH07	LMNA Δ50 Sequencing Forward 3	5'-AGGTGGTGACGATCTGGGC-3'
GH08	pBud EF1α Sequencing Reverse	5'-AGAAGGCACAGTCGAGGCTGATC-3'
pBud FOR	pBud CMV Sequencing Forward	5'-ATTGACGCAAATGGGCGG-3'
AL4	pBud CMV Sequencing Reverse	5'-TATCTTATCATGTCTGAATTCCCGGGGATC-3'
T7	General pBud Sequencing	5'-TAATACGACTCACTATAGG-3'

**AAGCTT** = *Hind*III restriction site

**TCTAGA** = *Xba*I restriction site

**GCGGCCGC** = *Not*I restriction site

**AGATCT** = *Bgl*II restriction site

GAACAAAACCTCATCTCAGAAGAGGATCTG = c-Myc tag

### **2.1.2: Construction of mCherry-LMNA WT-pBudCE and mCherry-LMNA $\Delta$ 50-pBudCE vectors**

DH5 $\alpha$  strains of *E. coli* transformed with pEGFP-LMNA  $\Delta$ 50 and pBABE-puro-GFP-LMNA WT vectors were purchased from Addgene. pEGFP-LMNA  $\Delta$ 50 vector and pBABE-puro-GFP-LMNA WT vector were extracted and purified using the QIAprep Spin Miniprep Kit (Qiagen). The primers GH03 and GH04 were used to perform PCR reactions on pEGFP-LMNA  $\Delta$ 50 and pBABE-puro-GFP-LMNA WT plasmids, introducing a *NotI* restriction site and a c-Myc tag at the 5' end, and a *BglIII* restriction site at the 3' end of the LMNA sequence (WT or  $\Delta$ 50). Products of the PCR reaction were electrophoresed on a 1% agarose gel and visualized with SYBR<sup>TM</sup> Safe DNA Gel Stain. Bands around 1500 bp were extracted from the gel with the MinElute Gel Extraction Kit (Qiagen). Extracted PCR products were ligated into the PCR 2.1 TOPO vector and transformed into DH5 $\alpha$  competent *E. coli* cells. Transformed *E. coli* were plated on LB plates containing ampicillin (50  $\mu$ g/mL) and X-gal (20 mg/mL), cultured and the plasmid DNA was then prepared by the QIAprep Spin Miniprep Kit (Qiagen). Extracted c-Myc-LMNA  $\Delta$ 50-TOPO and c-Myc-LMNA WT-TOPO plasmids were test-digested with *EcoRI* restriction enzyme. DNA samples displaying a band near 2000 bp after *EcoRI* digestion were sequenced. c-Myc-LMNA  $\Delta$ 50-TOPO plasmid and c-Myc-LMNA WT-TOPO plasmid with confirmed sequence and purified pBudCE4 were digested with *NotI* and *BglIII* restriction enzymes. The bands around 2000 bp in digested c-Myc-LMNA  $\Delta$ 50-TOPO and c-Myc-LMNA WT-TOPO samples and the bands around 5000 bp in digested mCherry-pBudCE4 samples were extracted from the gel with the MinElute Gel Extraction Kit (Qiagen). Extracted *NotI*-c-Myc-LMNA  $\Delta$ 50-*BglIII* and *NotI*-c-Myc-LMNA WT-*BglIII* were ligated into *NotI*-mCherry-pBudCE4-*BglIII* vector and were transformed into DH5 $\alpha$  competent *E. coli* cells. Transformed *E. coli* were

plated on LB plates containing zeocin (25 µg/mL), cultured and the plasmid DNA was then prepared by the QIAprep Spin Miniprep Kit (Qiagen). Extracted c-Myc-LMNA Δ50-mCherry-pBudCE4 and c-Myc-LMNA WT-mCherry-pBudCE4 plasmids were test-digested with *NotI* and *BglII* restriction enzymes, and sequenced with primers GH05, GH06, GH07 and GH08. Confirmed plasmids were prepared at large scale with the EndoFree Plasmid Maxi Kit (Qiagen).

## **2.2: Expression of LMNA Δ50, LMNA WT and mCherry in HEK293 tauRD-YFP cells**

### **2.2.1: Cell culture**

Human Embryonic Kidney 293 cells stably expressing tauRD-YFP fusion protein (HEK293 tauRD-YFP)[74][83] were grown in complete media: Delbecco's Modified Eagle Medium (Gibco™) containing 10% Fetal Bovine Serum (FBS, Gibco™) and 1% penicillin/streptomycin (Gibco™). Cells were cultured and passaged at 37 °C, 5% CO<sub>2</sub>, in a humidified incubator. 1x sterilized PBS was used for washing cells prior to trypsinization with 0.25% trypsin-EDTA (Gibco™).

### **2.2.2: Transient transfection of LMNA (Δ50, WT and empty vector) in HEK293 tauRD-YFP cells**

HEK293 tauRD-YFP cells were passed with complete media until reaching 70% confluency. 5 µg of each construct was mixed gently in a solution of Lipofectamine 3000 (Invitrogen) and OPTI-MEM media (Gibco™) at room temperature and incubated for 20 minutes prior to transfection. The DNA-lipofectamine mixture was then added to HEK293 tauRD-YFP cells and incubated at 37 °C with 5% CO<sub>2</sub> for 4 hours in a humidified incubator. OPTI-MEM was then removed and replaced with DMEM containing 10% FBS. Cells were rinsed with 1x PBS and lysed with RIPA buffer containing 50 mM Tris-HCl, 150 mM NaCl, 0.5% sodium deoxycholate,

1% NP-40, 0.1% SDS, 1 mM EDTA and cOmplete Mini EDTA-free protease inhibitor cocktail (Roche) in 48 hours, centrifuged at 12,000 rpm at 4 °C for 5 min and the supernatant was collected for further analyses.

### **2.2.3: Generation of stable progeric cell lines (HEK293 tauRD-YFP LMNA $\Delta$ 50 and ES1 LMNA $\Delta$ 50)**

HEK293 tauRD-YFP and ES1 cells transiently transfected with c-Myc-LMNA  $\Delta$ 50-mCherry-pBudCE4 plasmid were cultured with DMEM (10% FBS) in the presence of 20  $\mu$ g/mL zeocin (Invitrogen). Individual colonies were selected with cloning discs, expanded to reach confluency and designated as “polyclonal cell lines”. Single cell clones were established from these “polyclonal cell lines” by limiting dilutions.

### **2.2.4: Confocal microscopy**

18 mm coverslips were coated with poly-D-lysine (5  $\mu$ g/mL) and laminin (0.5  $\mu$ g/mL) for 1 hour and rinsed with 1x PBS. Cells were grown for 24 hours on double-coated coverslips in 12-well plates. Media was removed and cells were rinsed with 1x PBS for 5 minutes. PBS was removed and placed with 4% paraformaldehyde (PFA) for 15 minutes. Cells were washed with 1x PBS once and permeabilized with 0.25% Triton-X for 15 minutes. Triton-X was removed prior to a 5-minute rinse with 1x PBS. Coverslips were blocked with 1% BSA-PBST for 30 minutes and incubated with primary antibodies (diluted in 1% BSA-PBST) at 4 °C overnight. Primary antibodies were aspirated and replaced with 1x PBS for a 3x 5 min rinse. To visualize the target molecules, cells were then incubated with Alexa Fluor 647-conjugated secondary antibody (Invitrogen, 1:400 diluted in 1% BSA-PBST) at 22 °C, in dark, for 1 hour. Cells were washed with 1x PBS before mounted with Prolong Gold Antifade Mountant with DAPI (Invitrogen), sealed with nail polish and stored at 4 °C before confocal analysis. For confocal microscopy, a

Zeiss LSM 700 laser scanning confocal microscope was coupled to a X-Cite mini+ compact LED illumination system.

Table 10: Primary antibodies used in confocal microscopy.

Primary antibody	Supplier	Catalogue number	Dilution factor
Anti- $\gamma$ H2AX	Novus Biologicals	NB100-384	1:500
Anti-c-Myc	GenScript	A00704	1:500

### 2.2.5: Analyses of protein expression with capillary western immunoassay

The capillary western immunoassay (Wes) is a gel-free and blot-free platform that allows for automated protein separation, detection and quantitation[211]. Cell lysates (refer to 2.2.1 for complete details) were normalized to 2  $\mu\text{g}/\mu\text{L}$  with the bicinchoninic acid (BCA) assay. 0.1X Sample Diluent (ProteinSimple) was used to dilute cell lysate samples. Fluorescent 5X Master Mix (ProteinSimple) was used to denature protein samples at 95 °C for 5 minutes. Primary antibodies were diluted with Antibody Diluent 2 (ProteinSimple). Secondary antibodies (anti-mouse or anti-rabbit, ProteinSimple) were used undiluted according to the instructions from ProteinSimple. 12-230 kDa separation modules were used for all analyses.

Table 11: Primary antibodies used in capillary western immunoassay

Primary antibody	Supplier	Catalogue number	Dilution factor
Anti-tau (RD4)	MilliporeSigma	05-804	1:250
Anti- $\beta$ -tubulin	Novus Biologicals	NB600-936	1:400
Anti-c-Myc	GenScript	A00704	1:500
Anti-GAPDH	Novus Biologicals	NB300-221	1:25

### 2.3: Tau protein transduction in HEK293 tauRD-YFP cells

On day 1, 96-well plates (Greiner Bio-One) were double-coated with poly-D-lysine (5  $\mu\text{g}/\text{mL}$ ) and laminin (0.5  $\mu\text{g}/\text{mL}$ ) for 1 hour and rinsed with 1x PBS. HEK293 tauRD-YFP cells were seeded in a 96-well plate with a density of 5,000 cells/well before incubated at 37 °C with 5%

CO<sub>2</sub> for 24 hours in a humidified incubator. On day 2, tau extracts (brain-derived or cell lysate), Lipofectamine 3000 (Invitrogen) and OPTI-MEM media (Gibco™) were mixed at room temperature and incubated for 20 minutes prior to transduction. The working ratios between tau extracts and Lipofectamine 3000 were experimentally determined by titration. Complete media was aspirated and replaced with 100 μL of warm OPTI-MEM media per well. 10 μL of pre-mixed liposome-tau complex was added to each well. After a 4-hour incubation, 100 μL of warm complete media was added to each well and cells were incubated at 37 °C with 5% CO<sub>2</sub> for 24 hours in a humidified incubator. On day 3, cells were incubated at 30 °C with 5% CO<sub>2</sub> for 24 hours in a humidified incubator to prevent the cells from over-proliferating. On day 4, cell culture media was aspirated, and cells were fixed with 4% PFA for 15 minutes. 100 μL of mounting medium (70% glycerol, 500 μg/mL p-phenylenediamine and 10 μg/mL Hoechst stain) was then added to each well. Cells were imaged with DAPI and GFP channels at 10x resolution and quantified by the MetaXpress XLS High Content Analysis System (Molecular Devices).

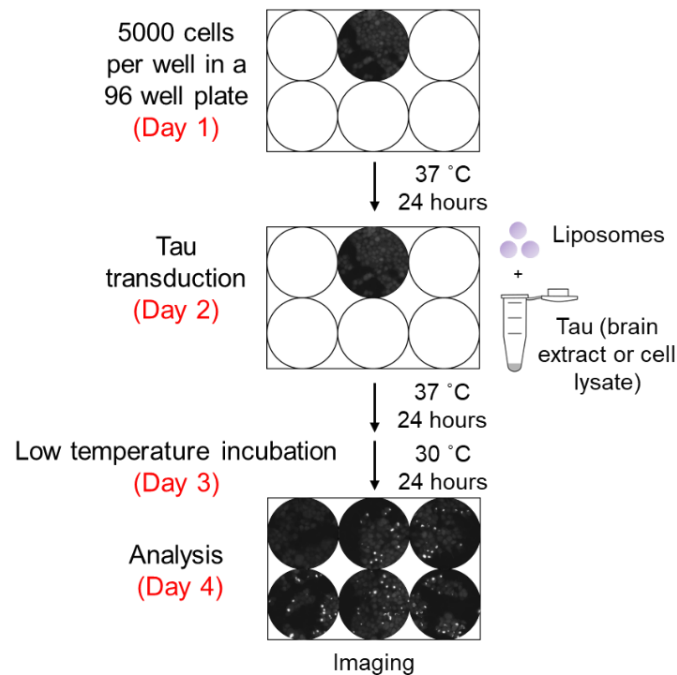


Figure 6: Schematic illustrating methods used to transduce brain-derived or cell lysate-derived tau extracts into HEK293 tauRD-YFP cells (progeric or non-progeric).

#### **2.4: Limited proteolysis**

ES1 cell pellets were frozen at -80 °C for storage. On the day of cell lysis, cell pellets were thawed on ice and lysed in 1x PBS with 0.05% Triton X-100 and a cOmplete mini protease inhibitor tablet (Roche). Sequential 5-minute centrifugations were performed at 500x g and 1,000x g to clarify the cell lysate at room temperature. A BCA assay with BSA standard curve was then performed and protein concentrations were normalized to 1.7 µg/µL with addition of lysis buffer. To sediment tau aggregates, clarified cell lysate was centrifuged at 48,000 rpm at 4 °C for 1 hour (rotor: TLA-55). Pellet was re-suspended with lysis buffer to a protein concentration of 0.7 µg/µL.

Lyophilized pronase E (Roche) was re-suspended in 1x PBS to a final concentration of 1 µg/µL and aliquots were stored at -80 °C. Lyophilized thermolysin (Sigma) was re-suspended in storage buffer (50% glycerol, 0.1 M sodium acetate, 0.5 mM calcium acetate, pH 7.5) to a final concentration of 1 µg/µL and aliquots were stored at -20 °C.

Titration experiments were performed to determine the working ratios between proteases and cell lysate. The cell lysates (1.7 µg/µL) or sedimented tau (0.7 µg/µL) were enzymatically digested with different concentrations of pronase E at 37 °C for 1 hour, or thermolysin at 65 °C for 30 minutes. Pronase E was quenched with protease inhibitors (Roche) and SDS-PAGE loading buffer; thermolysin was quenched with 0.5 M EDTA and SDS-PAGE loading buffer. The undigested tau fragments in each enzymatic reaction were determined by western blot analysis using anti-tau mAb ET3 or anti-tau mAb RD4.

## **2.5: Mass spectrometric analysis of cell lysate**

To explore progerin-induced changes in cellular proteome, six different cell lines (HEK293 tauRD-YFP reporter cell line, ES1 cell line, progeric HEK293 tauRD-YFP reporter clone 2 and clone 3-1, progeric ES1 clone 7 and clone 9) were analyzed by liquid chromatography with tandem mass spectrometry (LC-MS/MS) with a label-free quantitation approach (Fig. 7). Each cell line was analyzed in triplicates (approximately 5 million cells per sample). Cells were lysed in a urea-based lysis buffer (8 M urea, 100 mM Tris pH 8.5, 5 mM EDTA, 1 mM AEBSF, 1 mM PMSF and 4 mM IAM). Total protein concentration of each sample was determined by the BCA assay. 100 µg of cell lysate was digested with the automated digestion protocol on a Kingfisher Duo Prime instrument before being analyzed by the Orbitrap Fusion™ Lumos™ Tribrid™ Mass Spectrometer in three biological replicates. Acquired data was subject to label-free quantitation with ProteomeDiscoverer to generate a list of significantly up/downregulated proteins compared to the control cell lines ( $p \leq 0.05$  and  $\geq 2$ -fold change).

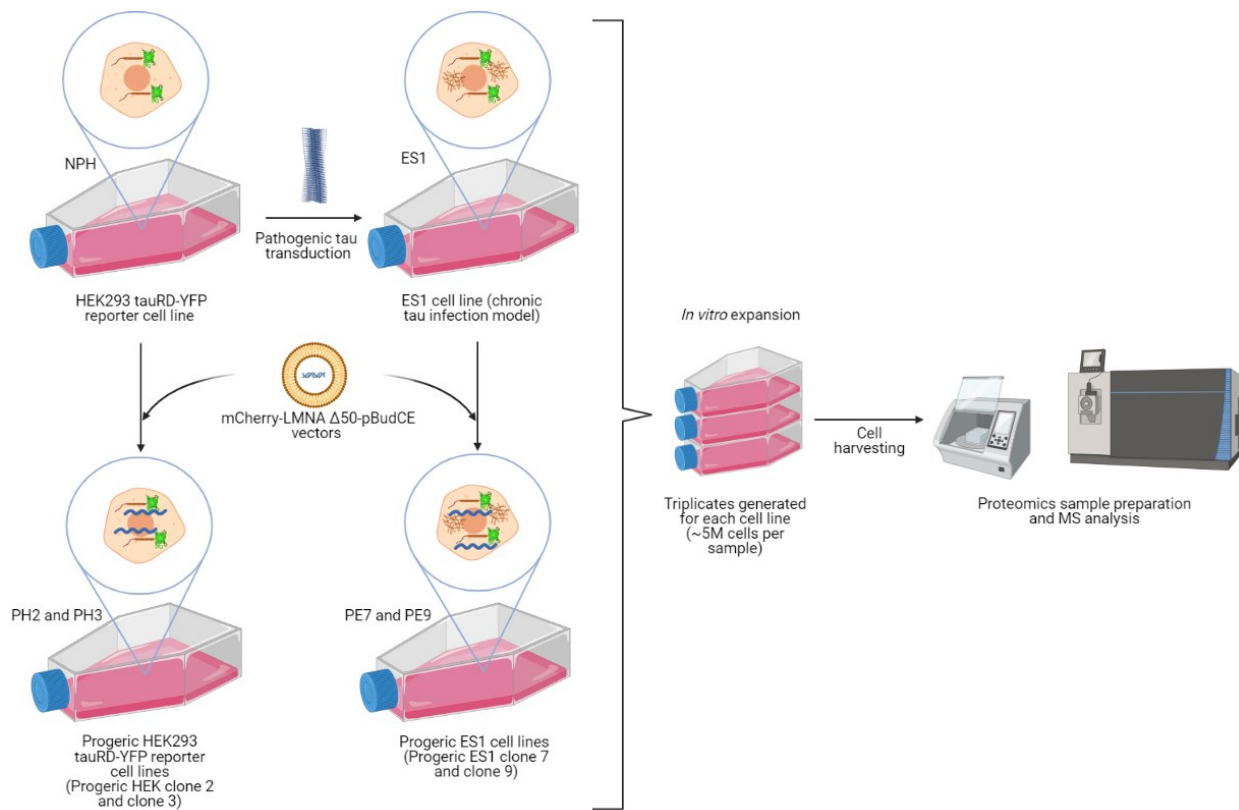


Figure 7: Schematic illustration of mass spectrometric analysis of different cell lines with/without progerin expression.

## 2.6: Statistical analysis

The number of independent experiments or biological replicates of compared groups were at least  $n=3$  for each observation. Statistical analysis for the quantitative data including capillary western immunoassay and tau transduction efficiency analysis and mass spectrometric analysis was performed using unpaired, two-tailed student t-test. The Benjamini-Hochberg Procedure was used to reduce the false discovery rate in mass spectrometry-based proteomics.

## Chapter 3: Results

### 3.1: Construction of mCherry-pBudCE, mCherry-LMNA WT-pBudCE and mCherry-LMNA $\Delta$ 50-pBudCE vectors

The mCherry red fluorescent protein expression cassette was molecularly cloned from a bacterial expression vector pBAD-mCherry by PCR (Fig. 8A). To obtain a sufficient amount of the mCherry PCR product with the appropriate restriction enzyme sites, it was first cloned into a PCR 2.1 TOPO vector (Fig. 8B), replicated in *E. coli* and test-digested (Fig. 8C). The mCherry cassette was then inserted into the multiple cloning site (under the control of the CMV promoter) of the pBudCE4.1 vector (Fig. 8D) in order to create a mammalian plasmid that will allow for post-transfection cell screening by fluorescence.

The wildtype and mutant LMNA genes (LMNA WT and LMNA  $\Delta$ 50) were molecularly cloned from bacterial vectors by PCR (Fig. 9A). Cloning into the pCR2.1-TOPO vector was conducted to amplify available DNA (Fig. 8B and 9B). LMNA WT and LMNA  $\Delta$ 50 genes were then inserted into the multiple cloning site adjacent to the EF1 $\alpha$  promoter of the previously constructed mCherry-pBudCE4 vector (Fig. 9C). Since promoters may have significant influence on transgene expression magnitude and stability, it needs to be carefully considered when designing expression vectors. Teschendorf *et al.* reported that when recombinant adeno-associated virus was used to transduce the colon carcinoma cell, the EF1 $\alpha$  promoter associates with higher and homogenous transgene expression level compared to the CMV promoter[212]. Wang *et al.* showed a similar observation for episomal vectors – in comparison with the CMV promoter, the EF1 $\alpha$  promoter maintains a higher and more stable transgene expression level in episomal vector-transfected Chinese hamster ovary K1 cells[213]. In our experiments, we chose

the CMV promoter for transfection marker (mCherry) and the EF1 $\alpha$  promoter for our target gene (LMNA) to ensure stable and homogenous expression of LMNA (Fig. 8D).

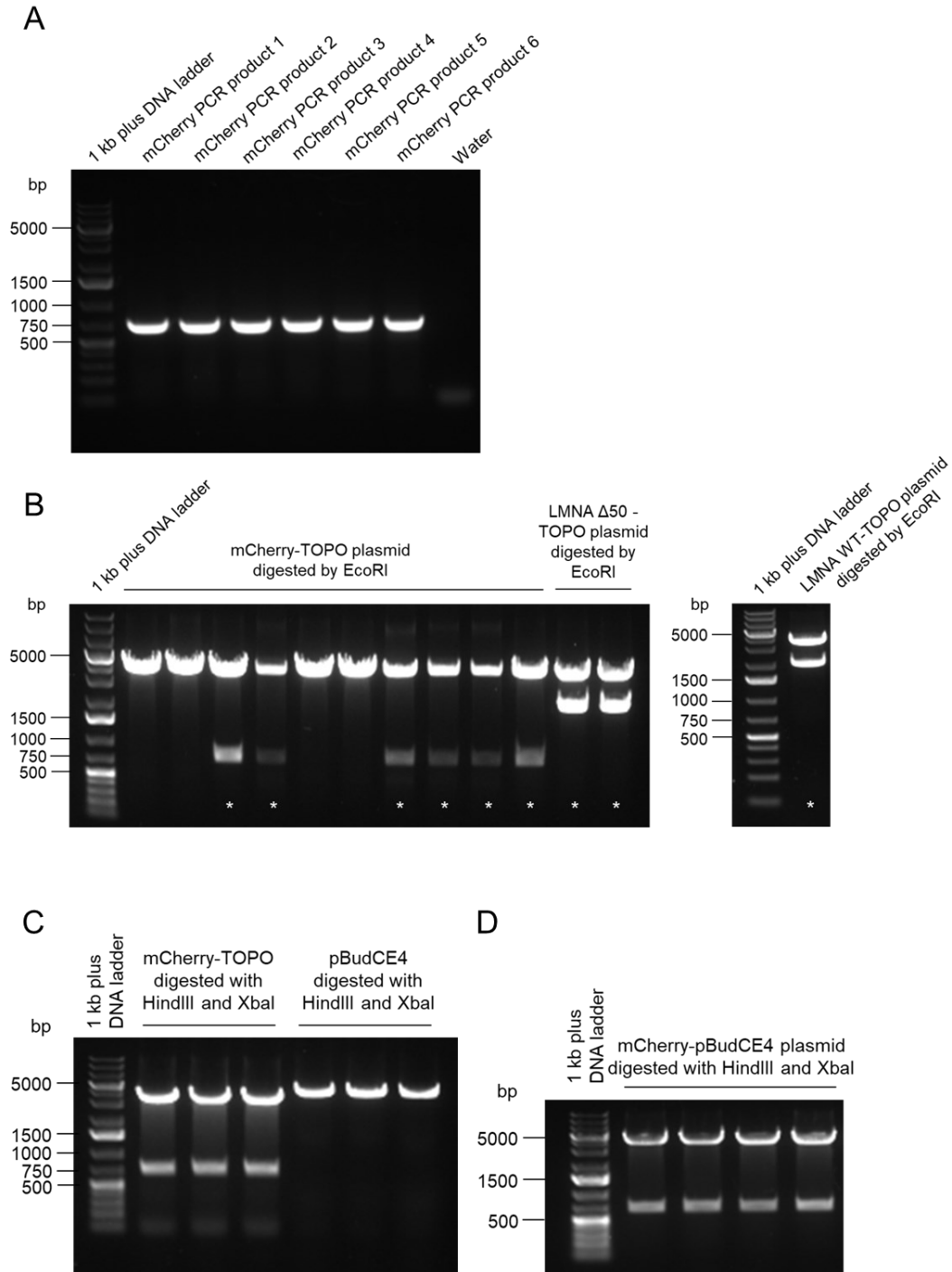


Figure 8: Construction of mCherry-pBudCE4 vector with molecular cloning. (A). PCR amplification of mCherry sequence from pBAD-mCherry bacterial vector. Agarose gel

electrophoresis was conducted to visualize the PCR products of six independently performed reactions (with GH01 and GH02 primers). PCR product bands (~750 bp) match expected size (732 bp). (B). *EcoRI* digestion of mCherry-TOPO plasmids and LMNA  $\Delta$ 50-TOPO plasmids. Samples with asterisk were sequenced. (C). *HindIII* and *XbaI* digestion of mCherry-TOPO and pBudCE4 plasmids. (D). *HindIII* and *XbaI* digestion of mCherry-pBudCE4 plasmid. All four samples were sequenced.

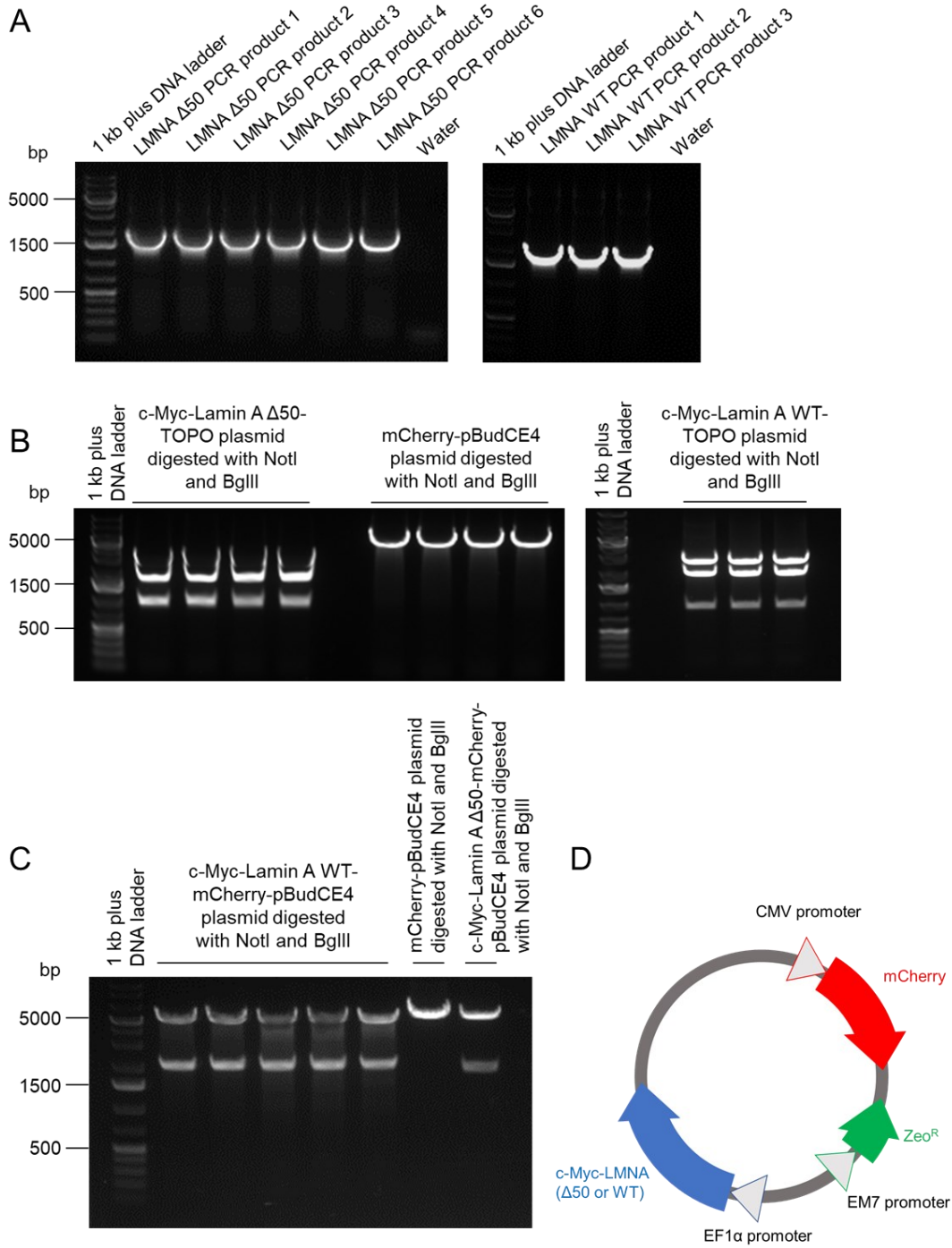


Figure 9: Construction of mCherry-LMNA WT-pBudCE and mCherry-LMNA  $\Delta$ 50-pBudCE4 vectors. (A). PCR amplification of LMNA  $\Delta$ 50 and LMNA WT sequences from purchased bacterial vectors. Agarose gel electrophoresis was conducted to visualize the PCR products (reactions performed with GH03 and GH04 primers). PCR product bands (~1500 bp) match expected size. (B). c-Myc-LMNA  $\Delta$ 50-TOPO, c-Myc-LMNA WT-TOPO and mCherry-pBudCE4 plasmids double-digested with *NotI* and *BglII*. (C). c-Myc-LMNA  $\Delta$ 50-mCherry-pBudCE4, c-Myc-LMNA WT-mCherry-pBudCE4 and mCherry-pBudCE4 plasmids double-digested with *NotI* and *BglII*. (D). Schematic diagram of constructed c-Myc-LMNA-mCherry-pBudCE4 plasmid. mCherry is under the control of the CMV promoter, c-Myc-LMNA is under the control of the EF1 $\alpha$  promoter and the zeocin resistance gene (*Zeo*<sup>R</sup>) is under the control of the EM7 promoter.

### 3.2: Transient transfection of LMNA-WT or - $\Delta$ 50 in HEK293 tauRD-YFP reporter cell line

To examine the effect of progerin in a tau aggregation reporter model, we transiently transfected an HEK293 tauRD-YFP reporter cell line[74] with c-Myc tagged progerin. The transfection efficiency was estimated by the percentage of mCherry-positive cells 24 hours after transfection. For LMNA-WT, LMNA- $\Delta$ 50 and empty vector, the transfection efficiency was nearly identical (35%) (Fig. 10A). Cell lysates were analyzed with the Wes capillary immunoassay on 1 day, 3 days and 6 days post-transfection. Significant amount of progerin is produced 1 day after transfection, yet it decreases by approximately 90% at day 3 and drops below the detection limit at day 6 (Fig. 10B). The expression level of tau in cells that were transfected with plasmids or mock transfected (i.e., exposed to liposomes without DNA cargo) also fluctuates significantly after transfection (Fig. 10C). This is a possible result of the cellular stress responses induced by liposome-based DNA carriers as lipofection may cause unintended changes in global gene expression[214]. These observations suggest the necessity of generating cell lines that stably express progerin.

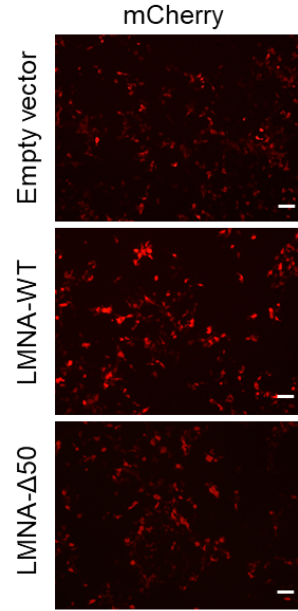
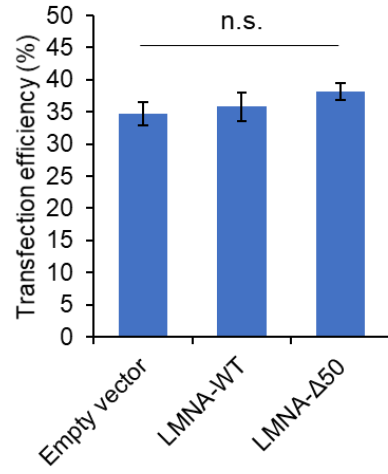
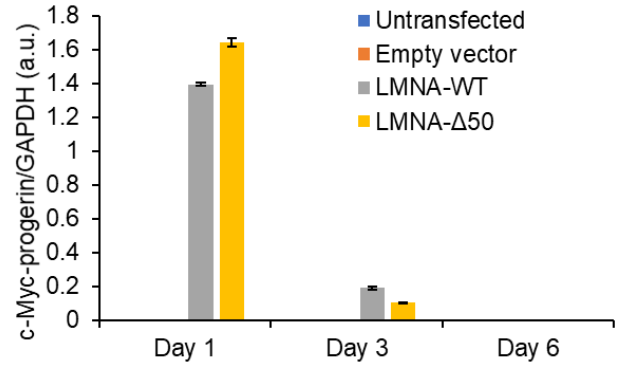
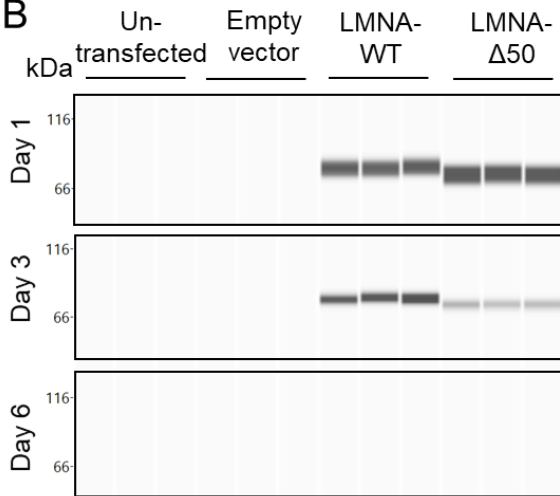
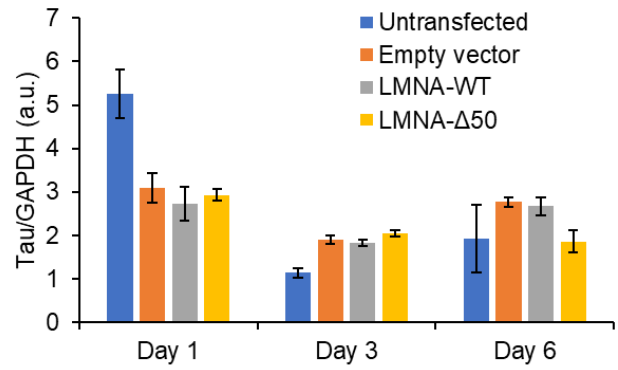
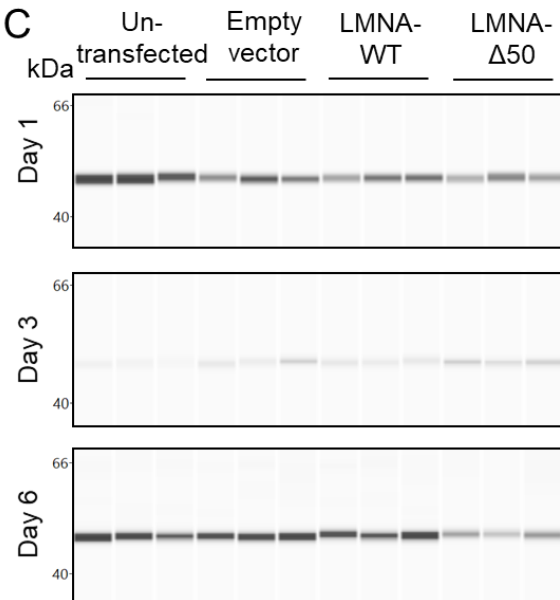
**A****B****C**

Figure 10: Transient transfection of progerin in HEK293 tauRD-YFP cells. (A). The transient transfection efficiency is similar in LMNA-WT, LMNA- $\Delta$ 50 and empty vector transfected cells. Scale bar = 100  $\mu$ m. (B). Expression of the LMNA transgene in transiently transfected cells declines below the detection limit in six days. (C). Tau expression level fluctuates in 1-6 days after transient transfection.

### 3.3: Generation of stable progeric HEK293 tauRD-YFP reporter cell lines

To study the influence of long-term expression of progerin, we selected four independent monoclonal cell lines (clones 2, 3, 11 and 12) after transient transfection. These progeric HEK293 tauRD-YFP reporter cell lines are named PH2, PH3, PH11 and PH12. Amongst these cell lines, all of them express c-Myc tagged progerin yet PH2 and PH3 clearly have the highest expression level (Fig. 11A). Due to their high progerin expression levels, PH2 and PH3 cell lines were subjected to more detailed characterization and used for most subsequent experiments.

Nuclear localization of c-Myc tagged progerin was confirmed with immunocytochemistry (Fig. 11B). Nuclear dysmorphology (blebbing and invagination) were observed in a small population of cells. It is worth mentioning that although folded/blebbed nuclear morphology appears to be a common phenotype for fibroblasts donated by aged individuals[204] and the HGPS fibroblasts[215], distorted nuclear envelop should not be considered an inevitable consequence of progerin expression, especially in the context of transfected cells[142]. In addition, a diffused signal from the tau-YFP fusion protein suggests that progerin expression does not result in spontaneous formation of tau aggregates. Trypan blue exclusion test of cell viability shows similar viability for progeric (PH2 and PH3) and non-progeric HEK293 TauRD-YFP clones (NPH, Fig. 11C). As expected, expression of progerin resulted in an increased level of double-stranded DNA damage, indicated by phosphorylated histone  $\gamma$ H2AX (Fig. 11D). It should be taken with caution that zeocin (used for selecting stable clones) may at least partially contribute to DNA damage as the zeocin-resistance gene may not offer full protection[216]. However, it is

also noteworthy that the concentration of zeocin used to select progeric clones (20  $\mu\text{g}/\text{mL}$ ) is significantly lower than the concentration used in Trastoy's experiments (100-800  $\mu\text{g}/\text{mL}$ ), which reduces the likelihood of zeocin-induced DNA damage in the context of our experiments. Progeric HEK clones 2, 3, 11 and 12 were also analyzed with the Wes capillary immunoassay for tau expression. All four stable progeric HEK clones showed significantly increased levels of immunoreactive tau (Fig. 12).

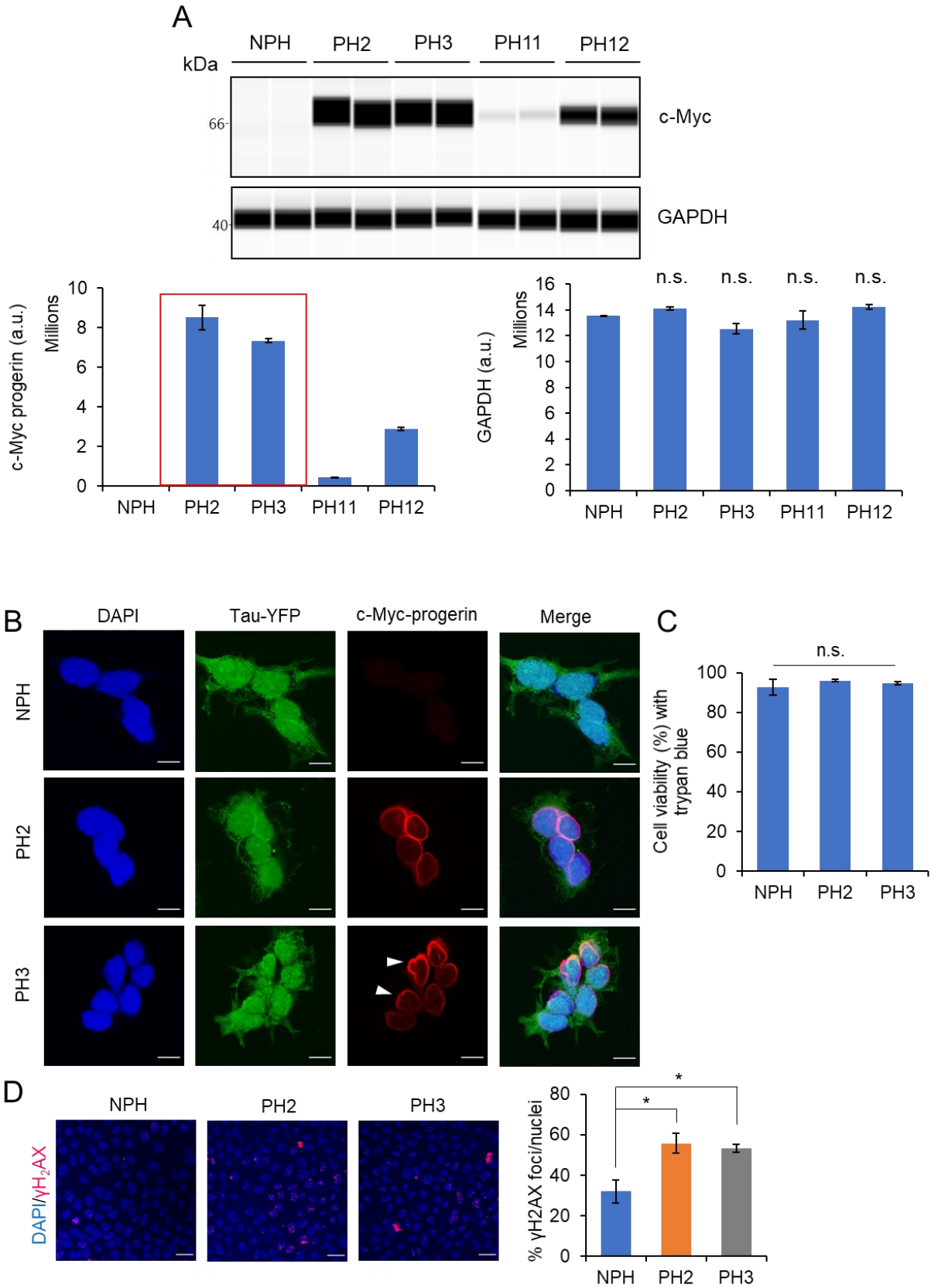


Figure 11: Characterization of progeric HEK293 tauRD-YFP clones. (A). Capillary western immunoassay analysis displays assimilation of the LMNA- $\Delta$ 50 transgene construct in four independent HEK progeric stable clones. Lane view of the immunoassay is shown and the average signal intensity for c-Myc-progerin and GAPDH are represented in the bar graphs. c-Myc tagged progerin was probed by anti-c-Myc antibody. Clone 2 and clone 3 (red box) were used for further experiments. (B). Immunocytochemistry analysis displays nuclear membrane-bound c-Myc-progerin. c-Myc tagged progerin was probed by anti-c-Myc antibody (primary) and Alexa Flour 647 (secondary). Scale bar = 10  $\mu$ m. (C). Trypan blue exclusion test of cell viability shows similar viability for progeric and non-progeric HEK293 TauRD-YFP clones. (D). Immunocytochemistry analysis of phosphorylated histone  $\gamma$ H2AX (DNA damage marker) in progeric and non-progeric clones. Scale bar = 20  $\mu$ m. Percentage of  $\gamma$ H2AX-positive nuclei is represented in the bar graph.

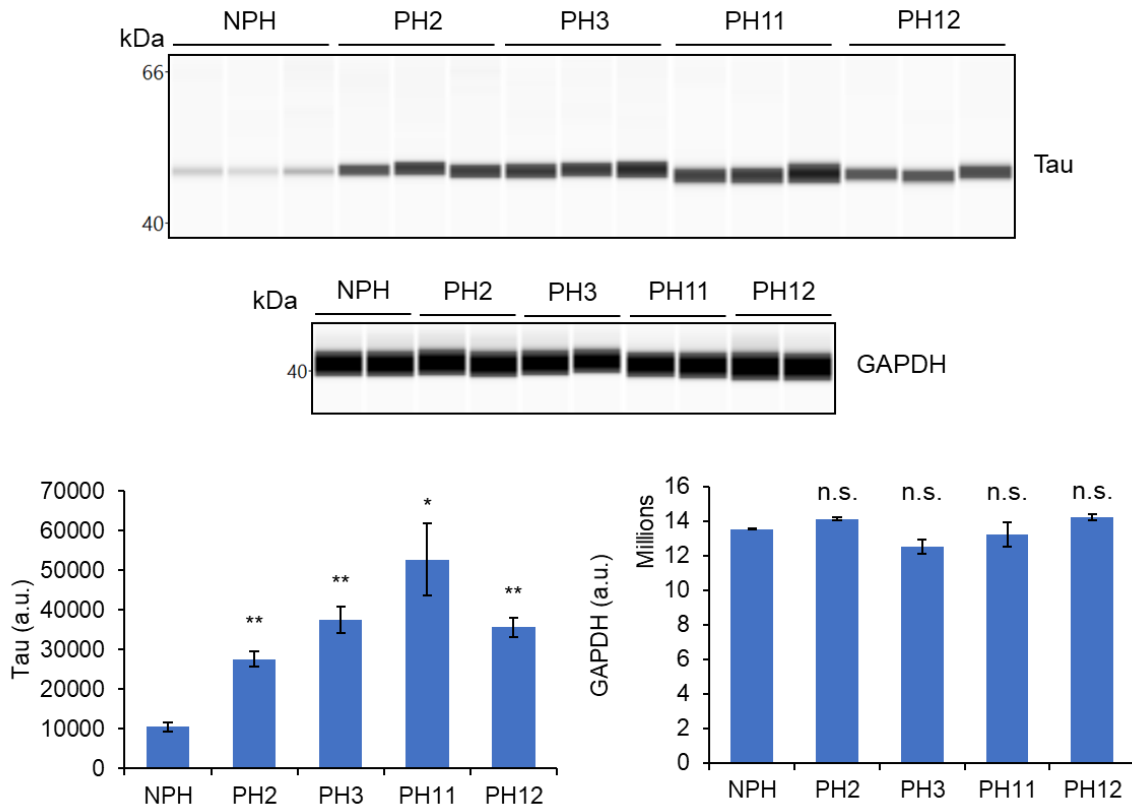


Figure 12: Wes capillary immunoassay of tau in progeric and non-progeric HEK cell lines. The total expression level of tau is elevated in all four HEK293 tauRD-YFP reporter cell lines that stably express progerin (PH2, PH3, PH11 and PH12). n=3 (technical replicates). Error bar = standard error of means. \*p<0.05, \*\*p<0.01, \*\*\*p<0.001.

### 3.4: Seeding of progeric HEK293 tauRD-YFP reporter cell lines

To analyze the effect of progerin on tau aggregation, we seeded cells (progeric and parental control) with transgenic mouse brain- or cell lysate-derived tau extracts. Evaluation of the frequency of cells with tauRD-YFP inclusions (seeding efficiency) was done with the high content screening fluorescence microscopy (Fig. 13). The working ratios between tau extract and lipofectamine 3000 were determined with titration experiments on NPH cells (Fig. 14). The results revealed that progeric HEK cells (PH2 and PH3) consistently associate with higher seeding efficiency (Fig. 15) compared to the control non-progeric HEK parental cells (NPH), regardless of the origin of tau seeds. Increased seeding efficiency may be explained by progerin-induced increase in tau expression level. It was previously reported that when our Tg mouse brain extracts were used to seed tau reporter cells, four tau inclusion morphologies were observed – amorphous, nuclear envelope, speckles and threads; and the proportion of each morphology varies between brain extracts[84]. Since tau is mechanistically intertwined with lamin B dysfunction and impaired nucleoskeleton in *Drosophila*[210], these data led us to hypothesize that nuclear envelope bound tau (TI-2) may interact with progerin differently, and progerin may sensitize the tau reporter cells for seeding events to a greater extent when tau extract preferentially results in TI-2 morphology. To test this possibility, progerin-induced fold increase of seeding efficiency was plotted against the proportion of TI-2 morphology (Fig. 16). When the Pearson correlation test was used to assess the correlation the percentage of nuclear envelope bound tau and the increase of seeding efficiency, it trended towards statistical significance ( $p = 0.052$  for PH2 cells and  $p = 0.049$  for PH3 cells), suggesting a possibility that progerin and tau on the nuclear membrane may have synergistic interactions.

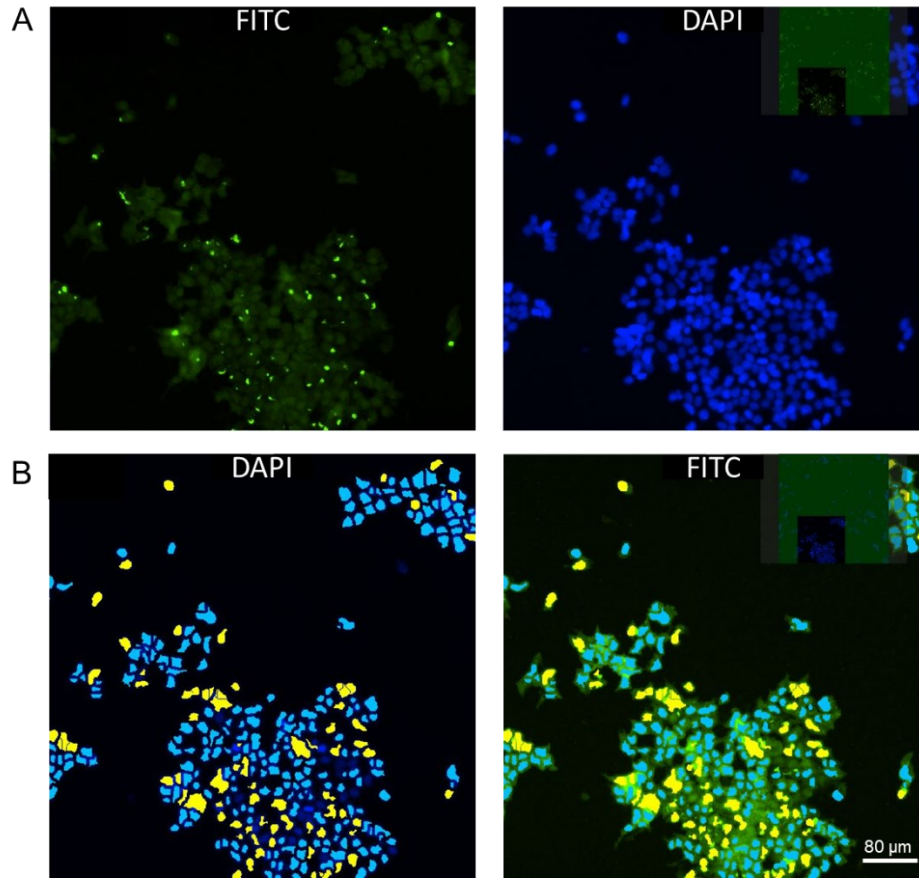


Figure 13: Tau seeding efficiency was quantified with the high content screening fluorescence microscopy. (A). Two channels were used for cell imaging (FITC for tauRD-YFP and DAPI for nuclear staining). (B). Cell images were subject to automated analyses to quantify tau inclusion positive cells (yellow, pseudocolor) and tau inclusion negative cells (blue, pseudocolor).

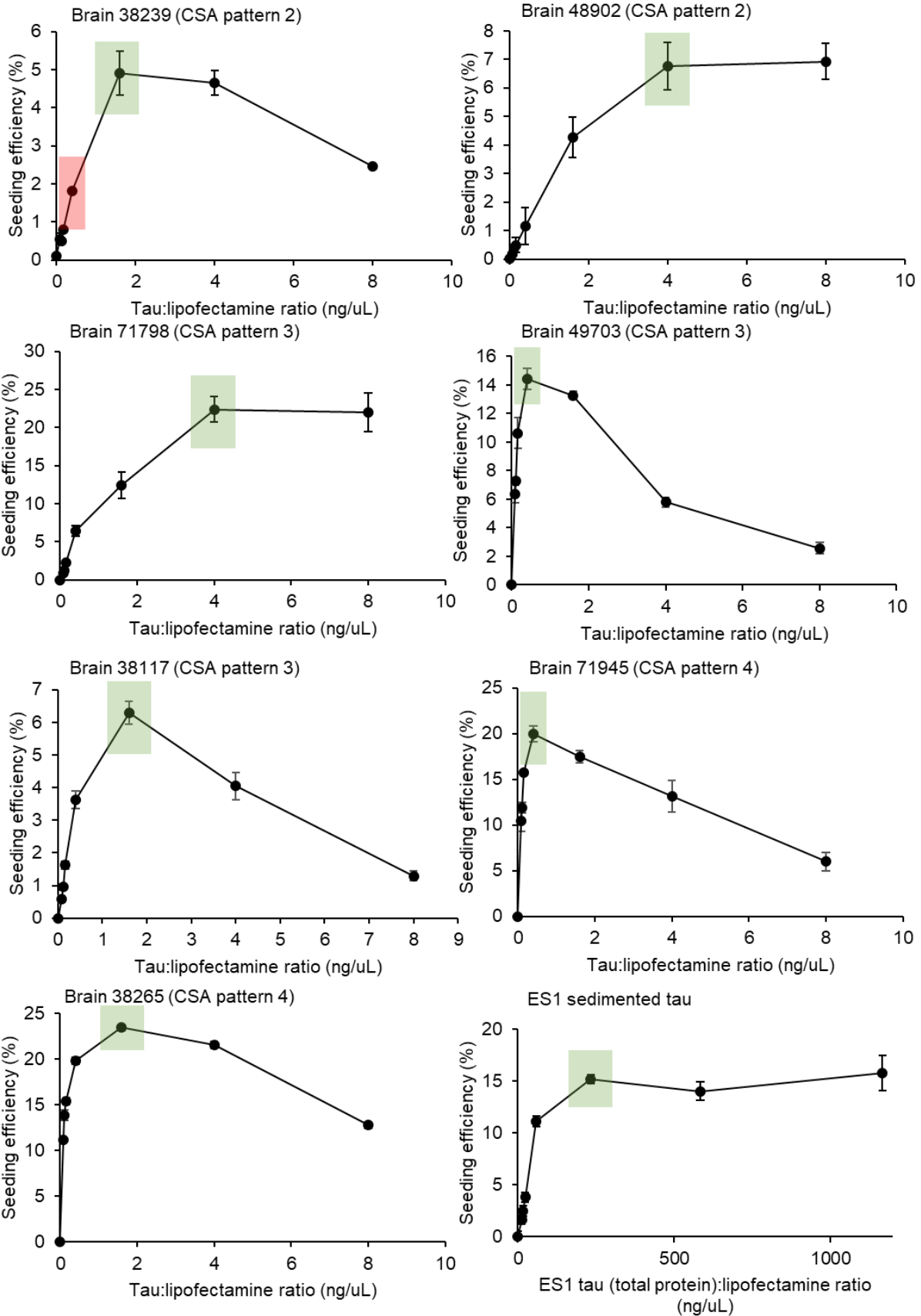


Figure 14: Tau-liposome titration assay used to determine the working ratio between tau extracts (from Tg mouse brain extracts or ES1 cell lysate) and lipofectamine 3000. Tg mouse brain extracts have been previously characterized by the conformational stability assay (CSA patterns 2-4) by the Safar Lab in Cleveland, Ohio, USA. Optimized tau:liposome ratios (highlighted in green boxes) are determined by 1) the highest seeding efficiency, or 2) the least amount of tau extract with reasonable high seeding efficiency. The red box represents a suboptimal ratio for brain 38239. n = 3 (biological replicates). Error bar = standard error of mean.

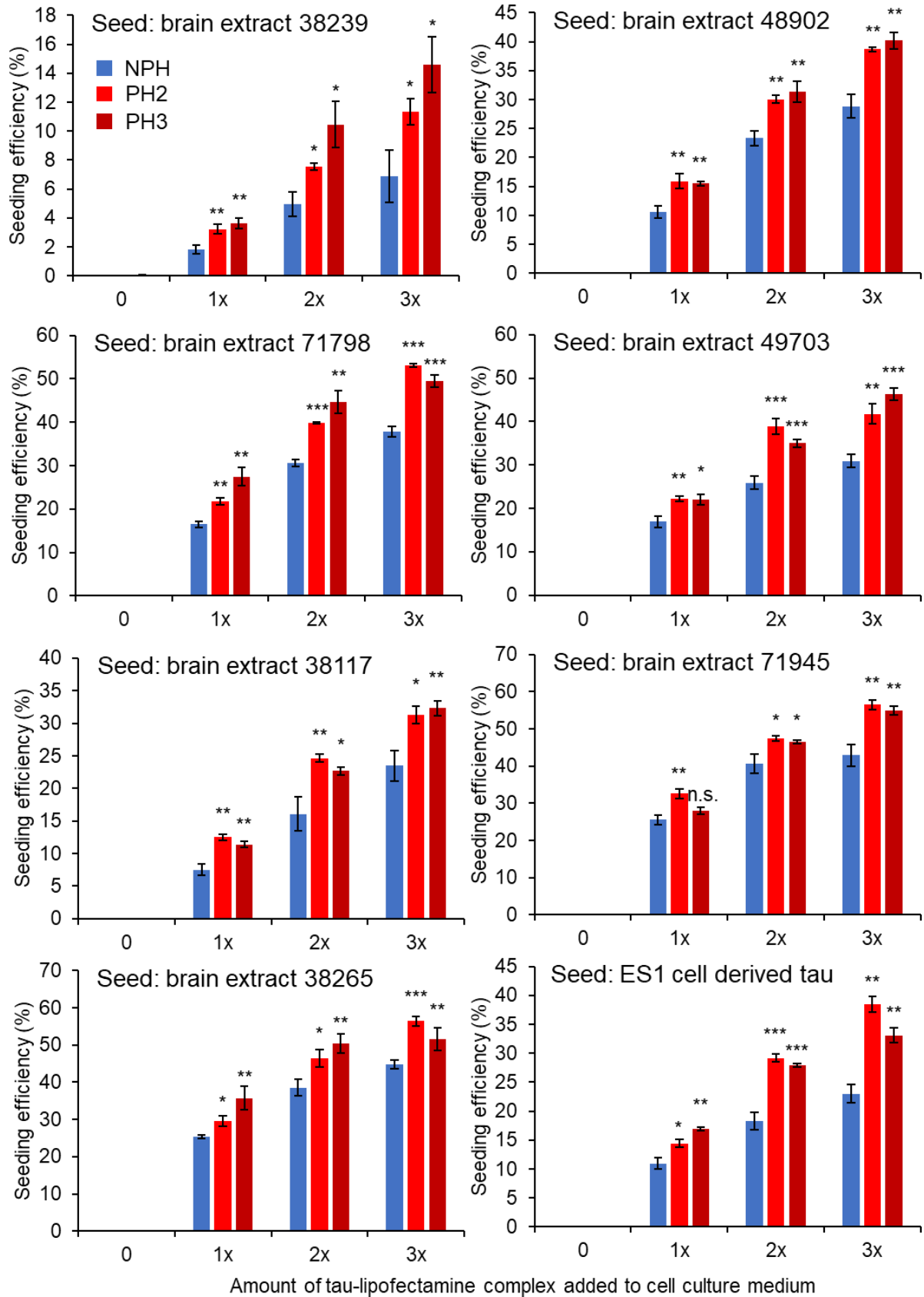


Figure 15: Quantitation of tau seeding efficiency. HEK293 cells (progeric and non-progeric) were transduced with preparations that contain pathogenic tau, including Tg mouse brain extracts and ES1 cell lysate. The seeding efficiency of two progeric clones (light red = PH2 and dark red = PH3) is compared to that of non-progeric cells (blue = NPH). n = 3 (biological replicates). Error bar = standard error of mean. \*p<0.05, \*\*p<0.01, \*\*\*p<0.001.

	Brain #	Fold increase in seeding efficiency (progeric HEK clone 2)	Fold increase in seeding efficiency (progeric HEK clone 3)	% Nuclear envelope tau
CSA2	38239	1.80	2.01	72.2
	48902	1.50	1.46	70.6
CSA3	38117	1.66	1.52	16.0
	71798	1.32	1.11	11.5
	49703	1.32	1.29	20.7
CSA4	38265	1.18	1.43	1.0
	71945	1.28	1.09	2.8

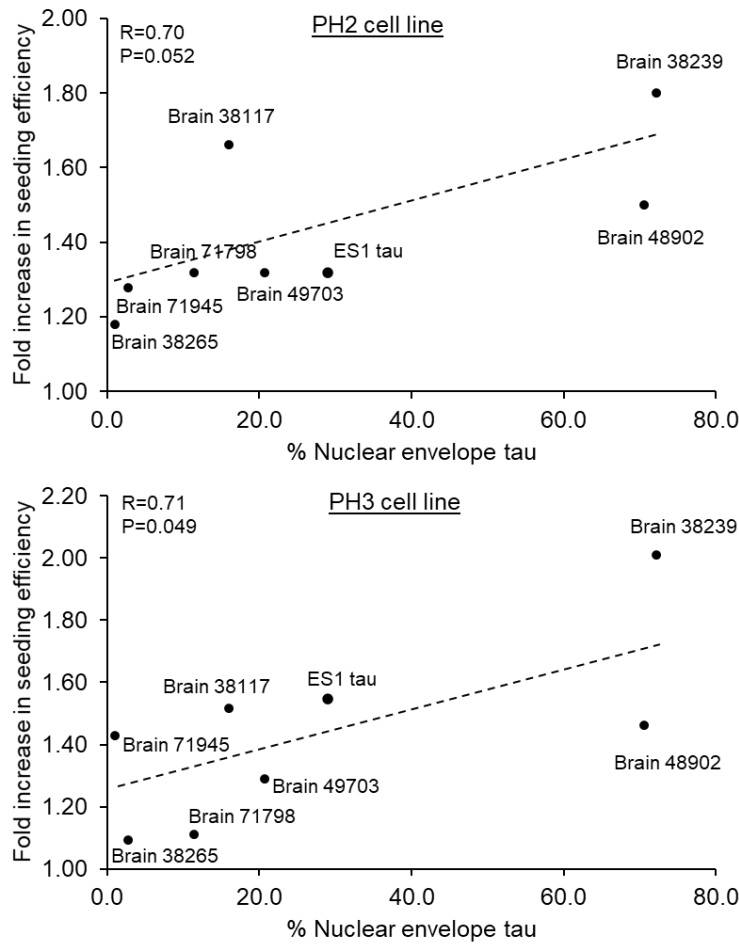


Figure 16: Correlation analysis for progerin-induced increase of seeding efficiency and the proportion of seeded cells that display nuclear envelope-bound tau. Seven Tg mouse brain

extracts were used in the analysis (two brains with CSA pattern 2, three brains with CSA pattern 3 and two brains with CSA pattern 4). Pearson correlation test was performed.

### **3.5: Generation and characterization of polyclonal progeric ES1 cell lines**

The ES1 cell line (NPE) was derived from the HEK293 tauRD-YFP reporter cell line by transducing the cells with preparations of pathogenic tau[217]. This cell line offers a unique cell culture model to investigate cellular responses when they are chronically burdened with tau aggregates. To study the effect of progerin in the presence of cellular tau inclusions, two polyclonal progeric ES1 cell lines (PE7 and PE9) were established. In contrast to HEK cells, progerin expression resulted in a 4-fold reduction of tau expression (Fig. 17A). In addition, progerin led to extensive dysmorphology of the nuclear membrane in ES1 cells – nearly all progeric ES1 cells exhibited nuclear blebbing (Fig. 17B). It suggests that tau aggregates and progerin act synergistically to aggravate nuclear membrane integrity. To determine if progerin expression associates with changes in the chemical signature of tau aggregates, we used proteinase K, thermolysin and pronase E to probe the fragments of tau after limited proteolytic digestion. The working concentrations of these three proteases were determined with titration experiments (Fig. 18). As all clones (ES1 and ES1-progerin) had the same size of protease-resistance core (Fig. 17C), it suggests that progerin does not alter the conformation of tau aggregates in HEK tau reporter cells.

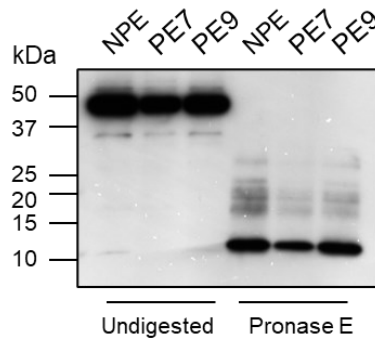
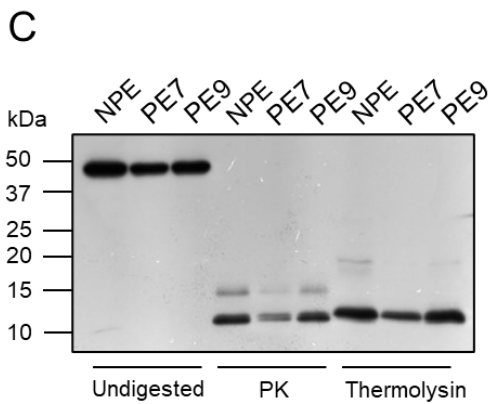
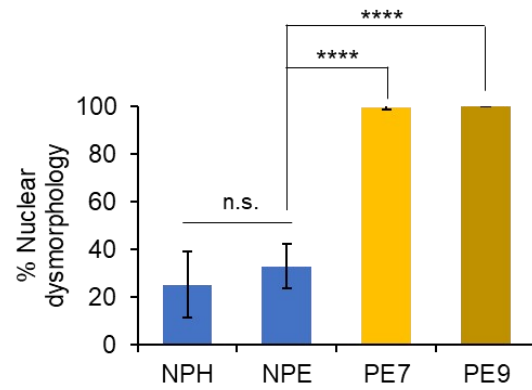
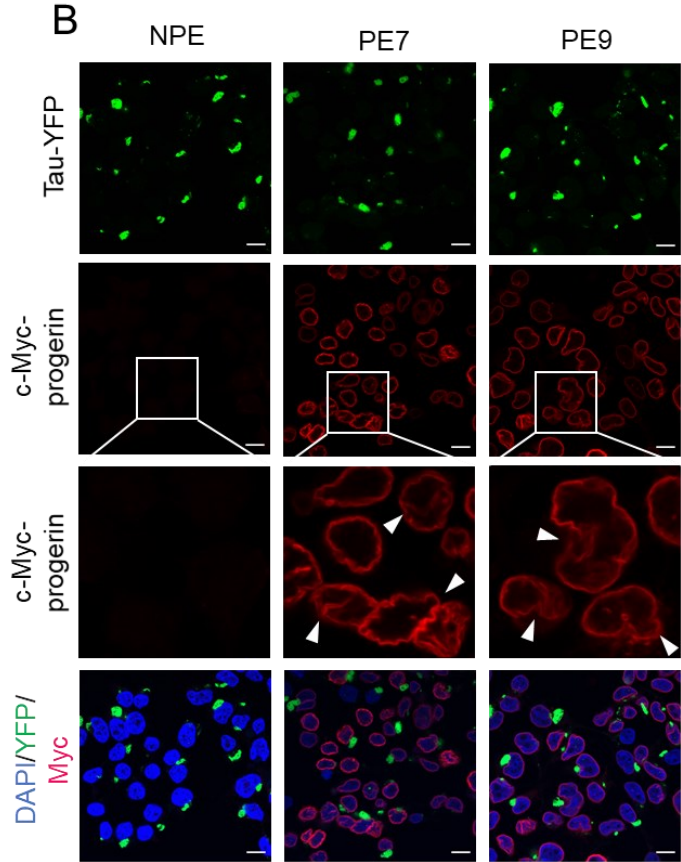
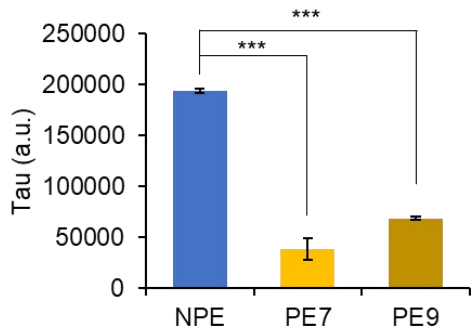
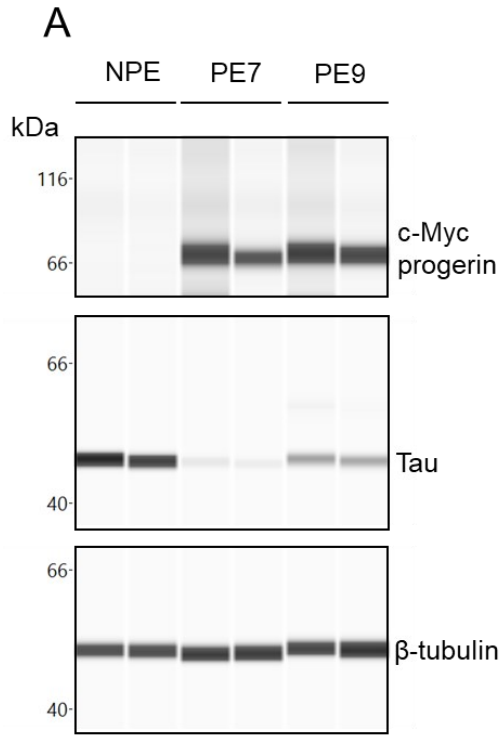


Figure 17: Characterization of polyclonal progeric ES1 cell lines. (A). Wes immunoassay shows that the total tau abundance is reduced in ES1 cells lines that stably express progerin (PE7 and PH9). (B). Immunocytochemistry displays extensive nuclear blebbing in progeric ES1 clones. Scale bar = 10  $\mu\text{m}$ . n = 5 (number of images) , \*p<0.0001. (C). Limited proteolysis (proteinase K, thermolysin and pronase E) demonstrates no conformational changes of tau aggregates in ES1 cells that stably express progerin.

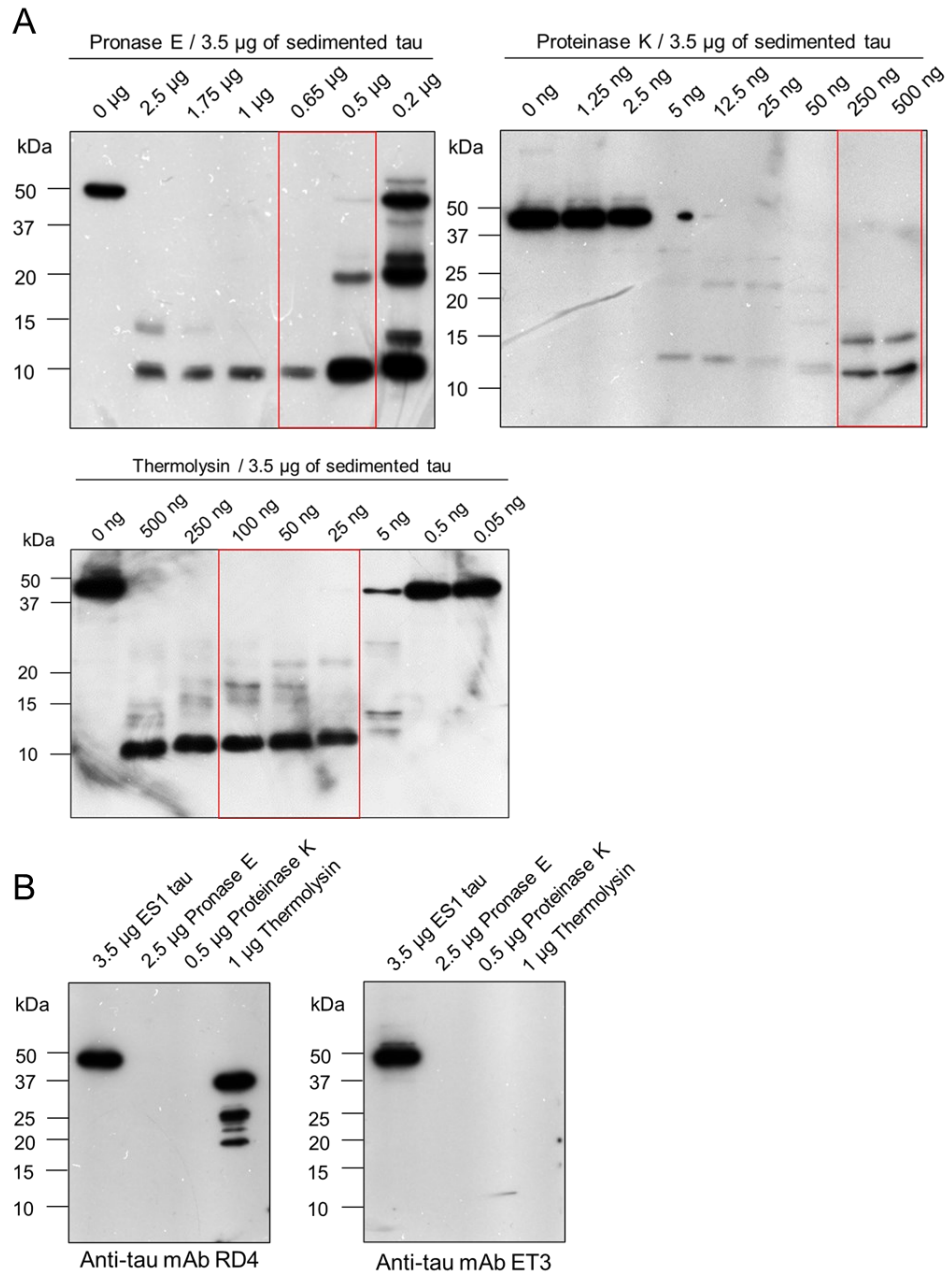


Figure 18: Limited proteolysis of ES1 cell-derived sedimented tau. (A). Working ratios between proteases (pronase E, proteinase K and thermolysin) and ES1 cell-derived sedimented tau were determined by titration. The ranges of working ratios are highlighted in red. (B). Spiking

experiment to demonstrate lack of cross-reactivity between ET3 antibodies and proteases (pronase E, proteinase K and thermolysin) used in limited proteolysis experiments. ES1 tau designates undigested cell lysate extracted from ES1 cells.

### 3.6: Mass spectrometric analysis of progeric and non-progeric tau reporter cell lines

#### 3.6.1: Progeric and non-progeric HEK cell lines

To understand the effect of progerin expression on the global proteomic changes in the HEK293 tauRD-YFP reporter cell line, the cell lysates of two independent progeric HEK clones (PH2 and PH3) and the non-progeric HEK parental cell line (NPH) were analyzed with mass spectrometry. Proteins from all samples were quantified in a label-free approach after being normalized against the total ion intensity (Fig. 19). In the following description of results, the protein IDs related to tryptic peptides that are devoid of post-translational modifications.

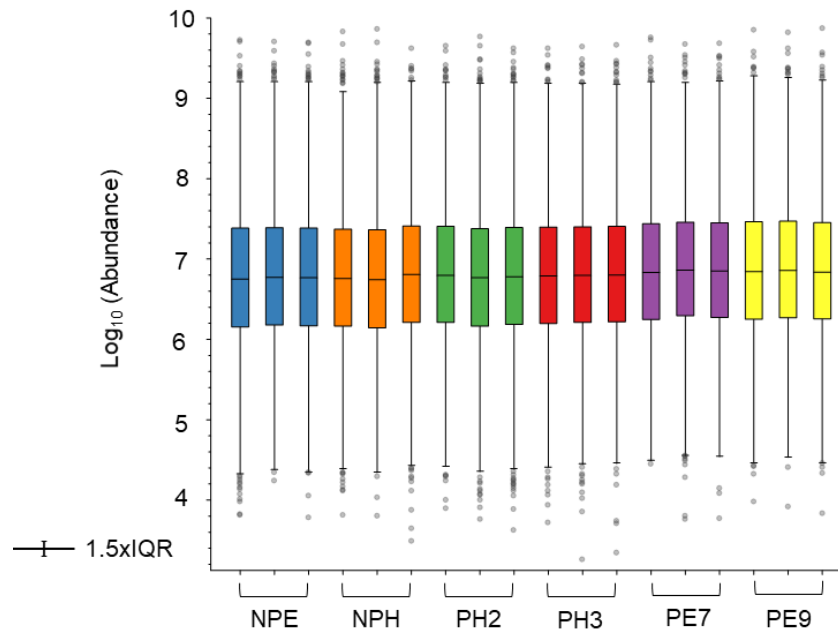


Figure 19: Adjustment of total protein abundance for cell lysate samples analyzed by mass spectrometry. Three biological replicates are analyzed for each cell line. Protein abundance is normalized according to total ion intensity by ProteomeDiscoverer before statistical comparison. Identified peptides are represented by grey dots. IQR=interquartile range. Image courtesy of Erik Gomez.

Using the criteria of >2-fold change and  $p < 0.05$ , when compared with the NPH cells, PH2 and PH3 cells had 54 and 62 significantly downregulated proteins, respectively, 24 of which were shared between PH2 and PH3. The PH2 and PH3 cells also had 58 and 96 upregulated proteins, respectively, with 37 being shared between these two independent progeric clones (Fig. 20A). In the list of shared modulated proteins, seven of them are endosomal and 25 are nuclear (Fig. 20B). These protein candidates were further investigated, by String (Search Tool for the Retrieval of Interacting Genes/Proteins) 11.0 analysis, to reveal the nuclear and endosomal pathways altered in progeric HEK293 tauRD-YFP cells. It is worth mentioning that in their comparison to NPH cells, besides lamin A (in effect, an internal control), the PH2 and PH3 cells share great similarity in fold change of protein abundance (Fig. 20C). Among the 25 nuclear proteins that changed significantly in abundance with progerin expression, four are involved in mRNA splicing (Fig. 21A), a biological process that is implicated in cellular senescence, organismal aging and age-related chronic diseases[218]. Using qRT-PCR, Holly *et al.* showed that the transcripts of core mRNA splicing factors and splicing regulators change in abundance with aging; the expression level of transformer-2 protein homolog beta (TRA2B), a splicing factor, increases significantly with age in fibroblasts[219]. However, opposing observations were made in brain and heart tissues where *TRA2B* was downregulated[220]. Tissue and cell type differences may at least partially explain the discrepancies between these observations. In our experiments, the protein abundance of TRA2B is also significantly higher in PH2 and PH3 cells (Fig. 21A), suggesting TRA2B is likely involved in both chronological and HGPS aging. Thioredoxin-like protein 4A (TXNL4A) is another spliceosomal protein that changes in abundance with age. Our proteomics dataset shows that TXNL4A is upregulated in both PH2 and PH3 cells. As Tollervey *et al.* demonstrated with microarray analyses that the transcript level

of TXNL4A decreases with age[221], the discrepancy between physiological aging and progerin-induced pathological aging in our cell model needs to be carefully examined. Among other mRNA splicing-related proteins, U2SURP was significantly upregulated and CSTF was significantly downregulated. To the best of our knowledge, progerin-induced or age-dependent modulations of these two genes have not been reported and may therefore need to be explored further.

While preliminary String analysis presented a complicated pattern about mRNA splicing pathways in the context of aging, it suggested two other biological processes that may be critically relevant to dementia-related cellular changes in PH2 and PH3 cells – protein deubiquitination (Fig. 21B) and endosomal trafficking (Fig. 20C). *CYLD* encodes for a ubiquitin carboxyl-terminal hydrolase. A mutant form of the *CYLD* protein (*CYLD*<sub>M719V</sub>) has increased activity and its overexpression in the HEK293 cells impairs autophagosome fusion to lysosomes[222], an important pathway in the pathogenesis of frontotemporal lobar degeneration[223]. Hamano *et al.* also demonstrated that autophagic-lysosomal disturbance delays tau clearance and promotes tau aggregation human neuroblastoma cells[224]. Thus, upregulation of *CYLD*, as shown in our experiments (Fig. 21B), may partially explain increased tau seeding efficiency in PH2 and PH3 cells. *OTULIN* (ubiquitin thioesterase), along with other components of the linear ubiquitination assembly complex, had been reported to be a genetic risk factor of AD and related dementia in a genome-wide association study[225]. Additionally, Van Well *et al.* demonstrated that *OTULIN* silencing decreased the percentage of transfected SH-SY5Y cells with TDP-43 inclusions (protein aggregates in frontotemporal lobar degeneration and amyotrophic lateral sclerosis) and Htt-Q97 inclusions (protein aggregates in Huntington's disease)[226], highlighting the importance of *OTULIN* in proteinopathies. As our data showed

that OTULIN is significantly upregulated in PH2 and PH3 cells (Fig. 21B), it may be a potential contributor to the increase in tau seeding efficiency noted for our progeric cell lines.

Dysregulation of the endosomal/lysosomal trafficking system has attracted great interest in the context of late-onset Alzheimer's disease[227][228]. Our proteomics analysis showed seven significantly modulated endosomal proteins; four of them are involved in early endosomes and three are involved in late endosomes (Fig. 21C). Two protein candidates in late endosomes, the Niemann-Pick type C1 (NPC1) protein and the cation-dependent mannose-6-phosphate receptor (M6PR), draw our special attention. *NPC1* encodes for a lysosomal membrane-bound cholesterol transporter that regulates the egress of cholesterol and fatty acids from the lysosomal/endosomal system[229]. Generally caused by mutations of the NPC1 protein[230], Niemann-Pick disease type C1 is a rare autosomal recessive lipid storage disease associated with a variety of phenotypic abnormalities, including neonatal jaundice and enlarged liver/spleen[231].

Progressive neurodegenerative changes encompass neurofibrillary tangles in many parts of the brain[232][233]. Interestingly, compared with non-demented individuals, the hippocampus and frontal cortex of Alzheimer's patients demonstrate an elevated level of NPC1 (both mRNA and protein levels)[234]. In our experiments, the progeric HEK293 tauRD-YFP reporter cell lines, PH2 and PH3, both showed a drastic increase in NPC1 protein abundance (Fig. 21C), suggesting a possible connection between progerin-mediated pathological aging and tau-related pathological alterations. M6PR is another significantly upregulated endosomal protein in our dataset. Using a mouse fibroblast-like cell line that stably overexpressed M6PR, Mathews *et al.* demonstrated that overexpression of M6PR (a receptor in the lysosomal/endosomal system) led to increased production of A $\beta$ 40 and A $\beta$ 42, possibly related to M6PR-induced redistribution of lysosomal hydrolases that are responsible for APP processing[235]. Interestingly, a more recent study,

using on a mouse model of AD, suggested that M6PR negatively regulates APP processing by the amyloidogenic pathway and A $\beta$  production[236]. Despite contradicting observations in the role of M6PR in A $\beta$  secretion in the literature, analyses of post-mortem human AD brains showed that the neuronal expression level of M6PR increases in sporadic AD when compared with non-demented control[237], supporting the involvement of M6PR in human AD. A dramatic increase in M6PR abundance in the progeric HEK cellular proteome compared with the non-progeric control (Fig. 21C) suggests a possible linkage between HGPS aging and molecular changes observed in AD.

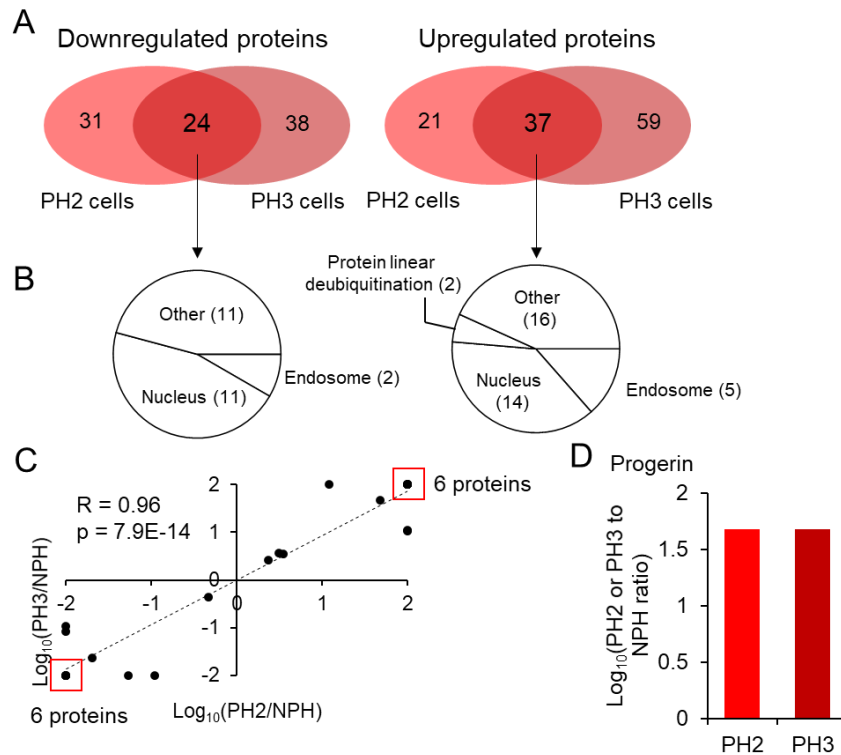


Figure 20: Mass spectrometric analysis of up/downregulated proteins in progeric HEK cells (PH2 and PH3) compared to non-progeric HEK cells (NPH). (A). Significantly up/downregulated proteins ( $p \leq 0.05$  and  $\geq 2$ -fold change in abundance) in two independent cell lines stably expressing progerin (PH2 and PH3). (B). General classification of modulated proteins shared between PH2 and PH3 cells. (C). Pearson correlation analysis between PH2 and PH3 cells against NPH control cells. Highlighted boxes represent multiple proteins having the

same fold change. (D). Protein abundance of progerin is significantly higher in PH2 ( $p=2.0E-16$ ) and PH3 ( $p=1.9E-16$ ) cells than in NPH cells.

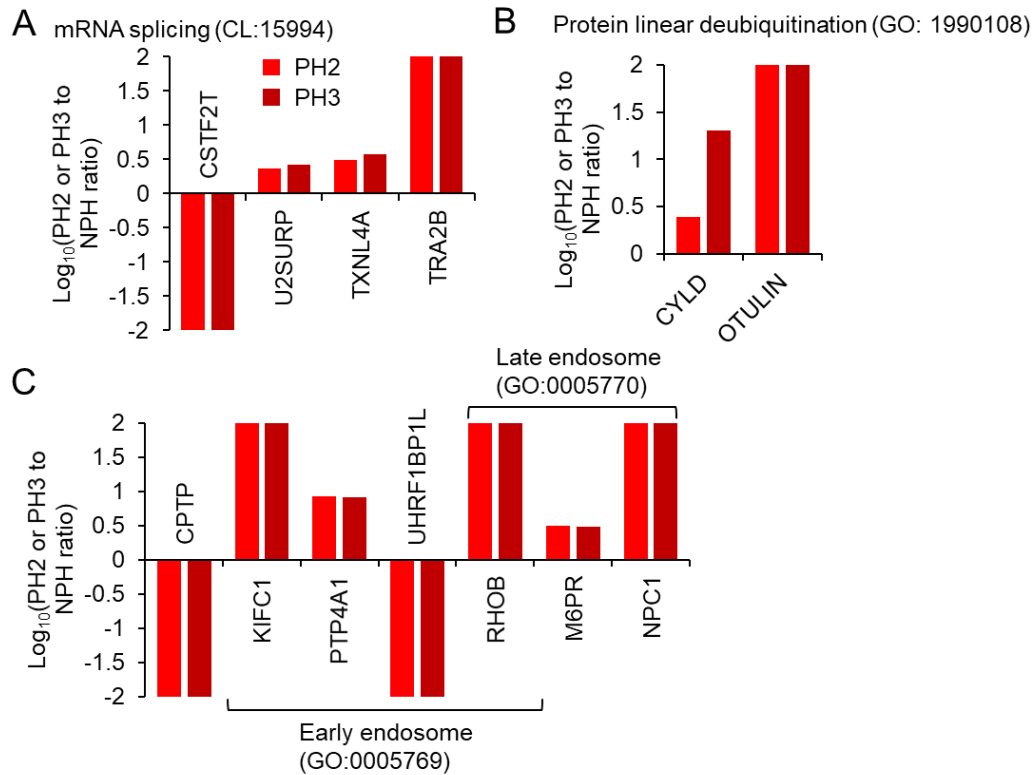


Figure 21: Preliminary analysis for pathways significantly modulated in progeric HEK cell lines (PH2/PH3) when compared to non-progeric HEK control. String pathway analysis reveals proteins involved in mRNA splicing (A), protein linear deubiquitination (B) and endosomal/lysosomal trafficking (C).

### 3.6.2: HEK and ES1 cell lines

The Edmonton Strain 1 (ES1) cell line was established by Dr. Sang-Gyun Kang in the Westaway lab by subcloning a tau inclusion-positive cell line from HEK293 tauRD-YFP cells that were infected with transgenic mouse brain-derived pathogenic tau. Specifically, the input pathogenic tau species were profiled chemically by a guanidine hydrochloride melting cure immunoassay (CSA) and found to resemble those of human P301L patients assigned a clinical diagnosis of semantic variant primary progressive aphasia (svPPA)[84][217]. The ES1 cells offer a valuable

model to investigate generic tau aggregation-related cellular changes for two reasons: 1) ES1 cells are chronically “burdened” with intracellular tau aggregates that do not disappear with passage number; 2) ES1 cells exhibit all the aforementioned tau inclusions morphologies (amorphous, nuclear envelope, speckles and threads) seen in acute protein transduction of sarkosyl-insoluble tau from mouse or human P301L brain samples[74][84][217].

When compared with the NPH cells and using the same cut-off parameter as Fig. 20, our proteomics analysis revealed 188 proteins that are significantly up- or downregulated in non-progeric ES1 (NPE) cells. Nuclear proteins, endosomal proteins and proteins that are involved in the protein linear deubiquitination pathways constituted a significant portion of the protein list and they were subjected to a more in-depth analysis (Fig. 22A). Among 65 nuclear proteins identified, four of them are involved in mRNA splicing, dysregulation of which is heavily implicated in different neurological disorders. In our dataset, the levels of cleavage stimulation factor subunit 2 (CSTF2) and a pre-mRNA-splicing factor SLU7 are significantly lower in ES1 cells comparing to parental HEK cells that are free of tau aggregates. Significant upregulation is observed in thioredoxin like 4A (TXNL4A) and pre-mRNA cleavage complex 2 protein PCF11 (Fig. 22B).

Compared to control NPH cells, NPE cells have a slower proliferation rate and a higher percentage of multinucleated cells[217]. To understand the effects of tau aggregation on cell cycle regulation, proteins involved in metaphase plate assembly and spindle organization were examined. Among 10 identified proteins, charged multivesicular body protein 2a (CHMP2A) and 2b (CHMP2B) drew our attention. As essential components of the endosomal sorting complexes required for transport (ESCRT-III), CHMP2A and CHMP2B play important roles in cell division. By knocking down these two proteins in HeLa cells, Morita *et al.* showed that

deficiency of CHMP2A and CHMP2B results in an elevated level of abscission defects (multinucleated cells and midbody) and mitotic defects (fragmented nuclei and unaligned chromosomes)[238]. Interestingly, CHMP2A and CHMP2B are both significantly downregulated in NPE cells when compared to NPH control (Fig. 22C). It suggests that proteins in the ESCRT-III complex may at least partially explain the aberrant cellular morphology and reduced proliferation rate in the ES1 cell line. To explore other regulators of cell division in ES1 cells, further screening will be needed to determine the involvement of the other eight proteins in this category.

Since endosomal/lysosomal trafficking is a heavily implicated biological process in tauopathies, we attempted to screen out the proteins associated with endosomes from the proteomic dataset. There were 11 proteins falling into the umbrella of endosomal proteins and they are further classified into four categories: early phagosome, ESCRT III complex, clathrin-coated vesicle membrane and late endosome (Fig. 22D). Apart from CHMP2A/2B, two significantly downregulated proteins, RAB3A and VPS29, have also been reported in the context of AD, as discussed in Section 4.2.

As shown earlier in Section 3.5.1, CYLD and OTULIN, two proteins involved in protein linear deubiquitination, undergo a significant increase in protein abundance in HEK cells stably expressing progerin (PH2 and PH3, Fig. 21B). Interestingly, CYLD and OTULIN are also significantly upregulated in NPE cells (Fig. 22E). The implications of CYLD and OTULIN dysregulation under two stressful conditions (progerin expression and tau aggregation) remain unclear, but their documented involvement in cell cycle[239] and endosomal trafficking[240] may offer a straightforward explanation.

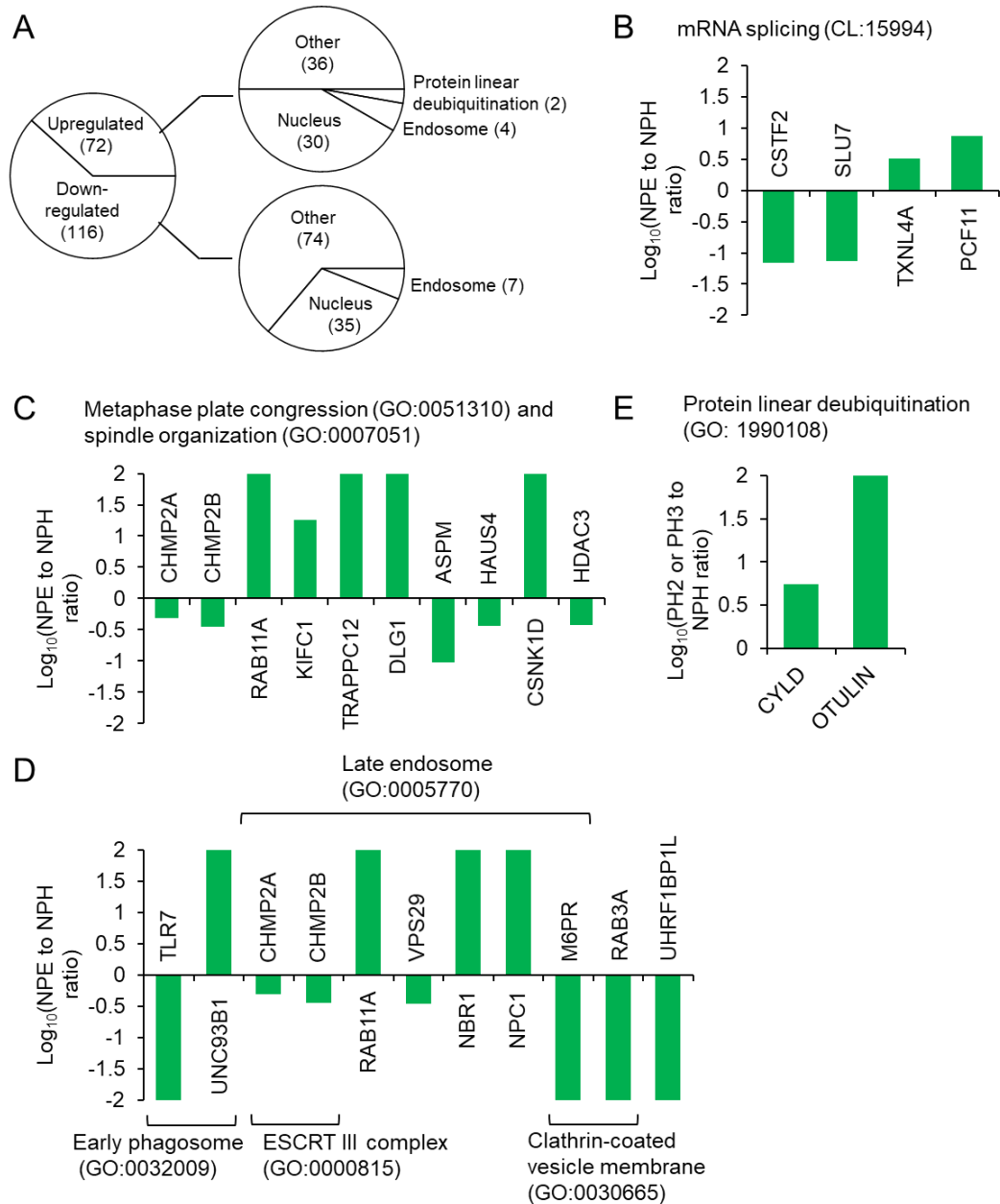


Figure 22: Mass spectrometric analysis of up/downregulated proteins in non-progeric ES1 cells (NPH) compared to non-progeric HEK cells (NPH). (A). General classification of Significantly up/downregulated proteins ( $p \leq 0.05$  and  $\geq 2$ -fold change in abundance) in NPH cells. (B). Four identified nuclear proteins are involved in mRNA splicing. (C). 10 identified nuclear proteins are involved in metaphase plate assembly and spindle organization. (D). 11 endosomal proteins are significantly modulated in NPE cells. (E). CYLD and OTULIN, two proteins involved in protein linear deubiquitination, are significantly upregulated in NPE cells.

### 3.6.3: Non-progeric HEK and progeric ES1 cell lines

Our proteomic approach suggested that progeric HEK cell lines (PH2 and PH3) and non-progeric ES1 cell line (NPE) offer useful tools to study cellular aging and tau aggregation, however, it remains unexplored what proteomic changes will be incurred when two stressors, progerin expression and tau aggregation, are present in the tau reporter cells simultaneously.

To analyze the synergistic effects of progerin and tau aggregates, the proteome datasets of two independent progeric ES1 cell lines (PE7 and PE9) were compared to that of non-progeric HEK cells (NPH), revealing 489 significantly modulated proteins shared by PE7 and PE9 cell lines, 368 being downregulated and 121 upregulated (Fig. 23A). The same analysis pipeline was applied to the dataset to categorize nuclear proteins, endosomal proteins and proteins that play a role in protein linear deubiquitination pathway (Fig. 23B). By performing a Pearson correlation test, it becomes clear that, despite some minor differences, PE7 and PE9 cell lines have similar general protein expression pattern (Fig. 23C). Reassuringly, the expression of progerin is confirmed by its increased abundance in progeric ES1 clones (Fig. 23D).

Among 211 identified nuclear proteins, proteins involved in mRNA splicing and components of the nuclear envelope are subjected to further analysis. As mentioned earlier, dysregulation of RNA splicing has been implicated in aging and neurological disorders. Our proteomic analysis for PE7 and PE9 cell lines revealed 10 spliceosomal proteins with significant expression differences (Fig. 24A). Interestingly, at least four of them fell into the protein clusters that have received great attention in the field of Alzheimer's disease – HNRNPs and SNRPs. Firstly, by analyzing human brain tissues from AD patients, Zhang *et al.* revealed that heterogeneous nuclear ribonucleoprotein K (HNRNPK) is an upregulated hub protein in AD[241]. As another related heterogeneous nuclear ribonucleoprotein, HNRNPC, is also shown to stabilize APP

mRNA and enhance its translation[242][243], it becomes evident that HNRNPs have critical functions in AD pathogenesis. Secondly, small nuclear ribonucleoproteins have a major role in APP production and toxicity of tau. Two independent studies using *Drosophila* models illustrated that: 1) knockdown of U2 small nuclear ribonucleoprotein B (SNRPB2) resulted in a significant increase of A $\beta$  secretion[244]; 2) silencing U1 small nuclear ribonucleoprotein C (SNRPC) augmented tau<sup>R406W</sup>-induced toxicity[245]. Because the protein abundance of HNRNPK, HNRNPC, SNRPB2 and SNRPF are significantly modulated in both PE7 and PE9 cells (Fig. 24A), it suggests that the progeric ES1 cells may recapitulate some unique changes in spliceosomal proteins in the context of tauopathies.

Since both OTULIN and CYLD are upregulated in progeric HEK cells (PH2 and PH3, Fig. 21B) and non-progeric ES1 cells (NPE, Fig. 24B), we attempted to observe their behavior in progeric ES1 cells (PE7 and PE9). To our surprise, only OTULIN increases in abundance in both PE7 and PE9 cell lines (Fig. 24B). CYLD is only upregulated in PE9 but not in PE7 cells (data not shown). Such a discrepancy between the progeric ES1 clones may be explained by intrinsic differences between independent clones.

Our proteomic comparison highlighted 29 endosomal proteins, 10 being upregulated and 19 downregulated. These protein candidates encompass constituents of early endosome, late endosome and lysosome (Fig. 22C). As three sets of endosomal proteins have been identified in PH vs. NPH comparison (Fig. 21C), NPE vs. NPH comparison (Fig. 22D) and PE vs. NPH comparison (Fig. 24C), we screened out the genes that are shared in all three sets. UHRF1BP1L, NPC1 and M6PR are the only mutual endosomal proteins (Fig. 24D), suggesting their potential roles in response to progerin-induced stress, tau aggregation-associated toxicity, or both, in HEK293 cells.

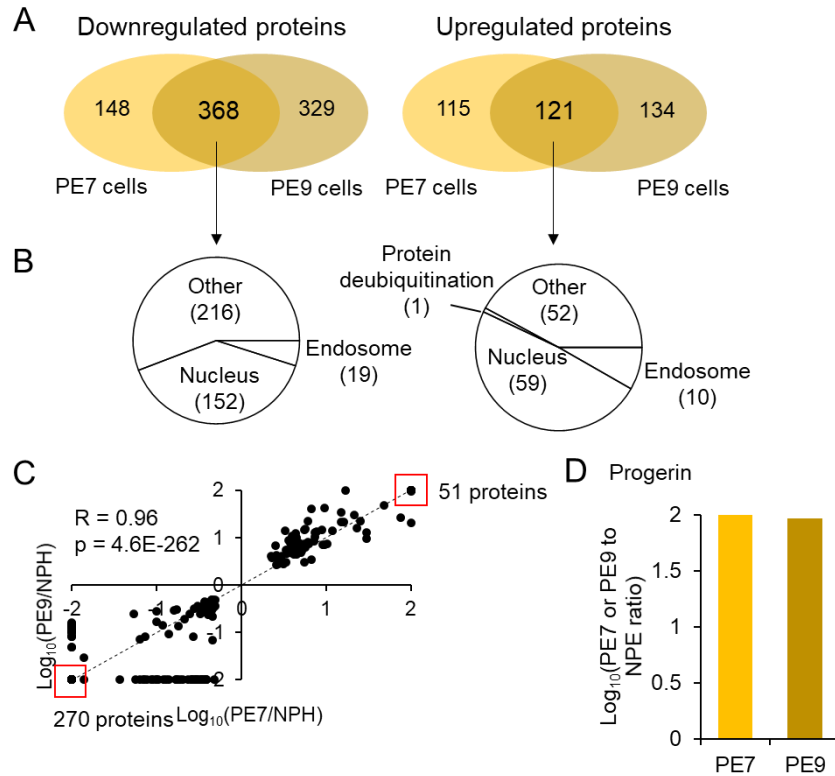


Figure 23: Mass spectrometric analysis of up/downregulated proteins in progeric ES1 cells (PE7 and PE9) compared to non-progeric HEK cells (NPH). (A). Significantly up/downregulated proteins ( $p \leq 0.05$  and  $\geq 2$ -fold change in abundance) in two independent ES1 cell lines stably expressing progerin (PE7 and PE9). (B). General classification of modulated proteins shared between PE7 and PE9 cells. (C). Pearson correlation analysis between PE7 and PE9 cells against NPH control cells. Highlighted boxes represent multiple proteins having the same fold change. (D). Protein abundance of progerin is significantly higher in PE7 ( $p=4.61E-17$ ) and PE9 ( $p=1.65E-14$ ) cells than in NPH cells.

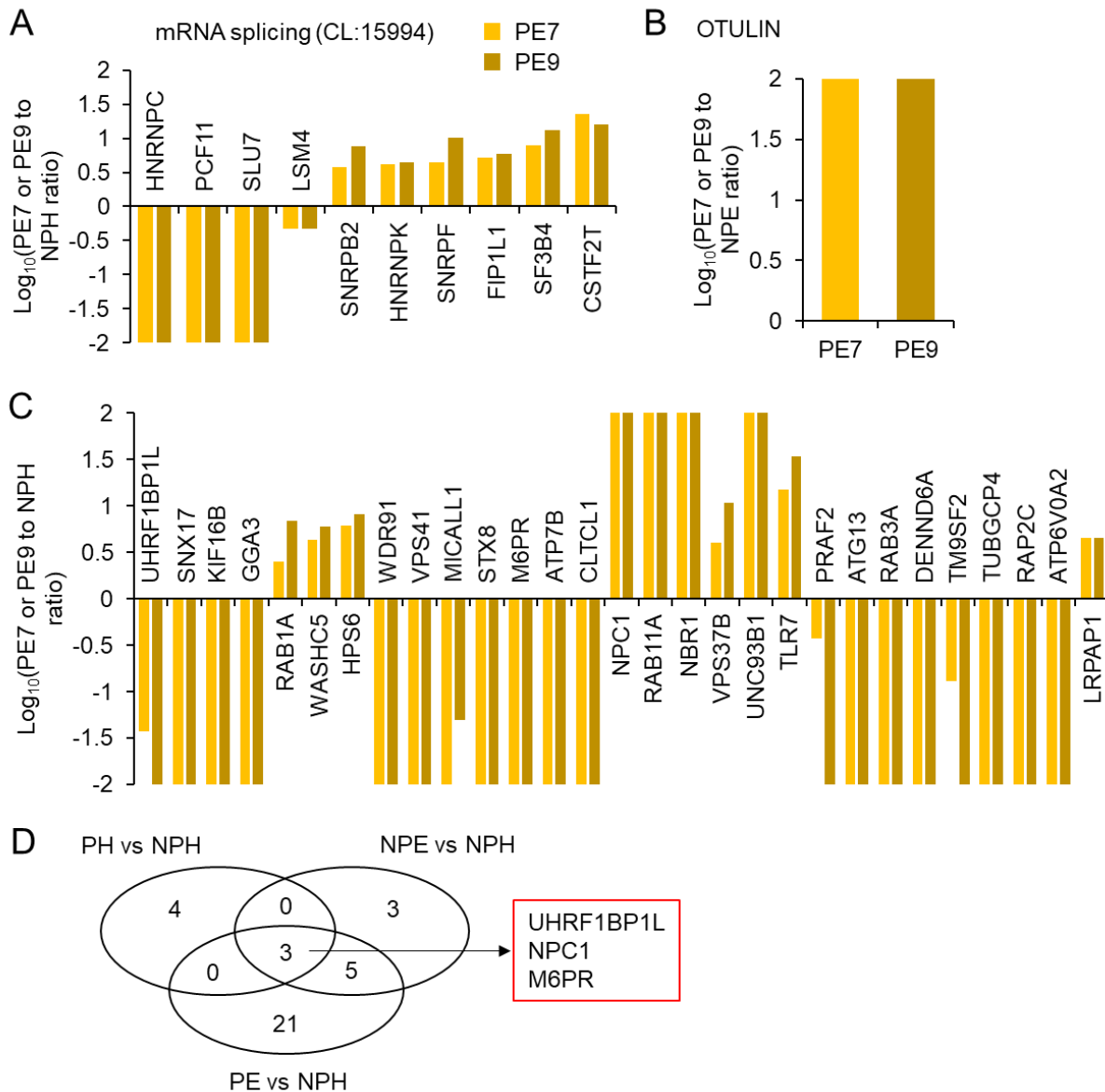


Figure 24: Analysis for pathways significantly modulated in progeric ES1 cell lines (PE7/PE9) compared to non-progeric HEK control. String pathway analysis reveals proteins involved in mRNA splicing (A), protein linear deubiquitination (B) and endosomal/lysosomal trafficking (C). (D). Three endosomal proteins (UHRF1BP1L, NPC1 and M6PR) are modulated in progeric HEK cells, ES1 cells and progeric ES1 cells when compared to non-progeric HEK cells.

## Chapter 4: Discussion

### 4.1: Progeric HEK cell lines – progerin-induced aging in a tau inclusion-free cell culture model

Cell culture models offer relatively inexpensive yet useful tools to establish causality between genetic mutations, cellular phenotypes and proteomic alterations, to thereby gain understanding into the pathogenesis of neurological disorders. Progerin (LMNA- $\Delta$ 50) is the “culprit” molecule of HGPS pathological aging[129] and its involvement in chronological aging has been confirmed in certain tissues[145]. Due to its potential to circumvent the fixed timeline of chronological aging in a lab setting, progerin has been used to model pathological phenotypes of late-onset Parkinson’s disease in human iPSC-derived neurons[204]. However, to the best of our knowledge, it remains unexplored if progerin can be used to model late-onset tauopathies in a cell culture system.

It is worth noting that the expression level of progerin and wildtype lamin A is reported to be low in the brain due to the existence of a brain-specific microRNA[199]. For this reason, HGPS aging is often considered an unsuitable model to study aging of the central nervous system. However, more recent analyses of human AD brains reveal that the transcript and protein level of lamin A increases in the hippocampus in late-stage AD[207][208], suggesting possible involvements of lamin A in neurodegeneration. Interestingly, neuronal cell may not be the only cell type under special lamin A regulation. Piekarowicz *et al.* suggested a posttranscriptional mechanism to explain low levels of lamin A in HEK293 cells[246]. In our experiments, using transfection of a heterologous expression vector (i.e., with promoter/enhancer, 5’ and 3’-UTR sequences that do not derive from the lamin A gene) bypasses potential regulatory mechanisms for lamin A in HEK293 cells. Although progerin exposure may not capture all aspects of

chronological aging, our study demonstrates that the induced aging strategy triggers modulation of some proteins that are known players in aging and tauopathies, as shown in our proteomics dataset.

The study presented here represents an attempt at modeling aging in a tau protein aggregation reporter cell line with progerin expression. By selecting two independent HEK293 tauRD-YFP reporter clones (PH2 and PH3) that stably express progerin, we observe c-Myc tagged progerin localizes at the nuclear envelope, causes nuclear dysmorphology in a subpopulation of cells and does not lead to spontaneous tau aggregate formation. As expected, significantly more double-stranded DNA damage markers are observed in both progeric HEK clones. After exposing the cells to preparations containing pathogenic tau, it becomes clear that both progeric cell lines associate with a higher seeding efficiency, implying that progeric cells become sensitized to receiving tau seeds or amplifying the pathogenic tau in a templated manner. In attempt to rationalize the increase of seeding efficiency in progeric cells, we show that the total tau protein abundance is increased in four independent progeric HEK clones, providing a straightforward explanation for this effect. But, importantly, our proteomic analysis reveals a set of significantly modulated proteins that are involved in a number of pathways related to cellular aging and tau protein biology (e.g., mRNA splicing, protein linear deubiquitination and endosomal trafficking), suggesting other possible explanations for progerin-induced seeding efficiency changes in HEK cells. Since it remains obscure why lamin A is uniquely regulated by microRNA in the brain, our observation raises a possible explanation that miR9-mediated downregulation of LMNA may serve as a protection mechanism against tau aggregation.

A critical requirement for our study is the evaluation of seeding events in tau reporter cell lines. Using an automated analysis pipeline (Fig. 13), we can quantify the number of tau inclusion-

positive cells. Future studies may include additional sources of pathogenic tau, such as human AD brain extract and *in vitro* generated tau fibrils, to investigate how progeric HEK cells respond to different tau seeds. It will also be interesting to assess the total amount of tau aggregates using filter trap assay[247]. As our observations for progeric HEK cells are generally consistent between PH2 and PH3 clones, the phenotypic changes are likely due to progerin expression, as opposed to the subcloning procedure yielding spontaneous cell variants unrelated to the biological properties of the expression constructs (subcloning effects as described in more detail in Section 4.4). Nevertheless, it will be interesting to include PH11 and PH12 clones in seeding experiments to confirm the effects of progerin expression on tau seeding efficiency.

#### **4.2: The ES1 cell line harboring tau aggregates exhibits changes in splicing and endosomal proteins**

In comparison to tau inclusion-free HEK cells, ES1 cells exhibit remarkable proteomic alterations, with multiple proteins selected from our proteomic dataset being involved in AD-related pathways. Three out of four identified mRNA splicing proteins, SLU7, TXNL4A and PCF11 (Fig. 22B), have been found to be associated with AD. For SLU7, in the study of Tollervey *et al.*, the transcript level appears to be significantly downregulated in brain tissues of AD patients when compared to cognitively normal individuals[221]. For TXNL4A, using serial analysis of gene expression, George *et al.* demonstrated that the transcript level of TXNL4A is significantly upregulated in a well characterized APP695, amyloid-depositing AD mouse model, Tg2576[248], when compared to non-transgenic control animals. Lastly, a microarray analysis by Wong *et al.* showed that the transcript level of PCF11 is significantly elevated in human AD brains[249]. To the best of our knowledge, the involvement of CSTF2 in human AD patients or AD-related transgenic animals remains unclear. As expected, our data of NPE cells to some

extent agree with previous gene expression analyses on human AD brains or transgenic animals, validating the modeling potential of the ES1 cell line for analyzing the involvement of tau aggregation in the context of mRNA splicing events.

With respect to significantly modulated endosomal proteins in the ES1 cell line (Fig. 22D), RAB3A and VPS29 have prominent connections to AD. *RAB3A* encodes for a Ras-related GTP-binding protein that has vital functions in synaptic vesicle transport in the nervous system[250][251]. Using quantitative western blotting, Blennow *et al.* demonstrated that the protein level of RAB3A is significantly reduced in the hippocampus and frontal cortex of AD patients compared to age-matched controls[252], yet the molecular mechanism behind RAB3A expression regulation is unclear. Interestingly, our experiments showed that the protein abundance of RAB3A is significantly lower in NPE cells when compared to NPH (Fig. 22D). Since NPE cells represent a derivative of control NPH cells that are chronically infected with pathogenic tau, it is tempting to speculate that transduction of pathogenic tau alone may lead to RAB3A dysregulation. This hypothesis may be tested by transducing different tau reporter cell lines with preparations containing pathogenic tau of different origins (human brain derived, transgenic mouse brain derived and *in vitro* generated).

In several neurodegenerative diseases, protein aggregation has been associated with dysregulation of retromer components (VPS35/VPS26/VPS29) that are responsible for endosomal cargo recycling[253][254][255]. In tauopathies, depletion of vacuolar protein sorting-associated protein 35 (VPS35) in transgenic mouse models blocks the resolution of autophagy, leading to an increased accumulation of pathological tau and defects in motor and learning behaviors[256][257]. A recent study from Ye *et al.* also suggested that VPS29 is required for retromer localization and function in the aging brain, thus having great impacts in synaptic

transmission, survival and locomotion, at least in the experimental context of *Drosophila*[258]. In our proteomic analysis, the protein level of VPS29 decreases significantly in NPE cells (Fig. 22D), agreeing with the notion that tau aggregation and retromer dysfunction may be mechanistically intertwined. Since it is not elucidated if retromer depletion precedes tau aggregation in the brain in human tauopathies, our data hints that pathogenic tau transduction alone may result in VPS29 downregulation in a tau reporter cell line. Further quantitative biochemical assays may be required to support this hypothesis.

#### **4.3: Progeric ES1 cell lines – progerin-induced aging in a tau inclusion-positive cell culture model**

To investigate the effects of progerin expression in the presence of intracellular tau inclusions, we established two polyclonal derivatives of the progeric ES1 cell line (i.e., PE7 and PE9). Wes capillary immunoassay demonstrates the total tau protein abundance being decreased in progeric ES1 cells (Fig. 17A). It does not escape our attention that in the parental HEK and the ES1 cells, that progerin expression results in tau levels to be modulated in opposite directions, disproving the possibility of progerin-induced changes in the efficiency of the ubiquitin c promoter. We also show that progerin expression significantly aggravates nuclear membrane defects, leading to nuclear perturbations in nearly all cells (Fig. 17B). Since progerin on its own only results in slight nuclear dysmorphology in progeric HEK cells, it becomes apparent that ES1 cells are more susceptible to the deleterious effects of progerin, suggesting possible interactions between tau aggregates and progerin. Such a remarkable alteration of nuclear integrity may be explained by the several modulated nuclear proteins that were identified in mass spectrometry-based proteomic analysis (Fig. 22B). Unsurprisingly, tau aggregates extracted from non-progeric ES1 cells and progeric ES1 cells yield highly similar, if not identical, fragments in limited proteolysis

experiments (Fig. 17C), arguing against the possibility of progerin-induced “strain” effects, i.e., selection of different tau conformers in a manner similar to the way in which alternative PrP conformers, prion strains, can be selected for under certain biological conditions.

Taken all proteomic comparisons together, UHRF1BP1L, NPC1 and M6PR appear to be the core changes when the cells are exposed to progerin alone, to pathogenic tau alone, or to a combined treatment of progerin and pathogenic tau (Fig. 24D). The endosomal origin of these three proteins highlights the importance of endo/lysosomal trafficking in aging and tau biology. Further investigation is needed to validate the involvement of these proteins in tau protein misfolding in other cell lines and animal models, and relationships to vesicular trafficking and/or specialized pathways relating to tau degradation.

#### **4.4: Technical considerations**

Using stable mammalian cell lines to investigate the effects of transgenes *in vitro* is a common practice but it has its own limitations/challenges. Cell type selection and subcloning conditions represent two areas that require careful considerations.

To study tau protein aggregation, immortalized cell lines are often used to stably express full-length or truncated forms of tau with or without pathogenic mutations, allowing for intracellular templated amplification. Commonly used cell lines include but not limited to N2a[259], HEK293[74][83][21][260], HeLa[261] and SH-SY5Y[262]. Since they are generally low-maintenance and easy-to-propagate, immortalized cell lines offer useful tools to investigate tau protein behaviors in a cellular environment. However, careful interpretation can only be made when we take the non-neuronal nature of these cell lines into consideration. Firstly, cell cycle regulation is vastly different between immortalized cell lines and neuronal cells – neurons are

terminally differentiated post-mitotic cells[263] yet immortalized cell lines undergo active cell division. Secondly, different cell types may differ significantly in their proteomes. As Geiger *et al.* demonstrated by deep proteomics analysis, different mammalian cell lines have cell type-specific clusters of protein expression[264]. In our experiments, expressing progerin in HEK293 tauRD-YFP reporter cells only represents a preliminary attempt to unveil the effects of HGPS aging in the context of tau aggregation. Systems that better represent neuronal biology, such as human iPSC derived neurons and transgenic animal models, are needed for future investigation.

To establish cell clones that stably express progerin, we used zeocin to select successfully transfected cells before performing limited dilution. Use of zeocin in mammalian cell culture has advantages and disadvantages. On one hand, compared to other antibiotics used for mammalian cell selection (hygromycin B, neomycin and puromycin), zeocin-selected population associates with high transgene expression level and better transgene stability in HT1080 and HEK293 cells[265]. On the other hand, zeocin causes DNA cleavage and its deleterious effects cannot be fully suppressed by the zeocin resistance gene[216]. Although use of a low concentration of zeocin (20  $\mu\text{g}/\text{mL}$  in our experiments) likely results in limited DNA damage versus concentrations of 100-800  $\mu\text{g}/\text{mL}$  used by Trastoy[216], it remains a critical variable when assessing nuclear integrity. Alternative methods may prove more suitable in subcloning, such as limited dilution without zeocin selection and flow cytometric selection based on fluorescent cell markers.

#### **4.5: Modeling aging to study tau biology – what is next?**

To date, we have only analyzed a limited number of proteins in our proteomics dataset. For this reason, the discussion in previous sections is restricted to significantly modulated proteins shown in Chapter 3. More in-depth analysis is needed to understand if other protein candidates in the

three cell culture models we established (PH2/PH3, NPE and PE7/PE9) have reported interactions with aging and generic tauopathies. We may need to pay special attention to proteins with known functions in autophagic pathways as experimental evidence supports the involvement of autophagy in a tau aggregation reporter cell line[266] and also in transgenic mice[267].

Progerin-induced aging associates with multifaceted alterations in cellular proteome. In future studies, it will be interesting to dissect the individual contribution of these proteins in tau seeding efficiency. It will also be intriguing to directly observe progerin-induced nuclear damage in progeric ES1 cells. As Ran (a small GTPase) is a cargo being constantly transported between the nucleus and the cytoplasm[268], loss of the Ran gradient across the nuclear membrane is used as an indicator for nuclear disintegrity[142][217]. By assessing the Ran gradient with immunocytochemistry or the Wes capillary immunoassay, we may gain direct evidence about functional nuclear perturbation caused by progerin expression. In addition, different proteomic technologies should be employed to assess changes in the post-translational modification status of tau with/without progerin expression. Finally, as new tools in our experimental paradigm, both non-progeric and progeric ES1 cell lines could be integrated into a drug discovery pipeline in attempt to identify compounds that counteract tau aggregation or nuclear impairment.

#### **4.6: Summary**

Using the HEK293 tauRD-YFP reporter cell line (established by Dr. Marc Diamond and co-workers) and the HEK293 tauRD-YFP-derived ES1 cell line (by Dr. Sang-Gyun Kang) as foundations, we have introduced a mutant LMNA allele into these cell culture models of tau aggregation (Fig. 25). Four progeric HEK cell lines and two progeric ES1 cell lines have been generated. We have employed a wide array of biochemical and cell biological methods to

investigate the differences between progeric cells and their non-progeric counterparts. We have observed significant alterations in protein abundance caused by progerin expression, particularly for those associated with endo/lysosomal trafficking, protein deubiquitination and mRNA splicing pathways. This underlines the importance of these biological processes in cellular aging and highlights specific protein targets for further investigation.

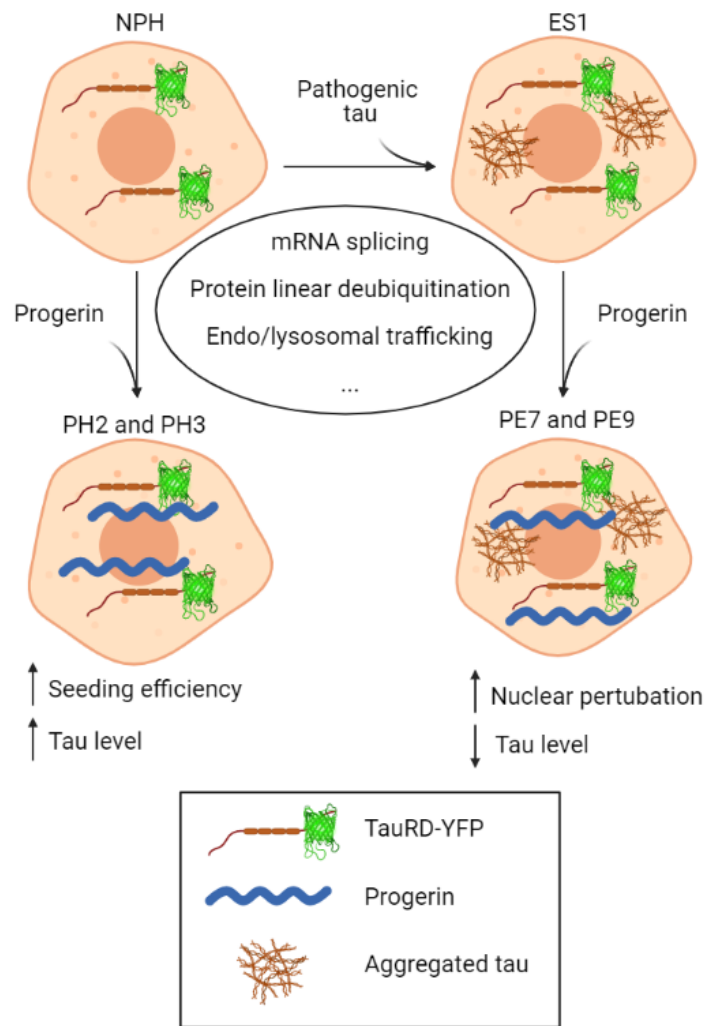


Figure 25: Schematic summary of main findings in progeric HEK cells, non-progeric ES1 cells and progeric ES1 cells. Filled circles represent nuclei.

## Chapter 5: References

- [1] M. Goedert, C. M. Wischik, R. A. Crowther, J. E. Walker, and A. Klug, “Cloning and sequencing of the cDNA encoding a core protein of the paired helical filament of Alzheimer disease: Identification as the microtubule-associated protein tau (molecular pathology/neurodegenerative disease/neurofibrillary tangles),” *Proc. Natl. Acad. Sci. USA*, vol. 85, no. June, pp. 4051–4055, 1988.
- [2] M. Goedert, M. G. Spillantini, R. Jakes, D. Rutherford, and R. A. Crowther, “Multiple isoforms of human microtubule-associated protein tau: sequences and localization in neurofibrillary tangles of Alzheimer’s disease,” *Neuron*, vol. 3, no. 4, pp. 519–526, 1989, doi: 10.1016/0896-6273(89)90210-9.
- [3] H. Takuma, S. Arawaka, and H. Mori, “Isoforms changes of tau protein during development in various species,” *Dev. Brain Res.*, vol. 142, no. 2, pp. 121–127, 2003, doi: 10.1016/S0165-3806(03)00056-7.
- [4] Himmler Adolf, “Structure of the bovine tau gene: alternatively spliced transcripts generate a protein family,” vol. 9, no. 4, pp. 1389–1396, 1989.
- [5] M. Chen, R. N. Martins, and M. Lardelli, “Complex splicing and neural expression of duplicated tau genes in zebrafish embryos,” *J. Alzheimer’s Dis.*, vol. 18, no. 2, pp. 305–317, 2009, doi: 10.3233/JAD-2009-1145.
- [6] Y. Gu, F. Oyama, and Y. Ihara, “Tau Is widely expressed in rat tissues,” *J. Neurochem.*, vol. 67, no. 3, pp. 1235–1244, 1996, doi: 10.1046/j.1471-4159.1996.67031235.x.
- [7] M. L. Wei and A. Andreadis, “Splicing of a regulated exon reveals additional complexity in the axonal microtubule-associated protein Tau,” *J. Neurochem.*, vol. 70, no. 4, pp. 1346–1356, 1998, doi: 10.1046/j.1471-4159.1998.70041346.x.
- [8] M. A. Kahlson and K. J. Colodner, “Glial tau pathology in tauopathies: Functional consequences,” *J. Exp. Neurosci.*, vol. 9s2, pp. 43–50, 2015, doi: 10.4137/JEN.S25515.
- [9] M. D. Weingarten, A. H. Lockwood, S. Hwo, and M. W. Kirschner, “A protein factor essential for microtubule assembly,” *bioRxiv*, vol. 72, no. 5, pp. 1858–1862, 2018, doi: 10.1101/468892.
- [10] P. Barbier *et al.*, “Role of tau as a microtubule-associated protein: Structural and functional aspects,” *Front. Aging Neurosci.*, vol. 10, no. JUL, pp. 1–14, 2019, doi: 10.3389/fnagi.2019.00204.
- [11] A. M. Pooler and D. P. Hanger, “Functional implications of the association of tau with the plasma membrane,” *Biochem. Soc. Trans.*, vol. 38, no. 4, pp. 1012–1015, 2010, doi: 10.1042/BST0381012.
- [12] X. C. Li *et al.*, “Human wild-type full-length tau accumulation disrupts mitochondrial dynamics and the functions via increasing mitofusins,” *Sci. Rep.*, vol. 6, pp. 1–10, 2016, doi: 10.1038/srep24756.
- [13] M. B. Maina, Y. K. Al-Hilaly, and L. C. Serpell, “Nuclear tau and its potential role in alzheimer’s disease,” *Biomolecules*, vol. 6, no. 1, pp. 2–20, 2016, doi:

10.3390/biom6010009.

- [14] T. Scholz and E. Mandelkow, “Transport and diffusion of Tau protein in neurons,” *Cell. Mol. Life Sci.*, vol. 71, no. 16, pp. 3139–3150, 2014, doi: 10.1007/s00018-014-1610-7.
- [15] F. J. Baird, “Microtubule Defects and Neurodegeneration,” *J. Genet. Syndr. Gene Ther.*, vol. 04, no. 11, 2013, doi: 10.4172/2157-7412.1000203.
- [16] A. Sultan *et al.*, “Nuclear Tau, a key player in neuronal DNA protection,” *J. Biol. Chem.*, vol. 286, no. 6, pp. 4566–4575, 2011, doi: 10.1074/jbc.M110.199976.
- [17] M. Violet *et al.*, “A major role for Tau in neuronal DNA and RNA protection in vivo under physiological and hyperthermic conditions,” *Front. Cell. Neurosci.*, vol. 8, no. MAR, pp. 1–11, 2014, doi: 10.3389/fncel.2014.00084.
- [18] T. L. Spires-Jones and B. T. Hyman, “The Intersection of Amyloid Beta and Tau at Synapses in Alzheimer’s Disease,” *Neuron*, vol. 82, no. 4, pp. 756–771, 2014, doi: 10.1016/j.neuron.2014.05.004.
- [19] J. Boehm, “A ‘danse macabre’: Tau and Fyn in STEP with amyloid beta to facilitate induction of synaptic depression and excitotoxicity,” *Eur. J. Neurosci.*, vol. 37, no. 12, pp. 1925–1930, 2013, doi: 10.1111/ejn.12251.
- [20] K. L. Fiock, M. E. Smalley, J. F. Crary, A. M. Pasca, and M. M. Hefti, “Increased tau expression correlates with neuronal maturation in the developing human cerebral cortex,” *eNeuro*, vol. 7, no. 3, pp. 1–9, 2020, doi: 10.1523/ENEURO.0058-20.2020.
- [21] S. G. Kang, G. Eskandari-Sedighi, L. Hromadkova, J. G. Safar, and D. Westaway, “Cellular Biology of Tau Diversity and Pathogenic Conformers,” *Front. Neurol.*, vol. 11, no. November, pp. 1–22, 2020, doi: 10.3389/fneur.2020.590199.
- [22] N. Sergeant, A. Delacourte, and L. Buée, “Tau protein as a differential biomarker of tauopathies,” *Biochim. Biophys. Acta - Mol. Basis Dis.*, vol. 1739, no. 2, pp. 179–197, 2005, doi: 10.1016/j.bbadis.2004.06.020.
- [23] F. Liu and C. X. Gong, “Tau exon 10 alternative splicing and tauopathies,” *Mol. Neurodegener.*, vol. 3, no. 1, pp. 1–10, 2008, doi: 10.1186/1750-1326-3-8.
- [24] R. Sud, E. T. Geller, and G. D. Schellenberg, “Antisense-mediated exon skipping decreases Tau protein expression: A potential therapy for tauopathies,” *Mol. Ther. - Nucleic Acids*, vol. 3, no. May, p. e180, 2014, doi: 10.1038/mtna.2014.30.
- [25] Y. Wang and E. Mandelkow, “Tau in physiology and pathology,” *Nat. Rev. Neurosci.*, vol. 17, no. 1, pp. 5–21, 2016, doi: 10.1038/nrn.2015.1.
- [26] X. Zhang *et al.*, “The proline-rich domain promotes Tau liquid-liquid phase separation in cells,” *J. Cell Biol.*, vol. 219, no. 11, 2020, doi: 10.1083/JCB.202006054.
- [27] M. D. Mukrasch *et al.*, “Structural polymorphism of 441-residue Tau at single residue resolution,” *PLoS Biol.*, vol. 7, no. 2, pp. 0399–0414, 2009, doi: 10.1371/journal.pbio.1000034.
- [28] T. N. Cordeiro *et al.*, “Small-angle scattering studies of intrinsically disordered proteins

- and their complexes,” *Curr. Opin. Struct. Biol.*, vol. 42, pp. 15–23, 2017, doi: 10.1016/j.sbi.2016.10.011.
- [29] T. F. Frappier, I. S. Georgieff, K. Brown, and M. L. Shelanski, “ $\tau$  Regulation of Microtubule-Microtubule Spacing and Bundling,” *J. Neurochem.*, vol. 63, no. 6, pp. 2288–2294, 1994, doi: 10.1046/j.1471-4159.1994.63062288.x.
- [30] J. Chen, Y. Kanai, N. J. Cowan, and N. Hirokawa, “Projection domains of MAP2 and tau determine spacings between microtubules in dendrites and axons,” *Nature*, vol. 360, no. 6405, pp. 674–677, 1992, doi: 10.1038/360674a0.
- [31] C. Liu and J. Götz, “Profiling murine tau with 0N, 1N and 2N isoform-specific antibodies in brain and peripheral organs reveals distinct subcellular localization, with the 1N isoform being enriched in the nucleus,” *PLoS One*, vol. 8, no. 12, pp. 1–18, 2013, doi: 10.1371/journal.pone.0084849.
- [32] Q. Zhong, E. E. Congdon, H. N. Nagaraja, and J. Kuret, “Tau isoform composition influences rate and extent of filament formation,” *J. Biol. Chem.*, vol. 287, no. 24, pp. 20711–20719, 2012, doi: 10.1074/jbc.M112.364067.
- [33] M. Goedert and R. Jakes, “Expression of separate isoforms of human tau protein: Correlation with the tau pattern in brain and effects on tubulin polymerization,” *EMBO J.*, vol. 9, no. 13, pp. 4225–4230, 1990, doi: 10.1002/j.1460-2075.1990.tb07870.x.
- [34] N. Sergeant *et al.*, “Two-dimensional characterization of paired helical filament-tau from Alzheimer’s disease: Demonstration of an additional 74-kDa component and age-related biochemical modifications,” *J. Neurochem.*, vol. 69, no. 2, pp. 834–844, 1997, doi: 10.1046/j.1471-4159.1997.69020834.x.
- [35] V. Lacovich *et al.*, “Tau isoforms imbalance impairs the axonal transport of the amyloid precursor protein in human neurons,” *J. Neurosci.*, vol. 37, no. 1, pp. 58–69, 2017, doi: 10.1523/JNEUROSCI.2305-16.2016.
- [36] G. G. Kovacs, “Invited review: Neuropathology of tauopathies: Principles and practice,” *Neuropathol. Appl. Neurobiol.*, vol. 41, no. 1, pp. 3–23, 2015, doi: 10.1111/nan.12208.
- [37] A. C. Ludolph *et al.*, “Tauopathies with parkinsonism: Clinical spectrum, neuropathologic basis, biological markers, and treatment options,” *Eur. J. Neurol.*, vol. 16, no. 3, pp. 297–309, 2009, doi: 10.1111/j.1468-1331.2008.02513.x.
- [38] M. G. and J. Q. T. Virginia M-Y Lee, “Neurodegenerative tauopathies,” *Genetics*, pp. 1121–1161, 2001.
- [39] E. H. Bigio *et al.*, “Frontal lobe dementia with novel tauopathy: Sporadic multiple system tauopathy with dementia,” *J. Neuropathol. Exp. Neurol.*, vol. 60, no. 4, pp. 328–341, 2001, doi: 10.1093/jnen/60.4.328.
- [40] J. F. Crary *et al.*, “Primary age-related tauopathy (PART): a common pathology associated with human aging,” *Acta Neuropathol.*, vol. 128, no. 6, pp. 755–766, 2014, doi: 10.1007/s00401-014-1349-0.
- [41] M. S. Pollanen *et al.*, “Nodding syndrome in Uganda is a tauopathy,” *Acta Neuropathol.*,

- vol. 136, no. 5, pp. 691–697, 2018, doi: 10.1007/s00401-018-1909-9.
- [42] Z. Mari *et al.*, “Clinico-Pathological Correlation in Progressive Ataxia and Palatal Tremor: A Novel Tauopathy,” *Mov. Disord. Clin. Pract.*, vol. 1, no. 1, pp. 50–56, 2014, doi: 10.1002/mdc3.12014.
- [43] A. F. Gao, A. Faust-Socher, M. Al-Murshed, M. R. Del Bigio, A. E. Lang, and D. G. Munoz, “Progressive ataxia and palatal tremor: Two autopsy cases of a novel tauopathy,” *Mov. Disord.*, vol. 32, no. 10, pp. 1465–1473, 2017, doi: 10.1002/mds.27074.
- [44] I. Grigg *et al.*, “Tauopathy in the young autistic brain: novel biomarker and therapeutic target,” *Transl. Psychiatry*, vol. 10, no. 1, 2020, doi: 10.1038/s41398-020-00904-4.
- [45] J. K. Chambers *et al.*, “The domestic cat as a natural animal model of Alzheimer’s disease,” *Acta Neuropathol. Commun.*, vol. 3, p. 78, 2015, doi: 10.1186/s40478-015-0258-3.
- [46] M. Jeffrey, P. Piccardo, D. L. Ritchie, J. W. Ironside, A. J. E. Green, and G. McGovern, “A naturally occurring bovine tauopathy is geographically widespread in the UK,” *PLoS One*, vol. 10, no. 6, pp. 1–13, 2015, doi: 10.1371/journal.pone.0129499.
- [47] W. Härtig *et al.*, “Abnormally phosphorylated protein tau in the cortex of aged individuals of various mammalian orders,” *Acta Neuropathol.*, vol. 100, no. 3, pp. 305–312, 2000, doi: 10.1007/s004010000183.
- [48] K. A. Josephs, “Current Understanding of Neurodegenerative Diseases Associated With the Protein Tau,” *Mayo Clin. Proc.*, vol. 92, no. 8, pp. 1291–1303, 2017, doi: 10.1016/j.mayocp.2017.04.016.
- [49] M. E. Murray, N. Kouri, W. L. Lin, C. R. Jack, D. W. Dickson, and P. Vemuri, “Clinicopathologic assessment and imaging of tauopathies in neurodegenerative dementias,” *Alzheimer’s Res. Ther.*, vol. 6, no. 1, pp. 1–13, 2014, doi: 10.1186/alzrt231.
- [50] “Mutations Database | ALZFORUM,” 2020. <https://www.alzforum.org/mutations/mapt>.
- [51] R. Mayeux and Y. Stern, “Epidemiology of Alzheimer disease,” *Cold Spring Harb. Perspect. Med.*, vol. 2, no. 8, p. a006239, 2012, doi: 10.1216/RMJ-1977-7-4-775.
- [52] E. Nichols *et al.*, “Global, regional, and national burden of Alzheimer’s disease and other dementias, 1990–2016: a systematic analysis for the Global Burden of Disease Study 2016,” *Lancet Neurol.*, vol. 18, no. 1, pp. 88–106, 2019, doi: 10.1016/S1474-4422(18)30403-4.
- [53] A. Wimo *et al.*, “The worldwide costs of dementia 2015 and comparisons with 2010,” *Alzheimer’s Dement.*, vol. 13, no. 1, pp. 1–7, 2017, doi: 10.1016/j.jalz.2016.07.150.
- [54] United Nations - Department of Economic and Social Affairs, *World Population Ageing 2019*. 2019.
- [55] “Global GDP - Worldometer.” <https://www.worldometers.info/gdp/>.
- [56] J. Xu, Y. Zhang, C. Qiu, and F. Cheng, “Global and regional economic costs of dementia: a systematic review,” *Lancet*, vol. 390, p. S47, 2017, doi: 10.1016/s0140-6736(17)33185-

9.

- [57] A. Wimo, B. Winblad, and L. Jönsson, “An estimate of the total worldwide societal costs of dementia in 2005,” *Alzheimer’s Dement.*, vol. 3, no. 2, pp. 81–91, 2007, doi: 10.1016/j.jalz.2007.02.001.
- [58] T. Karakaya, F. Fußer, D. Prvulovic, and H. Hampel, “Treatment options for tauopathies,” *Curr. Treat. Options Neurol.*, vol. 14, no. 2, pp. 126–136, 2012, doi: 10.1007/s11940-012-0168-7.
- [59] K. Tatiparti, S. Sau, M. A. Rauf, and A. K. Iyer, “Smart treatment strategies for alleviating tauopathy and neuroinflammation to improve clinical outcome in Alzheimer’s disease,” *Drug Discov. Today*, vol. 25, no. 12, pp. 2110–2129, 2020, doi: 10.1016/j.drudis.2020.09.025.
- [60] M. Novak, J. Kabat, and C. M. Wischik, “Molecular characterization of the minimal protease resistant tau unit of the Alzheimer’s disease paired helical filament,” *EMBO J.*, vol. 12, no. 1, pp. 365–370, 1993, doi: 10.1002/j.1460-2075.1993.tb05665.x.
- [61] G. Lippens and B. Gigant, “Elucidating Tau function and dysfunction in the era of cryo-EM,” *J. Biol. Chem.*, vol. 294, no. 24, pp. 9316–9325, 2019, doi: 10.1074/jbc.REV119.008031.
- [62] S. H. Scheres, W. Zhang, B. Falcon, and M. Goedert, “Cryo-EM structures of tau filaments,” *Curr. Opin. Struct. Biol.*, vol. 64, pp. 17–25, 2020, doi: 10.1016/j.sbi.2020.05.011.
- [63] A. W. P. Fitzpatrick *et al.*, “Cryo-EM structures of tau filaments from Alzheimer’s disease,” *Nature*, vol. 547, no. 7662, pp. 185–190, 2017, doi: 10.1038/nature23002.
- [64] H. Braak and E. Braak, “Staging of Alzheimer’s disease-related neurofibrillary changes,” *Neurobiol Aging*, vol. 16, no. 3, pp. 271–278, 1995, doi: 10.1007/s00134-002-1380-9.
- [65] B. Frost, R. L. Jacks, and M. I. Diamond, “Propagation of Tau misfolding from the outside to the inside of a cell,” *J. Biol. Chem.*, vol. 284, no. 19, pp. 12845–12852, 2009, doi: 10.1074/jbc.M808759200.
- [66] A. De Calignon *et al.*, “Propagation of Tau Pathology in a Model of Early Alzheimer’s Disease,” *Neuron*, vol. 73, no. 4, pp. 685–697, 2012, doi: 10.1016/j.neuron.2011.11.033.
- [67] Y. Wang *et al.*, “The release and trans-synaptic transmission of Tau via exosomes,” *Mol. Neurodegener.*, vol. 12, no. 1, pp. 1–25, 2017, doi: 10.1186/s13024-016-0143-y.
- [68] S. Dujardin *et al.*, “Ectosomes: A new mechanism for non-exosomal secretion of Tau protein,” *PLoS One*, vol. 9, no. 6, pp. 28–31, 2014, doi: 10.1371/journal.pone.0100760.
- [69] M. Tardivel *et al.*, “Tunneling nanotube (TNT)-mediated neuron-to neuron transfer of pathological Tau protein assemblies,” *Acta Neuropathol. Commun.*, vol. 4, no. 1, p. 117, 2016, doi: 10.1186/s40478-016-0386-4.
- [70] B. B. Holmes *et al.*, “Heparan sulfate proteoglycans mediate internalization and propagation of specific proteopathic seeds,” *Proc. Natl. Acad. Sci. U. S. A.*, vol. 110, no.

- 33, 2013, doi: 10.1073/pnas.1301440110.
- [71] L. D. Evans *et al.*, “Extracellular Monomeric and Aggregated Tau Efficiently Enter Human Neurons through Overlapping but Distinct Pathways,” *Cell Rep.*, vol. 22, no. 13, pp. 3612–3624, 2018, doi: 10.1016/j.celrep.2018.03.021.
- [72] G. Eskandari-Sedighi *et al.*, “The CNS in inbred transgenic models of 4-repeat Tauopathy develops consistent tau seeding capacity yet focal and diverse patterns of protein deposition,” *Mol. Neurodegener.*, vol. 12, no. 1, pp. 1–27, 2017, doi: 10.1186/s13024-017-0215-7.
- [73] C. Gonzalez, E. Armijo, J. Bravo-Alegria, A. Becerra-Calixto, C. E. Mays, and C. Soto, “Modeling amyloid beta and tau pathology in human cerebral organoids,” *Mol. Psychiatry*, vol. 23, no. 12, pp. 2363–2374, 2018, doi: 10.1038/s41380-018-0229-8.
- [74] D. W. Sanders *et al.*, “Distinct tau prion strains propagate in cells and mice and define different tauopathies,” *Neuron*, vol. 82, no. 6, pp. 1271–1288, 2014, doi: 10.1016/j.neuron.2014.04.047.
- [75] T. Guo, W. Noble, and D. P. Hanger, “Roles of tau protein in health and disease,” *Acta Neuropathol.*, vol. 133, no. 5, pp. 665–704, 2017, doi: 10.1007/s00401-017-1707-9.
- [76] K. Iqbal *et al.*, “Tau pathology in Alzheimer disease and other tauopathies,” *Biochim. Biophys. Acta - Mol. Basis Dis.*, vol. 1739, no. 2, pp. 198–210, 2005, doi: 10.1016/j.bbadis.2004.09.008.
- [77] G. Lindwall and R. D. Cole, “Phosphorylation affects the ability of tau protein to promote microtubule assembly,” *J. Biol. Chem.*, vol. 259, no. 8, pp. 5301–5305, 1984, doi: 10.1016/s0021-9258(17)42989-9.
- [78] E. M. Mandelkow, J. Biernat, G. Drewes, N. Gustke, B. Trinczek, and E. Mandelkow, “Tau domains, phosphorylation, and interactions with microtubules,” *Neurobiol. Aging*, vol. 16, no. 3, pp. 355–362, 1995, doi: 10.1016/0197-4580(95)00025-A.
- [79] J. J. Heinisch and R. Brandt, “Signaling pathways and posttranslational modifications of tau in Alzheimer’s disease: The humanization of yeast cells,” *Microb. Cell*, vol. 3, no. 4, pp. 135–146, 2016, doi: 10.15698/mic2016.04.489.
- [80] G. Lippens *et al.*, “Tau aggregation in Alzheimer’s disease: what role for phosphorylation?,” *Prion*, vol. 1, no. 1, pp. 21–25, 2007, doi: 10.4161/pri.1.1.4055.
- [81] K. Nakamura *et al.*, “Proline isomer-specific antibodies reveal the early pathogenic tau conformation in Alzheimer’s disease,” *Cell*, vol. 149, no. 1, pp. 232–244, 2012, doi: 10.1016/j.cell.2012.02.016.
- [82] S. Ikegami, A. Harada, and N. Hirokawa, “Muscle weakness, hyperactivity, and impairment in fear conditioning in tau-deficient mice,” *Neurosci. Lett.*, vol. 279, no. 3, pp. 129–132, 2000, doi: 10.1016/S0304-3940(99)00964-7.
- [83] S. K. Kaufman *et al.*, “Tau Prion Strains Dictate Patterns of Cell Pathology, Progression Rate, and Regional Vulnerability In Vivo,” *Neuron*, vol. 92, no. 4, pp. 796–812, 2016, doi: 10.1016/j.neuron.2016.09.055.

- [84] N. Daude *et al.*, “Diverse , evolving conformer populations drive distinct phenotypes in frontotemporal lobar degeneration caused by the same MAPT - P301L mutation,” *Acta Neuropathol.*, no. 0123456789, 2020, doi: 10.1007/s00401-020-02148-4.
- [85] Y. Fichou *et al.*, “Cofactors are essential constituents of stable and seeding-active tau fibrils,” *Proc. Natl. Acad. Sci. U. S. A.*, vol. 115, no. 52, pp. 13234–13239, 2018, doi: 10.1073/pnas.1810058115.
- [86] Y. Fichou, N. A. Eschmann, T. J. Keller, and S. Han, *Conformation-based assay of tau protein aggregation*, 1st ed., vol. 141. Elsevier Inc., 2017.
- [87] T. K. Karikari *et al.*, “Distinct Conformations, Aggregation and Cellular Internalization of Different Tau Strains,” *Front. Cell. Neurosci.*, vol. 13, no. July, pp. 1–16, 2019, doi: 10.3389/fncel.2019.00296.
- [88] B. Falcon *et al.*, “Conformation Determines the Seeding Potencies of Native and Recombinant Tau Aggregates,” *J. Biol. Chem.*, vol. 290, no. 2, pp. 1049–1065, 2015, doi: 10.1074/jbc.M114.589309.
- [89] A. M. Sharma, T. L. Thomas, D. R. Woodard, O. M. Kashmer, and M. I. Diamond, “Tau monomer encodes strains,” *Elife*, vol. 7, pp. 1–20, 2018, doi: 10.7554/eLife.37813.
- [90] D. Ajit *et al.*, “A unique tau conformation generated by an acetylation- mimic substitution modulates P301S-dependent tau pathology and hyperphosphorylation,” *J. Biol. Chem.*, vol. 294, no. 45, pp. 16698–16711, 2019, doi: 10.1074/jbc.RA119.009674.
- [91] Z. He *et al.*, “Transmission of tauopathy strains is independent of their isoform composition,” *Nat. Commun.*, vol. 11, no. 7, 2020, doi: 10.1038/s41467-019-13787-x.
- [92] G. Eskandari-sedighi, L. M. Cortez, J. Yang, N. Daude, and K. Shmeit, “Quaternary Structure Changes for PrP Sc Predate PrP C Downregulation and Neuronal Death During Progression of Experimental Scrapie Disease,” *Mol. Neurobiol.*, vol. 58, pp. 375–390, 2021.
- [93] C. Roe, M. Behrens, C. Xiong, J. Miller, and J. Morris, “Alzheimer disease and cancer,” *Neurology*, vol. 64, no. 5, pp. 895–8, 2005, doi: 10.1097/01.SMJ.0000167699.56872.56.
- [94] D. A. Bennett and S. Leurgans, “Is there a link between cancer and Alzheimer disease?,” *Neurology*, vol. 74, no. 2, pp. 100–101, 2010, doi: 10.1212/WNL.0b013e3181cbb89a.
- [95] C. M. Roe *et al.*, “Cancer linked to Alzheimer disease but not vascular dementia,” *Neurology*, vol. 74, no. 2, pp. 106–112, 2010, doi: 10.1212/WNL.0b013e3181c91873.
- [96] R. Inzelberg and J. Jankovic, “Are parkinson disease patients protected from some but not all cancers?: Reply,” *Neurology*, vol. 71, no. 20, pp. 1650–1651, 2008, doi: 10.1212/01.wnl.0000339367.54460.8c.
- [97] R. Gargini, B. Segura-Collar, and P. Sánchez-Gómez, “Novel functions of the neurodegenerative-related gene tau in cancer,” *Front. Aging Neurosci.*, vol. 11, no. AUG, pp. 1–11, 2019, doi: 10.3389/fnagi.2019.00231.
- [98] M. Sola *et al.*, “Tau affects P53 function and cell fate during the DNA damage response,”

- Commun. Biol.*, vol. 3, no. 1, pp. 1–15, 2020, doi: 10.1038/s42003-020-0975-4.
- [99] D. Hristodorov *et al.*, “Microtubule-associated protein tau facilitates the targeted killing of proliferating cancer cells in vitro and in a xenograft mouse tumour model in vivo,” *Br. J. Cancer*, vol. 109, no. 6, pp. 1570–1578, 2013, doi: 10.1038/bjc.2013.457.
- [100] R. Gargini *et al.*, “The IDH-TAU-EGFR triad defines the neovascular landscape of diffuse gliomas,” *Sci. Transl. Med.*, vol. 12, no. 527, pp. 1–16, 2020, doi: 10.1126/scitranslmed.aax1501.
- [101] A. Takashima, B. Wolozin, and L. Buee, *Tau Biology*, vol. 1184. 2019.
- [102] A. M. A. Brands, G. J. Biessels, E. H. F. de Jaan, L. J. Kappelle, and R. P. C. Kessels, “The effects of Type 1 Diabetes on cognitive performance: a meta-analysis,” *Diabetes Care*, vol. 28, no. December 2004, pp. 726–735, 2005.
- [103] T. Hershey, N. Bhargava, M. Sadler, N. H. White, and S. Craft, “Conventional versus intensive diabetes therapy in children with Type 1 Diabetes,” *Diabetes Care*, vol. 22, no. 8, pp. 1–7, 1999.
- [104] L. A. Profenno, A. P. Porsteinsson, and S. V. Faraone, “Meta-Analysis of Alzheimer’s Disease Risk with Obesity, Diabetes, and Related Disorders,” *Biol. Psychiatry*, vol. 67, no. 6, pp. 505–512, 2010, doi: 10.1016/j.biopsych.2009.02.013.
- [105] B. O’Nuallain, A. D. Williams, P. Westermark, and R. Wetzel, “Seeding Specificity in Amyloid Growth Induced by Heterologous Fibrils,” *J. Biol. Chem.*, vol. 279, no. 17, pp. 17490–17499, 2004, doi: 10.1074/jbc.M311300200.
- [106] P. Bharadwaj *et al.*, “Amylin and beta amyloid proteins interact to form amorphous heterocomplexes with enhanced toxicity in neuronal cells,” *Sci. Rep.*, vol. 10, no. 1, pp. 1–14, 2020, doi: 10.1038/s41598-020-66602-9.
- [107] J. N. Fawver *et al.*, “Islet Amyloid Polypeptide (IAPP): A Second Amyloid in Alzheimer’s Disease,” *Curr. Alzheimer Res.*, vol. 11, no. 10, pp. 928–40, 2014, [Online]. Available: <http://www.ncbi.nlm.nih.gov/>.
- [108] D. M. Ouwens *et al.*, “Cerebrospinal fluid levels of Alzheimer’s disease biomarkers in middle-aged patients with type 1 diabetes,” *Diabetologia*, vol. 57, no. 10, pp. 2208–2214, 2014, doi: 10.1007/s00125-014-3333-6.
- [109] C. Moran, R. Beare, T. G. Phan, D. G. Bruce, M. L. Callisaya, and V. Srikanth, “Type 2 diabetes mellitus and biomarkers of neurodegeneration,” *Neurology*, vol. 85, no. 13, pp. 1123–1130, 2015, doi: 10.1212/WNL.0000000000001982.
- [110] Y. D. Ke, F. Delerue, A. Gladbach, J. Götz, and L. M. Ittner, “Experimental diabetes mellitus exacerbates Tau pathology in a transgenic mouse model of Alzheimer’s disease,” *PLoS One*, vol. 4, no. 11, 2009, doi: 10.1371/journal.pone.0007917.
- [111] T. L. Platt, T. L. Beckett, K. Kohler, D. M. Niedowicz, and M. P. Murphy, “Obesity, diabetes, and leptin resistance promote tau pathology in a mouse model of disease,” *Neuroscience*, vol. 315, pp. 162–174, 2016, doi: 10.1016/j.neuroscience.2015.12.011.

- [112] T. Niccoli and L. Partridge, “Ageing as a risk factor for disease,” *Curr. Biol.*, vol. 22, no. 17, pp. R741–R752, 2012, doi: 10.1016/j.cub.2012.07.024.
- [113] E. Jaul and J. Barron, “Age-Related Diseases and Clinical and Public Health Implications for the 85 Years Old and Over Population,” *Front. Public Heal.*, vol. 5, no. December, pp. 1–7, 2017, doi: 10.3389/fpubh.2017.00335.
- [114] A. Quadros, O. I. Weeks, and G. Ait-Ghezala, “Role of tau in Alzheimer’s dementia and other neurodegenerative diseases,” *J. Appl. Biomed.*, vol. 5, no. 1, pp. 1–12, 2007, doi: 10.32725/jab.2007.001.
- [115] R. Guerreiro and J. Bras, “The age factor in Alzheimer’s disease,” *Genome Med.*, vol. 7, no. 1, pp. 1–3, 2015, doi: 10.1186/s13073-015-0232-5.
- [116] J. Vijg and Y. Suh, “Genome instability and aging,” *Annu. Rev. Physiol.*, vol. 75, pp. 645–668, 2013, doi: 10.1146/annurev-physiol-030212-183715.
- [117] G. Aubert and P. M. Lansdorp, “Telomeres and aging,” *Physiol. Rev.*, vol. 88, no. 2, pp. 557–579, 2008, doi: 10.1152/physrev.00026.2007.
- [118] A. Trifunovic and N. G. Larsson, “Mitochondrial dysfunction as a cause of ageing,” *J. Intern. Med.*, vol. 263, no. 2, pp. 167–178, 2008, doi: 10.1111/j.1365-2796.2007.01905.x.
- [119] S. N. Saldanha and L. P. Watanabe, “Epigenetics and Aging,” *Epigenetics and Dermatology*, vol. 4, no. July, pp. 379–406, 2015, doi: 10.1016/B978-0-12-800957-4.00018-7.
- [120] F. Martins, J. Sousa, C. D. Pereira, O. A. B. da Cruz e Silva, and S. Rebelo, “Nuclear envelope dysfunction and its contribution to the aging process,” *Aging Cell*, vol. 19, no. 5, pp. 1–17, 2020, doi: 10.1111/acel.13143.
- [121] E. Beauregard-Lacroix *et al.*, “A variant of neonatal progeroid syndrome, or Wiedemann–Rautenstrauch syndrome, is associated with a nonsense variant in POLR3GL,” *Eur. J. Hum. Genet.*, vol. 28, no. 4, pp. 461–468, 2020, doi: 10.1038/s41431-019-0539-6.
- [122] A. Masotti *et al.*, “Keppen-lubinsky syndrome is caused by mutations in the inwardly rectifying K<sup>+</sup> channel encoded by KCNJ6,” *Am. J. Hum. Genet.*, vol. 96, no. 2, pp. 295–300, 2015, doi: 10.1016/j.ajhg.2014.12.011.
- [123] T. Janse, A. De Paepe, N. Lutyinck, and G. Plewig, “COL3A1 mutation leading to acrogeria (Gottron type),” *Br. J. Dermatol.*, vol. 142, pp. 177–180, 2000.
- [124] H. Rezai-Delui, N. Lotfi, G. Mamoori, and M. B. Rahimi, “Hereditary Gottron’s acrogeria with recessive transmission: A report of four cases in one family,” *Pediatr. Radiol.*, vol. 29, no. 2, pp. 124–130, 1999, doi: 10.1007/s002470050555.
- [125] M. Ritelli, C. Dordoni, V. Cinquina, M. Venturini, P. Calzavara-Pinton, and M. Colombi, “Expanding the clinical and mutational spectrum of B4GALT7-spondylodysplastic Ehlers-Danlos syndrome,” *Orphanet J. Rare Dis.*, vol. 12, no. 1, pp. 1–7, 2017, doi: 10.1186/s13023-017-0704-3.
- [126] M. H. Guo *et al.*, “Redefining the Progeroid Form of Ehlers-Danlos Syndrome: Report of

- the Fourth Patient with B4GALT7 Deficiency and Review of the Literature,” *Am J Med Genet A*, vol. 161, no. 10, pp. 2519–2527, 2013, doi: 10.1055/s-0038-1632965.
- [127] L. B. Gordon *et al.*, “Impact of farnesylation inhibitors on survival in Hutchinson-Gilford progeria syndrome,” *Circulation*, vol. 130, no. 1, pp. 27–34, 2014, doi: 10.1161/CIRCULATIONAHA.113.008285.
- [128] K. Piekarowicz, M. Machowska, V. Dzianisava, and R. Rzepecki, “Hutchinson-Gilford Progeria Syndrome—Current Status and Prospects for Gene Therapy Treatment,” *Cells*, vol. 8, no. 2, p. 88, 2019, doi: 10.3390/cells8020088.
- [129] R. L. Pollex and R. A. Hegele, “Hutchinson-Gilford progeria syndrome,” *Clin. Genet.*, vol. 66, no. 5, pp. 375–381, 2004, doi: 10.1111/j.1399-0004.2004.00315.x.
- [130] F. L. DeBusk, “The Hutchinson-Gilford progeria syndrome. Report of 4 cases and review of the literature,” *J. Pediatr.*, vol. 80, no. 4 PART 2, pp. 697–724, 1972, doi: 10.1016/S0022-3476(72)80229-4.
- [131] Y. Y. Shevelyov and S. V. Ulianov, “The Nuclear Lamina as an Organizer of Chromosome Architecture,” *Cells*, vol. 8, no. 2, p. 136, 2019, doi: 10.3390/cells8020136.
- [132] C. J. Hutchison and H. J. Worman, “A-type lamins: Guardians of the soma?,” *Nat. Cell Biol.*, vol. 6, no. 11, pp. 1062–1067, 2004, doi: 10.1038/ncb1104-1062.
- [133] Q. Ye and H. J. Worman, “Protein-protein interactions between human nuclear lamins expressed in yeast,” *Exp. Cell Res.*, vol. 219, pp. 292–298, 1995.
- [134] T. Kolb, K. Maaß, M. Hergt, U. Aebi, and H. Herrmann, “Lamin A and lamin C form homodimers and coexist in higher complex forms both in the nucleoplasmic fraction and in the lamina of cultured human cells,” *Nucleus*, vol. 2, no. 5, 2011, doi: 10.4161/nucl.2.5.17765.
- [135] J. Ahn *et al.*, “Structural basis for lamin assembly at the molecular level,” *Nat. Commun.*, vol. 10, no. 1, pp. 1–12, 2019, doi: 10.1038/s41467-019-11684-x.
- [136] J. Swift *et al.*, “Nuclear lamin-A scales with tissue stiffness and enhances matrix-directed differentiation,” *Science (80-. )*, vol. 341, no. 6149, 2013, doi: 10.1126/science.1240104.
- [137] G. Schatten *et al.*, “Nuclear lamins and peripheral nuclear antigens during fertilization and embryogenesis in mice and sea urchins,” *Proc. Natl. Acad. Sci. U. S. A.*, vol. 82, no. 14, pp. 4727–4731, 1985, doi: 10.1073/pnas.82.14.4727.
- [138] H. D. M. Coutinho, V. S. Falcão-Silva, G. Gonçalves, and R. da Nóbrega, “Molecular ageing in progeroid syndromes: Hutchinson-Gilford progeria syndrome as a model,” *Immun. Ageing*, vol. 6, 2009, doi: 10.1186/1742-4933-6-4.
- [139] R. D. Goldman *et al.*, “Accumulation of mutant lamin A progressive changes in nuclear architecture in Hutchinson-Gilford progeria syndrome,” *Proc. Natl. Acad. Sci. U. S. A.*, vol. 101, no. 24, pp. 8963–8968, 2004, doi: 10.1073/pnas.0402943101.
- [140] J. Liu *et al.*, “HP1 $\alpha$  mediates defective heterochromatin repair and accelerates senescence in Zmpste24 -deficient cells,” *Cell Cycle*, vol. 13, no. 8, pp. 1237–1247, 2014, doi:

10.4161/cc.28105.

- [141] H. Zhang *et al.*, “Loss of H3K9me3 correlates with ATM activation and histone H2AX phosphorylation deficiencies in Hutchinson-Gilford progeria syndrome,” *PLoS One*, vol. 11, no. 12, pp. 1–25, 2016, doi: 10.1371/journal.pone.0167454.
- [142] J. B. Kelley *et al.*, “The Defective Nuclear Lamina in Hutchinson-Gilford Progeria Syndrome Disrupts the Nucleocytoplasmic Ran Gradient and Inhibits Nuclear Localization of Ubc9,” *Mol. Cell. Biol.*, vol. 31, no. 16, pp. 3378–3395, 2011, doi: 10.1128/mcb.05087-11.
- [143] C. J. Snow, A. Dar, A. Dutta, R. H. Kehlenbach, and B. M. Paschal, “Defective nuclear import of Tpr in Progeria reflects the Ran sensitivity of large cargo transport,” *J. Cell Biol.*, vol. 201, no. 4, pp. 541–557, 2013, doi: 10.1083/jcb.201212117.
- [144] P. Scaffidi and T. Misteli, “Lamin A-Dependent Nuclear Defects in Human Aging,” *Science (80-. )*, vol. 312, no. 5776, pp. 1059–1063, 2006.
- [145] D. Mcclintock *et al.*, “The Mutant Form of Lamin A that Causes Hutchinson- Gilford Progeria Is a Biomarker of Cellular Aging in Human Skin,” *PLoS One*, vol. 2, no. 12, p. e1269, 2007, doi: 10.1371/journal.pone.0001269.
- [146] V. V. Ashapkin, L. I. Kutueva, S. Y. Kurchashova, and I. I. Kireev, “Are there common mechanisms between the Hutchinson-Gilford progeria syndrome and natural aging?,” *Front. Genet.*, vol. 10, no. MAY, pp. 1–14, 2019, doi: 10.3389/fgene.2019.00455.
- [147] Y. Tonoyama *et al.*, “Abnormal nuclear morphology is independent of longevity in a *zmpste24*-deficient fish model of Hutchinson-Gilford progeria syndrome (HGPS),” *Comp. Biochem. Physiol. Part - C Toxicol. Pharmacol.*, vol. 209, no. December 2017, pp. 54–62, 2018, doi: 10.1016/j.cbpc.2018.03.006.
- [148] K. Cao *et al.*, “Progerin and telomere dysfunction collaborate to trigger cellular senescence in normal human fibroblasts,” *J. Clin. Invest.*, vol. 121, no. 7, pp. 2833–2844, 2011, doi: 10.1172/JCI43578.
- [149] S. Gonzalo and R. Kreienkamp, “DNA repair defects and genome instability in Hutchinson-Gilford Progeria Syndrome,” *Curr. Opin. Cell Biol.*, vol. 34, pp. 75–83, 2015, doi: 10.1016/j.ceb.2015.05.007.
- [150] E. J. Lesnefsky, Q. Chen, and C. L. Hoppel, “Mitochondrial Metabolism in Aging Heart,” *Circ. Res.*, vol. 118, no. 10, pp. 1593–1611, 2016, doi: 10.1161/CIRCRESAHA.116.307505.
- [151] I. Kasapoğlu and E. Seli, “Mitochondrial Dysfunction and Ovarian Aging,” *Endocrinol. (United States)*, vol. 161, no. 2, pp. 1–11, 2020, doi: 10.1210/endo/bqaa001.
- [152] J. Faitg, O. Reynaud, J. P. Leduc-Gaudet, and G. Gouspillou, “Dysfonctions mitochondriales et vieillissement musculaire,” *Medecine/Sciences*, vol. 33, no. 11, pp. 955–962, 2017, doi: 10.1051/medsci/20173311012.
- [153] J. Rivera-Torres *et al.*, “Identification of mitochondrial dysfunction in Hutchinson-Gilford progeria syndrome through use of stable isotope labeling with amino acids in cell culture,”

- J. Proteomics*, vol. 91, pp. 466–477, 2013, doi: 10.1016/j.jprot.2013.08.008.
- [154] D. McHugh and J. Gil, “Senescence and aging: Causes, consequences, and therapeutic avenues,” *J. Cell Biol.*, vol. 217, no. 1, pp. 65–77, 2018, doi: 10.1083/jcb.201708092.
- [155] K. Wheaton *et al.*, “Progerin-Induced Replication Stress Facilitates Premature Senescence in,” *Mol. Cell. Biol.*, vol. 37, no. 14, pp. 1–18, 2017.
- [156] M. A. Goodell and T. A. Rando, “Stem cells and healthy aging,” *Science (80-. )*, vol. 350, no. 6265, pp. 1199–1204, 2015, doi: 10.1126/science.aab3388.
- [157] T. M. Paola Scaffidi, “Lamin A-dependent misregulation of adult stem cells associated with accelerated ageing,” *Stem Cells*, vol. 10, no. 4, pp. 452–459, 2008.
- [158] Z. Wu *et al.*, “Differential stem cell aging kinetics in Hutchinson-Gilford progeria syndrome and Werner syndrome,” *Protein Cell*, vol. 9, no. 4, pp. 333–350, 2018, doi: 10.1007/s13238-018-0517-8.
- [159] C. L. Klaips, G. G. Jayaraj, and F. U. Hartl, “Pathways of cellular proteostasis in aging and disease,” *J. Cell Biol.*, vol. 217, no. 1, pp. 51–63, 2018, doi: 10.1083/jcb.201709072.
- [160] J. Mateos *et al.*, “iTRAQ-based analysis of progerin expression reveals mitochondrial dysfunction, reactive oxygen species accumulation and altered proteostasis,” *Stem Cell Res. Ther.*, vol. 6, no. 1, pp. 1–17, 2015, doi: 10.1186/s13287-015-0110-5.
- [161] R. C. M. Hennekam, “Hutchinson–Gilford Progeria Syndrome: Review of the Phenotype,” *Am. J. Med. Genet.*, vol. 140A, pp. 2603–2624, 2006, doi: 10.1002/ajmg.a.
- [162] N. J. Ullrich and L. B. Gordon, *Hutchinson-Gilford progeria syndrome*, 1st ed., vol. 132. Elsevier B.V., 2015.
- [163] C. N. Harada, M. C. Natelson Love, and K. Triebel, “Normal cognitive aging,” *Clin. Geriatr. Med.*, vol. 29, no. 4, pp. 737–752, 2013, doi: 10.1016/j.cger.2013.07.002.Normal.
- [164] A. Tripathi, “New cellular and molecular approaches to ageing brain,” *Ann. Neurosci.*, vol. 19, no. 4, pp. 177–182, 2012.
- [165] N. A. Bishop, T. Lu, and B. A. Yankner, “Neural mechanisms of ageing and cognitive decline,” *Nature*, vol. 464, no. 7288, pp. 529–535, 2010, doi: 10.1038/nature08983.
- [166] K. B. Walhovd *et al.*, “Consistent neuroanatomical age-related volume differences across multiple samples,” *Neurobiol. Aging*, vol. 32, no. 5, pp. 916–932, 2011, doi: 10.1016/j.neurobiolaging.2009.05.013.
- [167] L. Nyberg *et al.*, “Longitudinal evidence for diminished frontal cortex function in aging,” *Proc. Natl. Acad. Sci. U. S. A.*, vol. 107, no. 52, pp. 22682–22686, 2010, doi: 10.1073/pnas.1012651108.
- [168] S. M. Morillo, P. Escoll, A. De La Hera, and J. M. Frade, “Somatic tetraploidy in specific chick retinal ganglion cells induced by nerve growth factor,” *Proc. Natl. Acad. Sci. U. S. A.*, vol. 107, no. 1, pp. 109–114, 2010, doi: 10.1073/pnas.0906121107.
- [169] M. Pacal and R. Bremner, “Mapping differentiation kinetics in the mouse retina reveals an

- extensive period of cell cycle protein expression in post-mitotic newborn neurons,” *Dev. Dyn.*, vol. 241, no. 10, pp. 1525–1544, 2012, doi: 10.1002/dvdy.23840.
- [170] J. N. Trollor and M. J. Valenzuela, “Brain ageing in the new millennium,” *Aust. N. Z. J. Psychiatry*, vol. 35, no. 6, pp. 788–805, 2001, doi: 10.1046/j.1440-1614.2001.00969.x.
- [171] B. E. Tomlinson, G. Blessed, and M. Roth, “Observations on the brains of non-demented old people,” *J. Neurol. Sci.*, vol. 7, no. 2, pp. 331–356, 1968, doi: 10.1016/0022-510X(68)90154-8.
- [172] V. J. Lowe *et al.*, “Widespread brain tau and its association with ageing, Braak stage and Alzheimer’s dementia,” *Brain*, vol. 141, no. 1, pp. 271–287, 2018, doi: 10.1093/brain/awx320.
- [173] D. F. Fischer *et al.*, “Long-term proteasome dysfunction in the mouse brain by expression of aberrant ubiquitin,” *Neurobiol. Aging*, vol. 30, no. 6, pp. 847–863, 2009, doi: 10.1016/j.neurobiolaging.2008.06.009.
- [174] B. Ravikumar *et al.*, “Inhibition of mTOR induces autophagy and reduces toxicity of polyglutamine expansions in fly and mouse models of Huntington disease,” *Nat. Genet.*, vol. 36, no. 6, pp. 585–595, 2004, doi: 10.1038/ng1362.
- [175] S. W. Min *et al.*, “SIRT1 deacetylates tau and reduces pathogenic tau spread in a mouse model of tauopathy,” *J. Neurosci.*, vol. 38, no. 15, pp. 3680–3688, 2018, doi: 10.1523/JNEUROSCI.2369-17.2018.
- [176] M. Kuro-o *et al.*, “Mutation of the mouse *klotho* gene leads to a syndrome resembling ageing,” *Chemtracts*, vol. 12, no. 10, pp. 703–707, 1997.
- [177] K. Dolegowska, M. Marchelek-Mysliwiec, M. Nowosiad-Magda, M. Slawinski, and B. Dolegowska, “FGF19 subfamily members: FGF19 and FGF21,” *J. Physiol. Biochem.*, vol. 75, no. 2, pp. 229–240, 2019, doi: 10.1007/s13105-019-00675-7.
- [178] P. Gaudet, M. S. Livstone, S. E. Lewis, and P. D. Thomas, “Phylogenetic-based propagation of functional annotations within the Gene Ontology consortium,” *Brief. Bioinform.*, vol. 12, no. 5, pp. 449–462, 2011, doi: 10.1093/bib/bbr042.
- [179] M. Kuro-o, “Klotho and aging,” *Biochim. Biophys. Acta - Gen. Subj.*, vol. 1790, no. 10, pp. 1049–1058, 2009, doi: 10.1016/j.bbagen.2009.02.005.
- [180] T. Nagai *et al.*, “Cognition impairment in the genetic model of aging *klotho* gene mutant mice: a role of oxidative stress,” *The FASEB journal : official publication of the Federation of American Societies for Experimental Biology*, vol. 17, no. 1, pp. 50–52, 2003, doi: 10.1096/fj.02-0448fje.
- [181] J. Leon *et al.*, “Peripheral Elevation of a *Klotho* Fragment Enhances Brain Function and Resilience in Young, Aging, and  $\alpha$ -Synuclein Transgenic Mice,” *Cell Rep.*, vol. 20, no. 6, pp. 1360–1371, 2017, doi: 10.1016/j.celrep.2017.07.024.
- [182] D. B. Dubal *et al.*, “Life extension factor *klotho* prevents mortality and enhances cognition in hAPP transgenic mice,” *J. Neurosci.*, vol. 35, no. 6, pp. 2358–2371, 2015, doi: 10.1523/JNEUROSCI.5791-12.2015.

- [183] M. E. Belloy, V. Napolioni, S. S. Han, Y. Le Guen, and M. D. Greicius, “Association of Klotho -VS Heterozygosity with Risk of Alzheimer Disease in Individuals Who Carry APOE4,” *JAMA Neurol.*, vol. 77, no. 7, pp. 849–862, 2020, doi: 10.1001/jamaneurol.2020.0414.
- [184] I. Akiguchi *et al.*, “SAMP8 mice as a neuropathological model of accelerated brain aging and dementia: Toshio Takeda’s legacy and future directions,” *Neuropathology*, vol. 37, no. 4, pp. 293–305, 2017, doi: 10.1111/neup.12373.
- [185] A. R. Folgueras, S. Freitas-Rodríguez, G. Velasco, and C. López-Otín, “Mouse models to disentangle the hallmarks of human aging,” *Circ. Res.*, vol. 123, no. 7, pp. 905–924, 2018, doi: 10.1161/CIRCRESAHA.118.312204.
- [186] A. Zaghini *et al.*, “Long term breeding of the Lmna G609G progeric mouse: Characterization of homozygous and heterozygous models,” *Exp. Gerontol.*, vol. 130, no. October 2019, p. 110784, 2020, doi: 10.1016/j.exger.2019.110784.
- [187] A. Eggel and T. Wyss-Coray, “A revival of parabiosis in biomedical research,” *Swiss Med. Wkly.*, vol. 144, no. February, pp. 1–9, 2014, doi: 10.4414/smw.2014.13914.
- [188] S. A. Villeda *et al.*, “Young blood reverses age-related impairments in cognitive function and synaptic plasticity in mice,” *Nat. Med.*, vol. 20, no. 6, pp. 659–663, 2014, doi: 10.1038/nm.3569.
- [189] R. Pálovics, A. Keller, N. Schaum, W. Tan, and T. Fehlmann, “Molecular hallmarks of heterochronic parabiosis at single cell resolution,” 2020.
- [190] T. Murakami *et al.*, “Cortical neuronal and glial pathology in TgTauP301L transgenic mice: Neuronal degeneration, memory disturbance, and phenotypic variation,” *Am. J. Pathol.*, vol. 169, no. 4, pp. 1365–1375, 2006, doi: 10.2353/ajpath.2006.051250.
- [191] S. Dujardin *et al.*, “Tau molecular diversity contributes to clinical heterogeneity in Alzheimer’s disease,” *Nat. Med.*, vol. 26, no. 8, pp. 1256–1263, 2020, doi: 10.1038/s41591-020-0938-9.
- [192] M. Ramsden *et al.*, “Age-dependent neurofibrillary tangle formation, neuron loss, and memory impairment in a mouse model of human tauopathy (P301L),” *J. Neurosci.*, vol. 25, no. 46, pp. 10637–10647, 2005, doi: 10.1523/JNEUROSCI.3279-05.2005.
- [193] Y. Yoshiyama *et al.*, “Synapse Loss and Microglial Activation Precede Tangles in a P301S Tauopathy Mouse Model,” *Neuron*, vol. 53, no. 3, pp. 337–351, 2007, doi: 10.1016/j.neuron.2007.01.010.
- [194] B. Allen *et al.*, “Abundant tau filaments and neurodegeneration in mice transgenic for human P301S tau,” *J. Neuropathol. Exp. Neurol.*, vol. 22, no. 21, pp. 9340–9351, 2002, [Online]. Available: isi:000175724500174.
- [195] T. Ishihara *et al.*, “Age-dependent emergence and progression of a tauopathy in transgenic mice overexpressing the shortest human tau isoform,” *Neuron*, vol. 24, no. 3, pp. 751–762, 1999, doi: 10.1016/S0896-6273(00)81127-7.
- [196] J. Lewis *et al.*, “Neurofibrillary tangles, amyotrophy and progressive motor disturbance in

- mice expressing mutant (P301L)tau protein,” *Nat. Genet.*, vol. 25, no. 4, pp. 402–405, 2000, doi: 10.1038/78078.
- [197] C. Coffinier, H. Jung, C. Nobumori, S. Chang, Y. Tu, and T. M. Magin, “Deficiencies in lamin B1 and lamin B2 cause neurodevelopmental defects and distinct nuclear shape abnormalities in neurons,” *MBoC*, vol. 22, 2011, doi: 10.1091/mbc.E11-06-0504.
- [198] Y. Kim *et al.*, “Mouse B-Type Lamins Are Required for Proper Organogenesis But Not by Embryonic Stem Cells,” *Science (80-. )*, vol. 334, pp. 1706–1711, 2011.
- [199] H. J. Jung *et al.*, “Regulation of prelamin A but not lamin C by miR-9, a brain-specific microRNA,” *Proc. Natl. Acad. Sci. U. S. A.*, vol. 109, no. 7, pp. 423–431, 2012, doi: 10.1073/pnas.1111780109.
- [200] L. G. Fong *et al.*, “Prelamin A and lamin A appear to be dispensable in the nuclear lamina,” *J Clin Invest.*, vol. 116, no. 3, pp. 743–752, 2006, doi: 10.1172/JCI27125.with.
- [201] M. De Toledo *et al.*, “Lamin C Counteracts Glucose Intolerance in Aging , Obesity , and Diabetes Through b -Cell Adaptation,” *Diabetes*, vol. 69, pp. 647–660, 2020, doi: 10.2337/db19-0377/-/DC1.J.-S.A.
- [202] F. Wang *et al.*, “Generation of a Hutchinson–Gilford progeria syndrome monkey model by base editing,” *Protein Cell*, vol. 11, no. 11, pp. 809–824, 2020, doi: 10.1007/s13238-020-00740-8.
- [203] J. H. Baek *et al.*, “Expression of progerin in aging mouse brains reveals structural nuclear abnormalities without detectable significant alterations in gene expression, hippocampal stem cells or behavior,” *Hum. Mol. Genet.*, vol. 24, no. 5, pp. 1305–1321, 2015, doi: 10.1093/hmg/ddu541.
- [204] J. D. Miller *et al.*, “Human iPSC-based modeling of late-onset disease via progerin-induced aging,” *Cell Stem Cell*, vol. 13, no. 6, pp. 691–705, 2013, doi: 10.1016/j.stem.2013.11.006.
- [205] A. Hattori *et al.*, “A novel mutation in the LMNA gene causes congenital muscular dystrophy with dropped head and brain involvement,” *Neuromuscul. Disord.*, vol. 22, no. 2, pp. 149–151, 2012, doi: 10.1016/j.nmd.2011.08.009.
- [206] U. Bonati *et al.*, “Congenital muscular dystrophy with dropped head phenotype and cognitive impairment due to a novel mutation in the LMNA gene,” *Neuromuscul. Disord.*, vol. 24, no. 6, pp. 529–532, 2014, doi: 10.1016/j.nmd.2014.02.004.
- [207] I. Méndez-López *et al.*, “Hippocampal LMNA gene expression is increased in late-stage Alzheimer’s disease,” *Int. J. Mol. Sci.*, vol. 20, no. 4, 2019, doi: 10.3390/ijms20040878.
- [208] L. Gil *et al.*, “Perinuclear lamin a and nucleoplasmic lamin B2 characterize two types of hippocampal neurons through Alzheimer’s disease progression,” *Int. J. Mol. Sci.*, vol. 21, no. 5, pp. 1–19, 2020, doi: 10.3390/ijms21051841.
- [209] I. Rauschert *et al.*, *Promoter hypermethylation as a mechanism for Lamin A/C silencing in a subset of neuroblastoma cells*, vol. 12, no. 4. 2017.

- [210] B. Frost, F. H. Bardai, and M. B. Feany, “Lamin Dysfunction Mediates Neurodegeneration in Tauopathies,” *Curr. Biol.*, vol. 26, no. 1, pp. 129–136, 2016, doi: 10.1016/j.cub.2015.11.039.
- [211] “Simple Western systems,” 2021. [https://www.proteinsimple.com/simple\\_western\\_overview.html](https://www.proteinsimple.com/simple_western_overview.html) (accessed Jul. 18, 2021).
- [212] C. Teschendorf, K. J. Warrington, D. Siemann, and N. Muzyczka, “Comparison of the EF-1 alpha and the CMV promoter for engineering stable tumor cell lines using recombinant adeno-associated virus,” *Anticancer Res.*, vol. 22, no. 6A, pp. 3325–30, 2002.
- [213] X. Wang, Z. Xu, Z. Tian, X. Zhang, D. Xu, and Q. Li, “The EF-1 a promoter maintains high-level transgene expression from episomal vectors in transfected CHO-K1 cells,” *J. Cell. Mol. Med.*, vol. 21, no. 11, pp. 3044–3054, 2017, doi: 10.1111/jcmm.13216.
- [214] A. Fiszer-Kierzkowska *et al.*, “Liposome-based DNA carriers may induce cellular stress response and change gene expression pattern in transfected cells,” *BMC Mol. Biol.*, vol. 12, 2011, doi: 10.1186/1471-2199-12-27.
- [215] M. K. Driscoll, J. L. Albanese, Z. M. Xiong, M. Mailman, W. Losert, and K. Cao, “Automated image analysis of nuclear shape: What can we learn from a prematurely aged cell?,” *Aging (Albany. NY)*, vol. 4, no. 2, pp. 119–132, 2012, doi: 10.18632/aging.100434.
- [216] M. O. Trastoy, M. Defais, and F. Larminat, “Resistance to the antibiotic Zeocin by stable expression of the Sh ble gene does not fully suppress Zeocin-induced DNA cleavage in human cells,” *Mutagenesis*, vol. 20, no. 2, pp. 111–114, 2005, doi: 10.1093/mutage/gei016.
- [217] S.-G. Kang *et al.*, “Tau conformers in FTLD-MAPT undergo liquid-liquid phase separation and perturb the nuclear envelope,” 2020, doi: 10.1101/2020.07.04.187997.
- [218] M. Deschenes and B. Chabot, “The emerging role of alternative splicing in senescence and aging,” *Aging Cell*, vol. 16, pp. 918–933, 2017, doi: 10.1111/accel.12646.
- [219] A. C. Holly *et al.*, “Changes in splicing factor expression are associated with advancing age in man,” *Mech. Ageing Dev.*, vol. 134, no. 9, pp. 356–366, 2013, doi: 10.1016/j.mad.2013.05.006.
- [220] B. L. Angarola, “Splicing alterations in healthy aging and disease,” *WIREs RNA*, no. e1643, pp. 1–40, 2021, doi: 10.1002/wrna.1643.
- [221] J. R. Tollervey *et al.*, “Analysis of alternative splicing associated with aging and neurodegeneration in the human brain,” *Genome Res.*, vol. 21, pp. 1572–1582, 2011, doi: 10.1101/gr.122226.111.1572.
- [222] C. Dobson-stone *et al.*, “CYLD is a causative gene for frontotemporal dementia – amyotrophic lateral sclerosis,” *Brain*, pp. 783–799, 2020, doi: 10.1093/brain/awaa039.
- [223] H. D. C. Bain *et al.*, “The role of lysosomes and autophagosomes in frontotemporal lobar degeneration,” *Neuropathol. Appl. Neurobiol.*, pp. 244–261, 2019, doi: 10.1111/nan.12500.

- [224] T. Hamano *et al.*, “Autophagic-lysosomal perturbation enhances tau aggregation in transfectants with induced wild-type tau expression,” *Eur. J. Neurosci.*, vol. 27, pp. 1119–1130, 2008, doi: 10.1111/j.1460-9568.2008.06084.x.
- [225] C. Bellenguez, F. Küçükali, I. Jansen, V. Andrade, and S. Moreno-grau, “New insights on the genetic etiology of Alzheimer ’ s and related dementia,” pp. 1–35, 2020.
- [226] E. M. Van Well *et al.*, “A protein quality control pathway regulated by linear ubiquitination,” *EMBO J.*, vol. 38, no. e100730, pp. 1–21, 2019, doi: 10.15252/embj.2018100730.
- [227] Z. P. Van Acker, M. Bretou, and W. Annaert, “Endo-lysosomal dysregulations and late-onset Alzheimer ’ s disease : impact of genetic risk factors,” *Mol. Neurodegener.*, vol. 7, pp. 1–20, 2019.
- [228] R. A. Nixon, “The role of autophagy in neurodegenerative disease,” *Nat. Med.*, vol. 19, no. 8, pp. 983–997, 2013, doi: 10.1038/nm.3232.
- [229] S. R. Pfeffer, “NPC intracellular cholesterol transporter 1 ( NPC1 ) -mediated cholesterol export from lysosomes,” *J. Biol. Chem.*, vol. 294, no. 5, pp. 1706–1709, 2019, doi: 10.1074/jbc.TM118.004165.
- [230] M. T. Vanier, “Niemann-Pick disease type C,” *Orphanet J. Rare Dis.*, vol. 5, no. 16, 2010, [Online]. Available: <http://www.orphandis.com/content/5/1/16>.
- [231] A. U. Bräuer, A. Kuhla, C. Holzmann, A. Wree, and M. Witt, “Current challenges in understanding the cellular and molecular mechanisms in niemann-pick disease type C1,” *International Journal of Molecular Sciences*, vol. 20, no. 18. 2019, doi: 10.3390/ijms20184392.
- [232] S. Love, L. R. Bridges, and C. P. Case, “Neurofibrillary tangles in Niemann-Pick disease type C,” *Brain*, vol. 118, pp. 119–129, 1995.
- [233] K. Suzuki *et al.*, “Neurofibrillary tangles in Niemann-Pick disease type C,” *Acta Neuropathol*, vol. 89, pp. 227–238, 1995.
- [234] K. Kågedal *et al.*, “Increased expression of the lysosomal cholesterol transporter NPC1 in Alzheimer ’ s disease,” *Biochim. Biophys. Acta*, vol. 1801, pp. 831–838, 2010, doi: 10.1016/j.bbali.2010.05.005.
- [235] P. M. Mathews *et al.*, “Alzheimer’s Disease-related Overexpression of the Cation-dependent Mannose 6-Phosphate Receptor Increases Abeta Secretion,” *J. Biol. Chem.*, vol. 277, no. 7, pp. 5299–5307, 2002, doi: 10.1074/jbc.M108161200.
- [236] H. Gerber *et al.*, “The APMAP interactome reveals new modulators of APP processing and beta- amyloid production that are altered in Alzheimer ’ s disease,” *Acta Neuropathol. Commun.*, vol. 3, no. 7, pp. 1–18, 2019.
- [237] A. M. Cataldo, J. L. Barnett, C. Pieroni, and R. A. Nixon, “Increased Neuronal Endocytosis and Protease Delivery to Early Endosomes in Sporadic Alzheimer’s Disease: Neuropathologic Evidence for a Mechanism of Increased beta-Amyloidogenesis,” *J. Neurosci.*, vol. 17, no. 16, pp. 6142–6151, 1997.

- [238] E. Morita, L. A. Colf, M. A. Karren, V. Sandrin, C. K. Rodesch, and W. I. Sundquist, “Human ESCRT-III and VPS4 proteins are required for centrosome and spindle maintenance,” *Proc Natl Acad Sci U S A.*, vol. 107, no. 29, pp. 12889–12894, 2010.
- [239] C. Katarzyna and S. Khochbin, “CYLD negatively regulates cell-cycle progression by inactivating HDAC6 and increasing the levels of acetylated tubulin,” *EMBO J.*, vol. 29, pp. 131–144, 2010, doi: 10.1038/emboj.2009.317.
- [240] A. Stangl *et al.*, “Regulation of the endosomal SNX27-retromer by OTULIN,” *Nat. Commun.*, vol. 10, no. 4320, 2019, doi: 10.1038/s41467-019-12309-z.
- [241] Q. Zhang, C. Ma, M. Gearing, P. G. Wang, L. Chin, and L. Li, “Integrated proteomics and network analysis identifies protein hubs and network alterations in Alzheimer’s disease,” *Acta Neuropathol. Commun.*, vol. 6, no. 19, 2018.
- [242] L. E. Rajagopalan, C. J. Westmark, J. A. Jarzembowski, and J. S. Malter, “hnRNP C increases amyloid precursor protein ( APP ) production by stabilizing APP mRNA,” *Nucleic Acids Res.*, vol. 26, no. 14, pp. 3418–3423, 1998.
- [243] A. Borreca, K. Gironi, and G. Amadoro, “Opposite Dysregulation of Fragile-X Mental Retardation Protein and Heteronuclear Ribonucleoprotein C Protein Associates with Enhanced APP Translation in Alzheimer Disease,” *Mol. Neurobiol.*, vol. 53, pp. 3227–3234, 2016, doi: 10.1007/s12035-015-9229-8.
- [244] R. M. Page *et al.*, “Loss of PAFAH1B2 Reduces Amyloid- $\beta$  Generation by Promoting the Degradation of Amyloid Precursor Protein C-Terminal Fragments,” *J. Neurosci.*, vol. 32, no. 50, pp. 18204–18214, 2012, doi: 10.1523/JNEUROSCI.2681-12.2012.
- [245] M. Butzlaff *et al.*, “Impaired retrograde transport by the Dynein / Dynactin complex contributes to Tau-induced toxicity,” *Hum. Mol. Genet.*, vol. 24, no. 13, pp. 3623–3637, 2015, doi: 10.1093/hmg/ddv107.
- [246] K. Piekarowicz, M. Machowska, E. Dratkiewicz, D. Lorek, A. Madej-Pilarczyk, and R. Rzepecki, “The effect of the lamin A and its mutants on nuclear structure, cell proliferation, protein stability, and mobility in embryonic cells,” *Chromosoma.*, vol. 126, no. 4, pp. 501–517, 2017.
- [247] E. Chang and J. Kuret, “Detection and quantification of tau aggregation using a membrane filter assay,” *Anal. Biochem.*, vol. 373, no. 2, pp. 330–336, 2008, doi: 10.1016/j.ab.2007.09.015.
- [248] A. J. George *et al.*, “A Serial Analysis of Gene Expression Profile of the Alzheimer’s Disease Tg2576 Mouse Model,” *Neurotox Res.*, vol. 17, pp. 360–379, 2010, doi: 10.1007/s12640-009-9112-3.
- [249] J. Wong, “Altered Expression of RNA Splicing Proteins in Alzheimer’s Disease Patients : Evidence from Two Microarray Studies,” *Dement Geriatr Cogn Disord*, vol. 2522, pp. 74–85, 2013, doi: 10.1159/000348406.
- [250] M. Geppert, Y. Goda, and C. F. Stevens, “The small GTP-binding protein Rab3A regulates a late step in synaptic vesicle fusion,” *Nature*, vol. 387, pp. 810–814, 1997.

- [251] A. G. M. Leenders, F. H. Lopes, W. E. J. M. Ghijsen, and M. Verhage, “Rab3A Is Involved in Transport of Synaptic Vesicles to the Active Zone in Mouse Brain Nerve Terminals,” *Mol. Biol. Cell*, vol. 12, pp. 3095–3102, 2001.
- [252] K. Blennow, N. Bogdanovic, I. Alafuzoff, R. Ekman, and P. Davidsson, “Synaptic pathology in Alzheimer’s disease: relation to severity of dementia, but not to senile plaques, neurofibrillary tangles, or the ApoE4 allele,” *J Neural Transm*, vol. 103, no. 5, pp. 603–618, 1996.
- [253] J. Follett *et al.*, “Parkinson Disease-linked Vps35 R524W Mutation Impairs the Endosomal Association of Retromer and Induces  $\alpha$ -Synuclein,” *J. Biol. Chem.*, vol. 291, no. 35, pp. 18283–18298, 2016, doi: 10.1074/jbc.M115.703157.
- [254] S. A. Small *et al.*, “Model-Guided Microarray Implicates the Retromer Complex in Alzheimer’s Disease,” *Ann Neurol.*, vol. 58, no. 6, pp. 909–919, 2005, doi: 10.1002/ana.20667.
- [255] E. Zavodszky *et al.*, “Mutation in VPS35 associated with Parkinson’s disease impairs WASH complex association and inhibits autophagy,” *Nat. Commun.*, vol. 5, no. 3828, p. doi: 10.1038/ncomms4828., 2014, doi: 10.1038/ncomms4828.
- [256] A. N. Vagnozzi, J. L. Jin, C. Roshanak, R. Rebecca, and D. Praticò, “VPS35 regulates tau phosphorylation and neuropathology in tauopathy,” *Mol. Psychiatry*, pp. 10.1038/s41380-019-0453-x, 2019, doi: 10.1038/s41380-019-0453-x.
- [257] J. M. Carosi *et al.*, “Retromer regulates the lysosomal clearance of MAPT/tau,” *Autophagy*, pp. 1–21, 2020.
- [258] H. Ye *et al.*, “Retromer subunit, VPS29, regulates synaptic transmission and is required for endolysosomal function in the aging brain,” *Elife*, vol. 9, no. e51977, 2020.
- [259] G. Matsumoto, K. Matsumoto, T. Kimura, T. Suhara, and M. Higuchi, “Tau Fibril Formation in Cultured Cells Compatible with a Mouse Model of Tauopathy,” *Int J Mol Sci.*, vol. 19, no. 5, p. 1497, 2018, doi: 10.3390/ijms19051497.
- [260] B. Bandyopadhyay, G. Li, H. Yin, and J. Kuret, “Tau Aggregation and Toxicity in a Cell Culture Model of Tauopathy \*,” *J. Biol. Chem.*, vol. 282, no. 22, pp. 16454–16464, 2007, doi: 10.1074/jbc.M700192200.
- [261] L. Li *et al.*, “Alzheimer’s disease brain contains tau fractions with differential prion-like activities,” *Acta Neuropathol. Commun.*, vol. 9, no. 28, 2021, doi: 10.1186/s40478-021-01127-4.
- [262] T. Löffler *et al.*, “Stable Mutated tau441 Transfected SH-SY5Y Cells as Screening Tool for Alzheimer’s Disease Drug Candidates,” *J Mol Neurosci*, vol. 47, pp. 192–203, 2012, doi: 10.1007/s12031-012-9716-6.
- [263] A. Aranda-anzaldo, “The post-mitotic state in neurons correlates with a stable nuclear higher-order structure,” *Commun. Integr. Biol.*, vol. 5, no. 2, pp. 134–139, 2012.
- [264] T. Geiger, A. Wehner, C. Schaab, J. Cox, and M. Mann, “Comparative proteomic analysis of eleven common cell lines reveals ubiquitous but varying expression of most proteins,”

- Mol. Cell. Proteomics*, vol. 11, no. 3, pp. 1–11, 2012, doi: 10.1074/mcp.M111.014050.
- [265] A. M. Lanza, D. S. Kim, and H. S. Alper, “Evaluating the influence of selection markers on obtaining selected pools and stable cell lines in human cells,” *Biotechnol. J.*, vol. 8, no. 7, pp. 811–821, 2013, doi: 10.1002/biot.201200364.
- [266] J. L. Guo *et al.*, “The dynamics and turnover of tau aggregates in cultured cells: INSIGHTS INTO THERAPIES FOR TAUOPATHIES,” *J. Biol. Chem.*, vol. 291, no. 25, pp. 13175–13193, 2016, doi: 10.1074/jbc.M115.712083.
- [267] B. L. Heckmann *et al.*, “Noncanonical function of an autophagy protein prevents spontaneous Alzheimer’s disease,” *Sci. Adv.*, vol. 6, no. 33, 2020, doi: 10.1126/sciadv.abb9036.
- [268] T. Cavazza and I. Vernos, “The RanGTP Pathway: From Nucleo-Cytoplasmic Transport to Spindle Assembly and Beyond,” *Front. Cell Dev. Biol.*, vol. 3, no. 82, 2016, doi: 10.3389/fcell.2015.00082.